

Petrography and Geochemistry of volcanic rocks in Khao Sam Sip area, Sa Kaeo  
Province



A Thesis Submitted in Partial Fulfillment of the Requirements

for the Degree of Master of Science in Geology

Department of Geology

FACULTY OF SCIENCE

Chulalongkorn University

Academic Year 2019

Copyright of Chulalongkorn University

ศิลปวรรณนาและธรณีเคมีของหินภูเขาไฟในบริเวณพื้นที่เขาสามสืบ จังหวัดสระแก้ว



วิทยานิพนธ์นี้เป็นส่วนหนึ่งของการศึกษาตามหลักสูตรปริญญาวิทยาศาสตรมหาบัณฑิต

สาขาวิชาธรณีวิทยา ภาควิชาธรณีวิทยา

คณะวิทยาศาสตร์ จุฬาลงกรณ์มหาวิทยาลัย

ปีการศึกษา 2562

ลิขสิทธิ์ของจุฬาลงกรณ์มหาวิทยาลัย



เมธิรา ศรีวิชัย : ศิลาวรรณนาและธรณีเคมีของหินภูเขาไฟในบริเวณพื้นที่เขาสามสิบ จังหวัด  
สระแก้ว. ( Petrography and Geochemistry of volcanic rocks in Khao Sam Sip area, Sa  
Kaeo Province) อ.ที่ปรึกษาหลัก : ดร.อภิสิทธิ์ ซาล้า

หินภูเขาไฟในบริเวณพื้นที่เขาสามสิบจังหวัดสระแก้วเป็นส่วนหนึ่งของแนวภูเขาไฟเลย-เพชรบูรณ์-  
สระแก้ว จากการศึกษารากคสนาม การศึกษาศิลาวรรณนา และธรณีเคมี พบว่าหินในพื้นที่ศึกษาสามารถแบ่ง  
ออกเป็นหน่วยหินได้ 4 หน่วยหิน ได้แก่ 1) หน่วยหินบะซอลต์-แอนดีไซต์ 2) หน่วยหินโพลีเมติก (Polymictic)  
แอนดีซิติค 3) หน่วยหินเนื้อประสมผิวพื้น และ 4) หน่วยหินเนื้อประสม หน่วยหินที่ 1 เป็นหน่วยที่ลำดับต่ำ  
ที่สุด ซึ่งประกอบด้วย หินโอลิวีน-ไพรอกซีน-แพลซิโอเคลสบะซอลต์ หินไพรอกซีนบะซอลต์ หินฮอร์นเบลนด์-  
แพลซิโอเคลสแอนดีไซต์ และหินแพลซิโอเคลสแอนดีไซต์ หน่วยหินที่ 2 ประกอบด้วย หินกรวดเหลี่ยมแอนดีซิติค  
ติก และหินทรายแอนดีซิติค หน่วยหินที่ 3 เป็นหน่วยหน่วยหินเนื้อประสมผิวพื้น ที่ประกอบไปด้วยหินทรายที่มี  
เศษชิ้นแร่และเศษชิ้นหินมาก หน่วยหินที่ 4 ประกอบด้วยหินเนื้อประสมเนื้อละเอียดและหินปูน

ในการศึกษาธรณีเคมีหน่วยหินบะซอลต์-แอนดีไซต์ได้รับการคัดเลือกสำหรับการวิเคราะห์ทาง  
ธรณีเคมี ประกอบด้วย ธาตุองค์ประกอบหลักและธาตุหายาก โดยชนิดหินในหน่วยหินบะซอลต์-แอนดีไซต์มี  
ความหลากหลายในองค์ประกอบ ได้แก่ หินแทร์โคต์แอนดีไซต์ และหินแอลคาไลบะซอลต์ บางส่วนพบเป็น  
หินไรโอเดไซต์ หินแอนดีไซต์และหินบาซาลต์ ซึ่งมีองค์ประกอบเป็นแอลคาไล จากปริมาณของธาตุร่องรอย  
และปริมาณของธาตุหายาก สามารถแบ่งย่อยชนิดหินออกเป็นสี่กลุ่ม โดยทั้งสี่กลุ่มมีลักษณะทางเคมีที่  
คล้ายคลึงกัน ในการเพิ่มปริมาณของธาตุ HFS และธาตุหายากเบาพร้อมกับค่าความผิดปกติของธาตุยูเรเนียม  
เชิงลบ และสิ่งนี้อาจบ่งชี้ว่าหินนั้นเกิดจากหินหนืดที่ตกผลึกและแยกส่วนในระบบแนวภูเขาไฟรูปโค้งในช่วง  
อายุไทรแอสซิกตอนต้น ซึ่งเป็นส่วนหนึ่งของแนวรอยคดโค้งเลย ในการศึกษานี้ไม่พบทองคำปรากฏ โดย  
ทองคำอาจเกิดขึ้นเป็นทองคำทนไฟ (ในโครงสร้างไฟไรต์) หรืออนุภาคขนาดนาโนที่รวมอยู่ในแร่ซัลไฟด์  
อย่างไรก็ตามสายแร่/สายแร่ร่างแหที่อุดมด้วยทองแดงนั้น พบอยู่ในหินภูเขาไฟเนื้อเดียวและอาจเป็นแสดงถึง  
การเกิดแหล่งแร่แบบสการ์นหรือแหล่งแร่ร้อนอุณหภูมิต่ำ

สาขาวิชา ธรณีวิทยา

ลายมือชื่อผู้ผลิต .....

ปีการศึกษา 2562

ลายมือชื่อ อ.ที่ปรึกษาหลัก .....

## 6172043623 : MAJOR GEOLOGY

KEYWORD: Volcanic Rock, Alkaline, Sa Kaeo, Loei-Phetchabun-Sa Kaeo Volcanic Belt,  
Petrography, Geochemistry, Copper veins/veinlets

Maythira Sriwichai : Petrography and Geochemistry of volcanic rocks in Khao Sam Sip  
area, Sa Kaeo Province. Advisor: ABHISIT SALAM, Ph.D.

The volcanic rocks at Khao Sam Sip, Sa Kaeo province is part of the Loei-Phetchabun-Sa Kaeo Volcanic Belt. Based on field observation, petrographic and geochemical studies, the rocks in the study area can be divided into four rock units namely, 1) Basalt-andesite unit, 2) Polymictic andesitic unit, 3) Epiclastic unit, and 4) Clastic unit. Unit 1 is the lowest unit in sequence consisting of olivine-pyroxene-plagioclase basalt, pyroxene basalt, hornblende-plagioclase andesite, and plagioclase andesite. Unit 2 consists of polymictic andesitic breccia and polymictic andesitic sandstone. Unit 3 is epiclastic unit comprising of crystal-lithic sandstone and polymictic conglomerate. Units 4 includes fine-grained clastic rock and limestone.

In the geochemical study, the basalt-andesite unit was selected for geochemical analyzes including major, trace and rare earth elements. They are ranging in composition of trachyandesite and alkali basalt with few rhyodacite, andesite, and basanite and classified dominantly as alkaline affinity. Based on the results of trace elements and REE abundances, the rocks can be subdivided into four groups. All four groups have similar chemical characters of enrichment in high field strength elements (HFSE) and light rare earth elements (LREE) with distinct negative Eu anomalies, and this may suggest the rocks were formed by Early Triassic fractionated magma of volcanic arc system as a part of Loei Fold Belt. Gold has not been identified during this study. It could have occurred as refractory gold (in pyrite structure) or nano-size particles included in sulfide minerals. However, copper-rich veins/veinlets are hosted in coherent volcanic rocks and they may represent either skarn or epithermal style mineralization.

Field of Study: Geology

Student's Signature .....

Academic Year: 2019

Advisor's Signature .....

## ACKNOWLEDGEMENTS

The author would like to gratefully thank my supervisor, Dr. Abhisit Salam for his supervision, encouragement, and criticism during the preparation of this thesis. My thank also goes to the Department of Geology, Faculty of Science, Chulalongkorn University for giving me knowledge and facilities, the graduate school Chulalongkorn University for financial support during my study, and the Department of Mineral Resources for giving access to the drill core samples, XRF analysis, and staff at the Resources Office Region 3 and Resources Analysis and Identification Division for the great support. Thanks, are also extended to many people who assisted during this study, in particular, Mr. Takayuki Manaka for his suggestion and revision; Mr. Thanaz Watcharamai, Miss Amporn Chaikham, Miss Chanista Chansom, Mr. Srett Santitharangkun, Miss Phattharawadeee Wacharapornpinthu, Miss Pimolpat Ardkham, Miss Saowapap Utthairat for their advice and encouragement; Ms. Sopit Poompuang, Ms. Bunjong Puangthong, and Mr. Suriya Chokmo (Department of Geology, Faculty of Science, Chulalongkorn University) for their help on laboratory work; Ms. Jongkonkanok Kamonchum for her advice on the scholarship and also the graduate documents; and all members of the Department of Geology, Faculty of Science, Chulalongkorn University, who have no been earlier mentioned, for their hospitality, companionship, support, encouragement and many facilities.

Finally, very special thanks are given to Sriwichai's Family, Mr. Jirat Konkhayan, and Mr. Rujaroj Techakajeonkiet for their encouragement, and financial support throughout the study.

## TABLE OF CONTENTS

	Page
.....	iii
ABSTRACT (THAI).....	iii
.....	iv
ABSTRACT (ENGLISH) .....	iv
ACKNOWLEDGEMENTS.....	v
TABLE OF CONTENTS.....	vi
LIST OF TABLES.....	viii
LIST OF FIGURES .....	ix
CHAPTER 1 INTRODUCTION .....	1
1.1. General Statement .....	1
1.2. Objective of the study.....	2
1.3. Physiographic description .....	2
1.4. Scope of study .....	3
1.5. Thesis structure and conventions.....	3
CHAPTER 2 TECTONIC SETTING AND REGIONAL GEOLOGY .....	5
2.1. Tectonic evolution of Thailand and adjacent areas .....	5
2.2. Volcanic rocks in Thailand.....	8
2.3. An overview geology of the study area .....	16
2.4. Economic Potential .....	18
CHAPTER 3 VOLCANIC PETROGRAPHY .....	19
3.1. Introduction .....	19

3.2. Method of study .....	19
3.3. Petrography.....	19
3.4. Interpretation .....	31
CHAPTER 4 GEOCHEMISTRY .....	33
4.1. Introduction .....	33
4.2. Sampling and analytical methods .....	33
4.3. Geochemistry of volcanic rocks in the Khao Sam Sip area .....	36
4.4. Tectonic Discrimination Diagrams.....	52
CHAPTER 5 MINERALIZATION .....	55
5.1. Introduction .....	55
5.2. Paragenesis and Mineralogy.....	55
5.3. Mineralogy.....	59
CHAPTER 6 DISCUSSION AND CONCLUSION.....	62
6.1. Magmatic suites at the Khao Sam Sip.....	62
6.2. Magma sources .....	63
6.3. Tectonic setting implication.....	64
6.4. Mineralization .....	66
6.5. Conclusion .....	67
6.6. Recommendations for future works .....	68
REFERENCES.....	69
VITA .....	79

## LIST OF TABLES

	Page
Table 1 Geochemistry of least altered volcanic rocks in the Khao Sam Sip area, Sa Kaeo Province.....	38
Table 2 Trace elements and REE compositions (in ppm) determined by ICP-MS analysis of least altered volcanic rocks from the Khao Sam Sip Area, Sa Kaeo Province. ....	40
Table 3 Paragenetic diagram showing order of veins formation and the relative amount of mineral abundance (e.g. ore and gangue minerals).....	56



## LIST OF FIGURES

	Page
Fig. 1 Topographic map of the Khao Sam Sip area (Modified from Royal Thai Survey Department (1999)).	2
Fig. 2 Tectonic map of showing the major tectonic terranes and suture zones (modified after Metcalfe (2009); Sone and Metcalfe (2008)).	6
Fig. 3 The distribution of Paleozoic-Mesozoic volcanic rocks in Thailand (after Junyusuk and Khositantont (1992); Kosuwan et al. (2017); Panjasawatwong (2003); Panjasawatwong et al. (2006)).	9
Fig. 4 Regional geology of the Khao Sam Sip area (Modified from Chaodumrong (1992); Polprasit et al. (1985)).	17
Fig. 5 Geological map of volcanic rocks and sedimentary rocks in the Khao Sam Sip area.	20
Fig. 6 Characteristics of olivine-pyroxene-plagioclase basalt and pyroxene basalt found at quarry and diamond drill core (BDH-3) at the north of Khao Moei Choi. A) Photograph of pit wall showing the olivine-pyroxene-plagioclase basalt and the pyroxene basalt on the pit wall of quarry. B) Photograph of Sample from the outcrop of olivine-pyroxene-plagioclase basalt showing dominated olivine phenocrysts. C) Photograph of hand specimen of olivine-pyroxene-plagioclase basalt showing olivine and pyroxene phenocrysts. D) Photomicrograph of olivine-pyroxene-plagioclase basalt showing plagioclase-rich groundmass with olivine, pyroxene and plagioclase phenocrysts. ....	22
Fig. 7 Characteristics of pyroxene basalt found at quarry at the north of Khao Moei Choi. A) Photograph of hand specimen of pyroxene basalt showing pyroxene phenocrysts (black) and calcite veinlets. B) Photomicrograph of pyroxene basalt showing groundmass consisting of plagioclase with pyroxene phenocrysts. ....	23

Fig. 8 Characteristics of hornblende-plagioclase andesite from drill core in the north of Khao Moei Choi area. A) Photograph hand specimen of hornblende-plagioclase andesite showing slightly porphyritic texture with calcite veinlets. B) Photomicrograph of hornblende-plagioclase andesite showing groundmass plagioclase with pyroxene, and hornblende crystals. ....24

Fig. 9 Characteristics of plagioclase andesite from drill core and outcrop in the north of Khao Moei Choi. A) Photograph of outcrop of plagioclase andesite at the north of Khao Moei Choi. B) Photograph of float rock of monomictic breccia showing clast supported. C) Hand specimen showing blocky clasts of plagioclase andesite. D) Photomicrograph from clast in Fig. 9C showing groundmass and phenocryst of pyroxene (Px), plagioclase (Pl) with quartz and calcite. E) Photomicrograph from matrix in Fig. 9C showing groundmass and phenocrysts of clinopyroxene (Cpx) and plagioclase (Pl). ....26

Fig. 10 Characteristics of polymictic andesitic breccia. A) Photograph of polymictic breccia and polymictic sandstone outcrop located at the north of the Khao Sam Sip B) Photograph of polymictic breccia outcrop showing clasts of gabbro and andesite. C) Photomicrograph of matrix of polymictic breccia consisting of plagioclase (Pl), K-feldspar (Kfs), clinopyroxene (Cpx), sphene (Spn) and rock fragments (Rf). D) Photomicrograph of andesitic breccia clast consisting of plagioclase (Pl) and clinopyroxene (Cpx) phenocrysts. E) Photomicrograph of gabbro clast consisting of orthopyroxene (Opx) and clinopyroxene (Cpx). ....27

Fig. 11 Characteristics of lithic-crystal sandstone and mudstone. A) Photograph of outcrop located at the Khao Thung Plueai showing sandstone interbedded with siltstone and mudstone. B) Photograph of hand specimen of lithic-crystal sandstone showing gradation in grain size. C) Photograph of hand specimen of lithic-crystal sandstone and mudstone showing sandstone interbedded with mudstone layers. D) Photomicrograph of lithic-crystal sandstone consisting of plagioclase fragments (Pl), K-feldspar (Kfs), quartz (Qtz), rock fragments (Rf) and clinopyroxene (Cpx). ....29

- Fig. 12 Characteristics of polymictic conglomerate. A) Photograph of polymictic conglomerate outcrop located at the north of the Khao Sam Sip showing clasts of granite, basaltic rock fragments. B) Photograph of hand specimen of polymictic conglomerate showing clasts of basaltic rock fragments, clasts of mudstone and quartz pebble. C) Photomicrograph of polymictic conglomerate showing clast of basaltic rock in sandstone matrix which consists of quartz (Qtz), plagioclase (Pl), K-feldspar (Kfs), Clinopyroxene (Cpx) and rock fragments (Rf)..... 30
- Fig. 13 Limestone outcrop located at the south of Khao Sam Sip A) Photograph of bedded limestone. B) Photograph of limestone hand specimen showing deformed texture..... 31
- Fig. 14 Geological map of the Khao Sam Sip area with sampling stations. .... 34
- Fig. 15 Histograms of whole rock SiO<sub>2</sub> content for the volcanic rocks from the Khao Sam Sip area. Note: Ranging of SiO<sub>2</sub> for basalt, basaltic andesite, andesite and dacite field are based on Cox et al. (1979). .... 36
- Fig. 16 Molar K/Al vs. molar (K + Na + 2Ca)/Al (Booden et al., 2010; Madeisky, 1996). In this diagram, the alteration minerals kaolinite, illite and adularia plot on a line of slope 1. Unaltered basaltic to andesitic volcanic rocks typically have molar (K + Na + 2Ca)/Al values > 1. Potassium metasomatism leads to decreasing molar (K + Na + 2Ca)/Al and increasing molar K/Al values. Most of the Khao Sam Sip rocks have molar (K + Na + 2Ca)/Al > 1 and are considered to be the least-altered rocks..... 37
- Fig. 17 TAS diagram (Na<sub>2</sub>O + K<sub>2</sub>O vs SiO<sub>2</sub> diagram) (Irvine and Barager, 1971; Le Maitre et al., 1989)..... 42
- Fig. 18 Nb/Y and Zr/TiO<sub>2</sub> discrimination diagram by (Winchester and Floyd, 1977). ..... 43
- Fig. 19 Major element bivariate diagrams plotted against Mg# for the volcanic rocks from the Khao Sam Sip area. A) TiO<sub>2</sub> vs Mg# number showing an increase TiO<sub>2</sub> with decrease Mg#, B) FeO<sub>t</sub> vs Mg# showing a slightly positive trend to more mafic composition, C) CaO vs Mg# showing the different fields for the volcanic rocks. .... 43

Fig. 20 Trace element bivariate diagrams plotted against Mg# for the volcanic rocks from the Khao Sam Sip area. A) Ni vs Mg#, B) Sr vs Mg#, C) Nb vs Mg#, D) Zr vs Mg#, and E) Y vs Mg#.	44
Fig. 21 Chondrite-normalized REE patterns for the olivine-pyroxene-plagioclase basalt. The chondrite-normalizing values are from (Sun and McDonough, 1989).	46
Fig. 22 N-MORB normalized multi-elements for the representative of the olivine-pyroxene-plagioclase basalt. The N-MORB normalizing values are from (Sun and McDonough, 1989).	47
Fig. 23 Chondrite-normalized REE pattern for the pyroxene basalt. The chondrite normalizing values are from (Sun and McDonough, 1989).	48
Fig. 24 N-MORB normalized multi-elements for the representative of the pyroxene-phyric basalt. The N-MORB normalizing values are from (Sun and McDonough, 1989).	48
Fig. 25 Chondrite-normalized REE patterns for the hornblende-plagioclase andesite. The chondrite normalizing values are from (Sun and McDonough, 1989).	50
Fig. 26 N-MORB normalized multi-elements for the representative of the hornblende-plagioclase andesite. The N-MORB normalizing values are from (Sun and McDonough, 1989).	50
Fig. 27 Chondrite-normalized REE patterns for the plagioclase andesite. The chondrite normalizing values are from (Sun and McDonough, 1989).	51
Fig. 28 N-MORB normalized multi-elements for the representative of the plagioclase andesite. The N-MORB normalizing values are from (Sun and McDonough, 1989).	52
Fig. 29 Tectonic discrimination diagrams for volcanic rocks from the Khao Sam Sip area. A) Plot of $MnO \cdot 10 - TiO_2 - P_2O_5 \cdot 10$ showing the field for MORB = mid ocean ridge basalt; OIT = ocean-island tholeiite or sea mount tholeiite; OIA = ocean-island alkali basalt or seamount alkali basalt; CAB = island-arc calc alkaline basalt; IAT = island-arc tholeiite; Bon = boninite (Mullen, 1983). Note that the volcanic rocks plot in the island arc calc-alkalic basalt field, B) Plot of $TiO_2$ against Zr (Pearce and Cann, 1973). Note that the	

- volcanic rocks plot in the volcanic arc basalt field, C) Plot of Zr/Y against Ti/Y (Pearce, 1982). Note that the volcanic rocks plot in the plate margin field. .... 53
- Fig. 30 Chondrite-normalized REE patterns of representative the volcanic rocks in the Khao Sam Sip plotted using chondrite normalizing values of (Sun and McDonough, 1989)..... 54
- Fig. 31 N-MORB normalised trace elements patterns for the volcanic rocks in the Khao Sam Sip area. The N-MORB composition is taken from (Sun and McDonough, 1989)... 54
- Fig. 32 Characteristics of Stage 1 veins/veinlets: A. Photograph of hand specimen showing Stage 1 vein consisting of massive pyrite aggregate and crosscut by Stage 2 quartz-carbonate-sulfides vein. B. Photomicrograph showing Stage 1 pyrite aggregate crosscut by Stage 2 quartz-carbonate-sulfide (mainly chalcopyrite) vein. C. Photomicrograph of Stage 2 zooming from area C in Fig. B showing vein dominated by chalcopyrite and minor pyrite. D. Photomicrograph enlarged from Fig. C. showing presence of chalcopyrite and pyrite. .... 57
- Fig. 33 Characteristics of Stage 2 veins: A. Photograph of diamond drill core showing Stage 2 vein consisting mainly of quartz and sulfide patches (dark). B. Photomicrograph showing mineral assemblage of Stage 2 vein comprising subhedral to euhedral quartz at the vein wall and pyrite (Py) and chalcopyrite (Cpy) at vein center. C. Photomicrograph showing presence of chalcopyrite crystals confined at the contact between quartz and carbonate bands. D. Photomicrograph showing massive chalcopyrite with euhedral pyrites at rim. .... 58
- Fig. 34 Characteristics of Stage 3 veins/veinlets: A. Photograph of hand specimen showing Stage 3 vein consisting of quartz and chlorite. B. Photomicrograph showing minerals in Stage 3 comprise chlorite..... 58
- Fig. 35 Characteristics of Stage 4 veins/veinlets. A. Photograph of diamond drill core showing Stage 4 vein consisting mainly of quartz and carbonate..... 59

- Fig. 36 Characteristics of vein infills: A. Photomicrograph showing Stage 1 pyrite aggregate. B. Photomicrograph showing mineral assemblage of Stage 2 vein comprising pyrite (Py), chalcopyrite (Cpy) and sphalerite (Sp). ..... 60
- Fig. 37 EPMA Mapping of pyrite-chalcopyrite bearing quartz vein (Stage 1) showing mostly pyrite with small amount of fine-grained chalcopyrite..... 61
- Fig. 38 EPMA Mapping of chalcopyrite-pyrite bearing quartz vein (Stage 2) confirming the present of chalcopyrite and pyrite but no gold. .... 61



# CHAPTER 1

## INTRODUCTION

### 1.1. General Statement

In Thailand, pre-Cenozoic volcanic rocks are found to be an important host rocks for mineral deposits for instance, Chatree (epithermal gold-silver), Khao Phanom Pha (gold skarn), Khao Lek and Khao Thap Kwai (Fe skarn). Many volcanic host rocks have been studied to analyze for economic potential because their properties, such as composition, control the possibility of base/precious metal deposits. Thus, recognition of volcanic composition is necessary to evaluate the potential and distribution of mineral deposits.

Volcanic rocks in Thailand have been studied in many disciplines, such as petrography, volcanic stratigraphy, geochemistry, age dating and their relationship with mineral deposits. However, research works in the field of volcanology (e.g. petrography, geochemistry, geochronology) are very limited. In general, the volcanic rocks particularly the pre-Cenozoic ages are widely distributed through the country with exception of the northeastern region. Based on the previous works, the volcanic rocks in Thailand are confined to two major periods namely, Permo-Triassic and Cenozoic periods. The former one can be grouped into four major volcanic belts, 1) the Chiang Rai–Chiang Mai Volcanic Belt, 2) the Chiang Khong–Lampang-Tak Volcanic Belt, 3) the Nan– Chanthaburi suture zone and the 4) the Loei–Phetchabun–Nakhon Nayok Volcanic Belt (Junyusuk and Khositantont, 1992; Kosuwan et al., 2017; Panjasawatwong et al., 2006). The Cenozoic volcanic rocks are mainly found in N-S trending basins which are also formed during the Cenozoic age, for example: Lam Narai basalt and Wichian Buri basalt along the eastern margin of Phetchabun basin and Bo Ploi basalt along the western margin of Chao Phraya Basin (Junyusuk and Khositantont, 1992). Although, the pre-Cenozoic volcanic rocks have been studied in several areas. Informative data of the Loei-Phetchabun-Nakorn Nayok volcanic rocks in Sa Kaeo area are still insufficient.

Therefore, in this study, petrochemical analysis of volcanic rocks in this area have been planned in order to determine their characteristic and tectonic setting of the formation.

### 1.2. Objective of the study

The aim of this study is to analyze petrography and geochemistry of the volcanic rocks in the Khao Sam Sip area as well as their tectonic setting.

### 1.3. Physiographic description

The Khao Sam Sip study area is located at Khao Sam Sip sub district, Khao Chakan district, Sa Kaeo Province, southeastern Thailand. It covers an area of approximately 60 sq. km in the central part of Sa Kaeo Province. The area is in three district administration zones including Khao Chakan, Watthana Nakhon and Muang Sa Kaeo. It locates between longitudinal grid references of 190000-202000 East and latitudinal grid references of 1510000-1517000 North in Topographic Map, scale 1: 50,000, Series L 7018 (WGS), Sheet Amphoe Khao Chakan (5436 III) (Fig. 1).

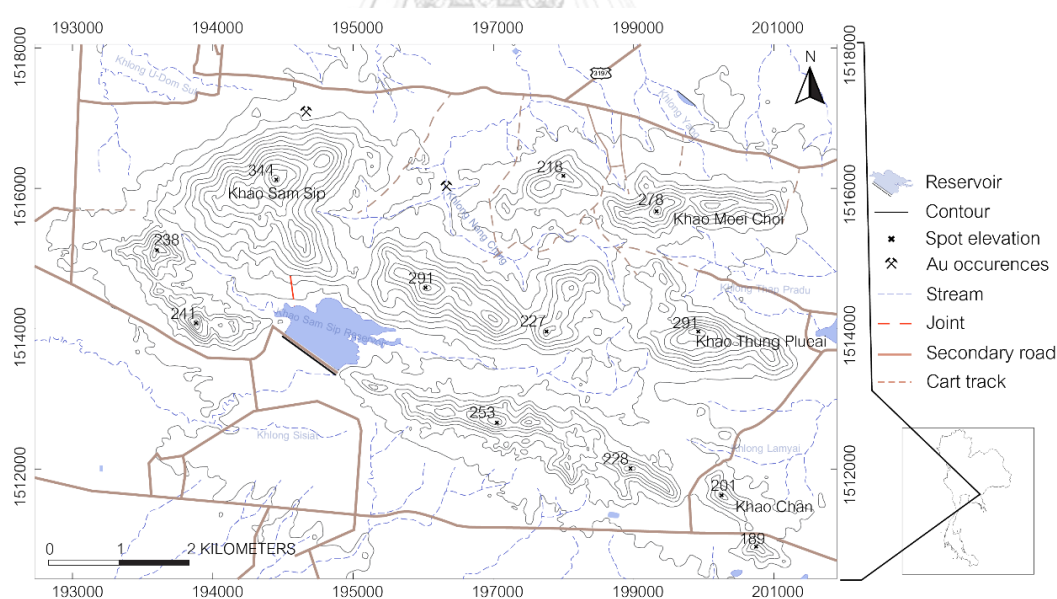


Fig. 1 Topographic map of the Khao Sam Sip area (Modified from Royal Thai Survey Department (1999)).

The Khao Sam Sip area is composed of 25% flat-lying with elevations ranging between 90 m and 344 m MSL with 75% mountainous areas with the highest peak is at Khao Sam Sip (~344 m above mean sea level-MSL). The plain area is extensively used

for agricultural and settlements. Rivers and related tributaries are sparse, short and narrow including Khlong Bo Nang Ching, Khlong Sisiat, Khlong Lamyai and Khlong Thap Pradu. Two reservoirs present in the study area, in the south (Khao Sam Sip Reservoir) and the west (Thap Pradu Reservoir) of Khao Sam Sip (Fig. 1).

The area is accessible all year round. From Bangkok, used Highway No. 7 to Chachoengsao Province about 60 kilometers, turn left onto Highway No. 314 for 20 kilometers and turn right to Highway No. 304. Following Highway No. 304 (Chachoengsao – Krabinburi) to the east for about 60 kilometers will be arrived in Krabinburi district, turn right again onto Highway No. 359 (Krabinburi – Aranyaprathet) for approximately 70 kilometers to the north of the study area in Sa Kaeo province. Within the survey area, accessibility can be done by using rural roads.

#### **1.4. Scope of study**

This study focused principally on the field investigation (e.g. recheck pre-existing geologic map covering approximately 60 square kilometers and collect geological information), and field samples collection. Field survey has been conducted in two times, the first field work was undertaken during October 24-25, 2019 and the second field work from November 26-27, 2019. Drill core logging and additional sampling from 3 diamond drill holes (BDH-1, BDH-2, and BDH-3) have been undertaken at Royal Thai Department of Mineral Resources, Sample warehouse, the Resources Office Region 3. Detailed petrographic investigation including ore petrography and geochemistry of least-altered volcanic rocks was also undertaken. Whole-rock geochemical analysis (X-Ray Fluorescence) for major oxides, and some trace elements solution ICP-MS for REE were conducted to clarify their tectonic setting and imply the relationship between volcanic rocks and mineral deposit.

#### **1.5. Thesis structure and conventions**

The thesis is divided into the following chapters:

- CHAPTER 1 (INTRODUCTION) provides the general background of this study including the volcanic rocks, the location and transportation to the Khao Sam Sip area, scope of study, and thesis structure and conventions.
- CHAPTER 2 (TECTONIC SETTING AND REGIONAL GEOLOGY) includes tectonic evolution of Thailand, pre-Cenozoic volcanic rocks in Thailand, an overview the geology of the Khao Sam Sip area and its economic potential.
- CHAPTER 3 (VOLCANIC PETROGRAPHY) documents characteristic of volcanic rocks and relation of volcanic rocks and mineralization in the Khao Sam Sip area supported by petrographic work.
- CHAPTER 4 (GEOCHEMISTRY) describes characteristic of volcanic rocks by geochemistry and implies for their tectonic setting in the Khao Sam Sip area.
- CHAPTER 5 (MINERALIZATION) give basic description of mineralization in terms of ore petrography and mineral paragenesis.
- CHAPTER 6 (DISCUSSION AND CONCLUSION) involves discussion and conclusions of all the collected data in this study.

## CHAPTER 2

### TECTONIC SETTING AND REGIONAL GEOLOGY

This chapter summarizes the tectonic and geological framework of Thailand and its adjacent areas. Geological setting and volcanism of the Loei-Phetchabun-Nakorn Nayok volcanic belt and ore deposits of the Loei Fold Belt (LFB) also are emphasized based on the available literatures. In addition, district-scale geology of the Khao Sam Sip area also is described based on existing literatures.

#### 2.1. Tectonic evolution of Thailand and adjacent areas

Thailand and its adjacent areas are composed of two continental terranes namely, Shan-Thai terrane in the west and Indochina terrane in the east. Between these terranes, there are Sukhothai fold belt (SFB) located on the eastern edge of Shan-Thai terrane; Loei fold belt (LFB) located on the western edge of Indochina terrane; and a volcano-plutonic zones along the SFB and the LFB (Fig. 2) (Barr and Macdonald, 1991; Bunopas and Vella, 1983; Sone and Metcalfe, 2008)

The Shan-Thai terrane, Indochina terrane and South China terrane were believed as parts of Gondwana Australia in the southern hemisphere during the Precambrian to Lower Paleozoic. Indochina terrane which amalgamated to the South China terrane along the Song Ma suture was separated from the Gondwana by the opening of Paleo Tethys in the late Devonian to Carboniferous. Subsequently, Paleo Tethys began to subduct under the Indochina terrane and the Shan-Thai terrane were separated from the Gondwana by rifting of Meso Tethys in the Late Carboniferous time (Bunopas and Vella, 1983; Metcalfe, 2009).

Significantly, during the Middle Permian to Late Triassic period, the continuous subduction of the Paleo Tethys was leading to magmatism of the Truong Son Fold Belt (TSFB) in northern Vietnam; Sukhothai Island Arc; the Nan-Uttaradit Suture (NUS)-Sa Kaeo Suture, and probably volcano-plutonic zone in the LFB (Bunopas and Vella, 1983; Intasopa, 1993; Sone and Metcalfe, 2008). The TSFB was a part of the Indochina terrane

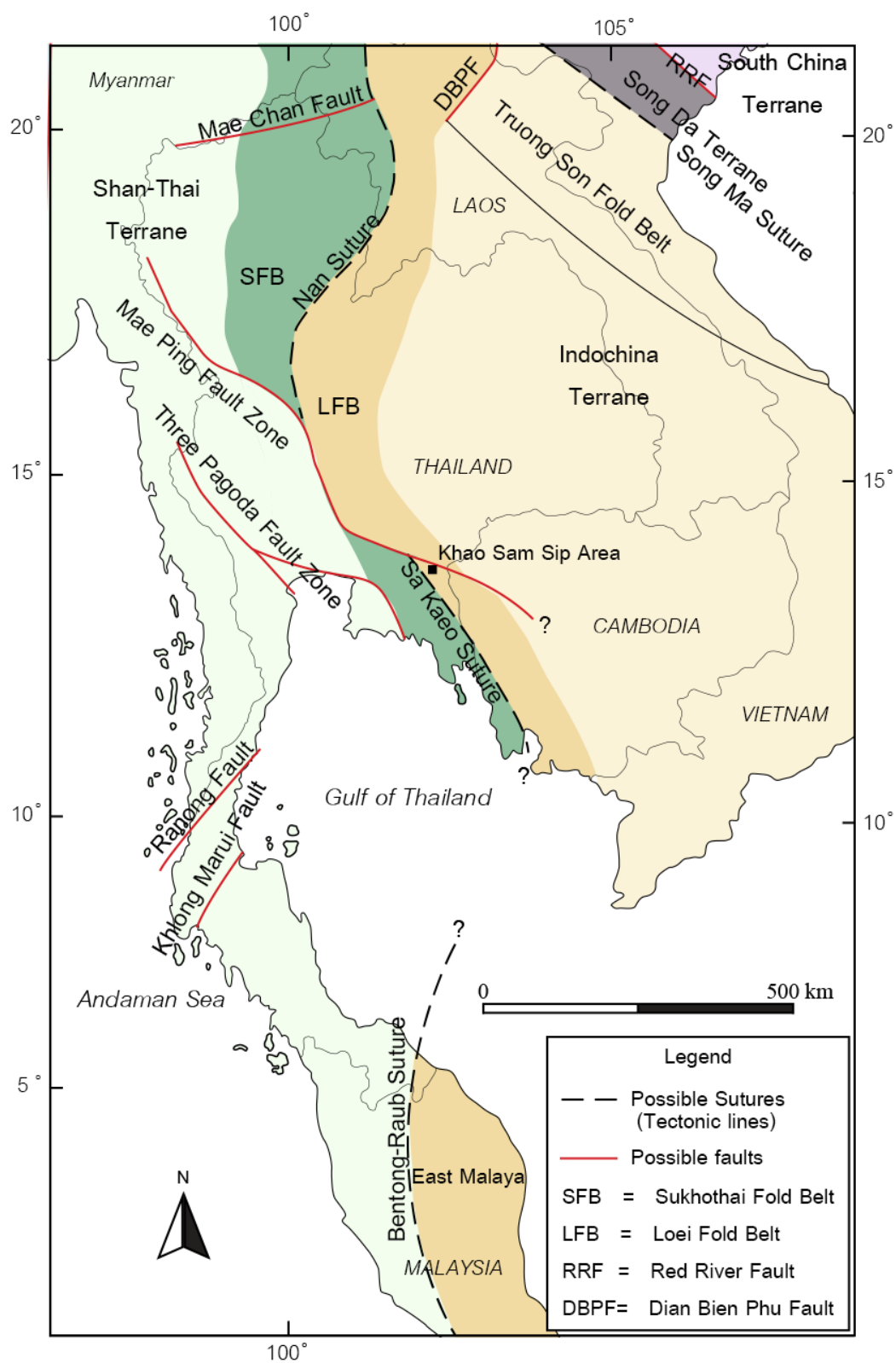


Fig. 2 Tectonic map of showing the major tectonic terranes and suture zones (modified after Metcalfe (2009); Sone and Metcalfe (2008)).

and considered to be the result of the closure of Laos-North Vietnam Strait of Paleo-Tethys (Intasopa, 1993) while the Sukhothai Island Arc was formerly believed to be the closure of westward subduction of the Paleo Tethys underneath the eastern margin of the Shan-Thai terrane (Bunopas and Vella, 1978; Singharajwarapan, 1994; Singharajwarapan and Berry, 2000). The Nan-Uttaradit Suture was formerly regarded to represent the remnant of the Paleo-Tethys with a pair subduction, because of the existence of dismembered ophiolite suites and volcanism along the east and west plate margin (Bunopas and Vella, 1978). However, Sone and Metcalfe (2008) modified the tectonic evolution model showing the new location of the Paleo Tethys along the west of the SFB (also known as Inthanon zone) instead of the Nan-Uttaradit Suture and the belt was a result of eastward subduction of Paleo Tethys underneath the western margin of the Indochina (Wakita and Metcalfe, 2005). Thus, the Nan-Uttaradit Suture has been re-interpreted as a closure of back-arc basin which probably continued to the Sa Kaeo Suture (Ueno and Hisada, 2001).

The volcano-plutonic rocks in LFB have been reported as the products of arc-related magmatism. Almost all of granitic rocks in the LFB have I-type affinity and almost all of volcanic rocks have calc-alkalic affinity (Charusiri et al., 1993; Junyusuk and Khositant, 1992; Khin et al., 2014; Nakapadungrat and Putthapiban, 1992). The ages of magmatism in the LFB have been suggested to be active in the three main periods: 1) Silurian to Early Carboniferous, 2) Late Permian to Late Triassic, and 3) Cenozoic (Intasopa, 1994; Qian et al., 2017).

In the Late Permian, the Shan-Thai terrane and Indochina terrane were beginning to amalgamate, and the Nan-Uttaradit back arc basin and the Sa Kaeo back arc basin were collapsed resulting in Nan-Uttaradit Suture and Sa Kaeo Suture (Metcalfe, 2009, 2011; Metcalfe, 2013; Sone and Metcalfe, 2008). In addition, Khin et al. (2014) also reported that the subduction of oceanic crust underneath the SFB resulted in the emplacement of volcanic rocks ranging in composition from basalt to rhyolite and plutonic rocks such as granite to diorite of I-type affinity.

Subsequently, during the Late Triassic to Early Jurassic, the Paleo Tethys was closed and the collision between Shan-Thai and Indochina terrane resulted in volcano-plutonic zones of post-collision magmatism (Barr and Charusiri, 2011; Junyusuk and Khositant, 1992; Khin et al., 2014). Meanwhile, in the Cenozoic, the collision between the Indian and the Eurasian plates caused the extension of several basins of Thailand. This event provoked rifting-related magmatism as the Cenozoic volcanic rocks and several strike slip faults such as Red River, Three Pagoda, and Mae Ping Faults (Barr and Macdonald, 1978; Junyusuk and Khositant, 1992; Morley, 2014).

## 2.2. Volcanic rocks in Thailand

The volcanic rocks in Thailand have been considered to synchronously form during the subduction, collision and extensional tectonic events. There are two major periods of tectonic evolution in Thailand: 1) Permo-Triassic period and 2) Cenozoic period. In this work, the volcanic rocks which are related with the subduction and collision during the Permo-Triassic period and before, are called as pre-Cenozoic rocks and will be thoroughly focused.

### Pre-Cenozoic volcanic rocks in Thailand

The pre-Cenozoic volcanic rocks were separated into four belts as Chiang Rai-Chiang Mai volcanic belt, Chiang Khong-Lampang-Tak volcanic belts, Nan-Uttaradit-Sa Kaeo suture, and Loei-Phetchabun-Nakhon Nayok volcanic belts (Junyusuk and Khositant, 1992; Kosuwan et al., 2017; Panjasawatwong, 2003; Panjasawatwong et al., 2006).

The Chiang Rai-Chiang Mai (CR-CM) volcanic belt (Fig. 3) extends southward from the Changning-Menglian suture in Yunnan through Chiang Rai and Chiang Mai to Lamphun (Shen et al., 2009; Yang, Mo, and Zhu, 1994). Macdonald and Barr (1978) suggested that the Chiang Mai volcanic belt appears to be mainly basaltic tuffs, agglomerate and lava with olivine-bearing pyroxenite and are probably cumulates. Geochemically, these volcanic rocks are characterized by tholeiitic basalts and generated in an island arc environment. However, Barr and Macdonald (1991) studied

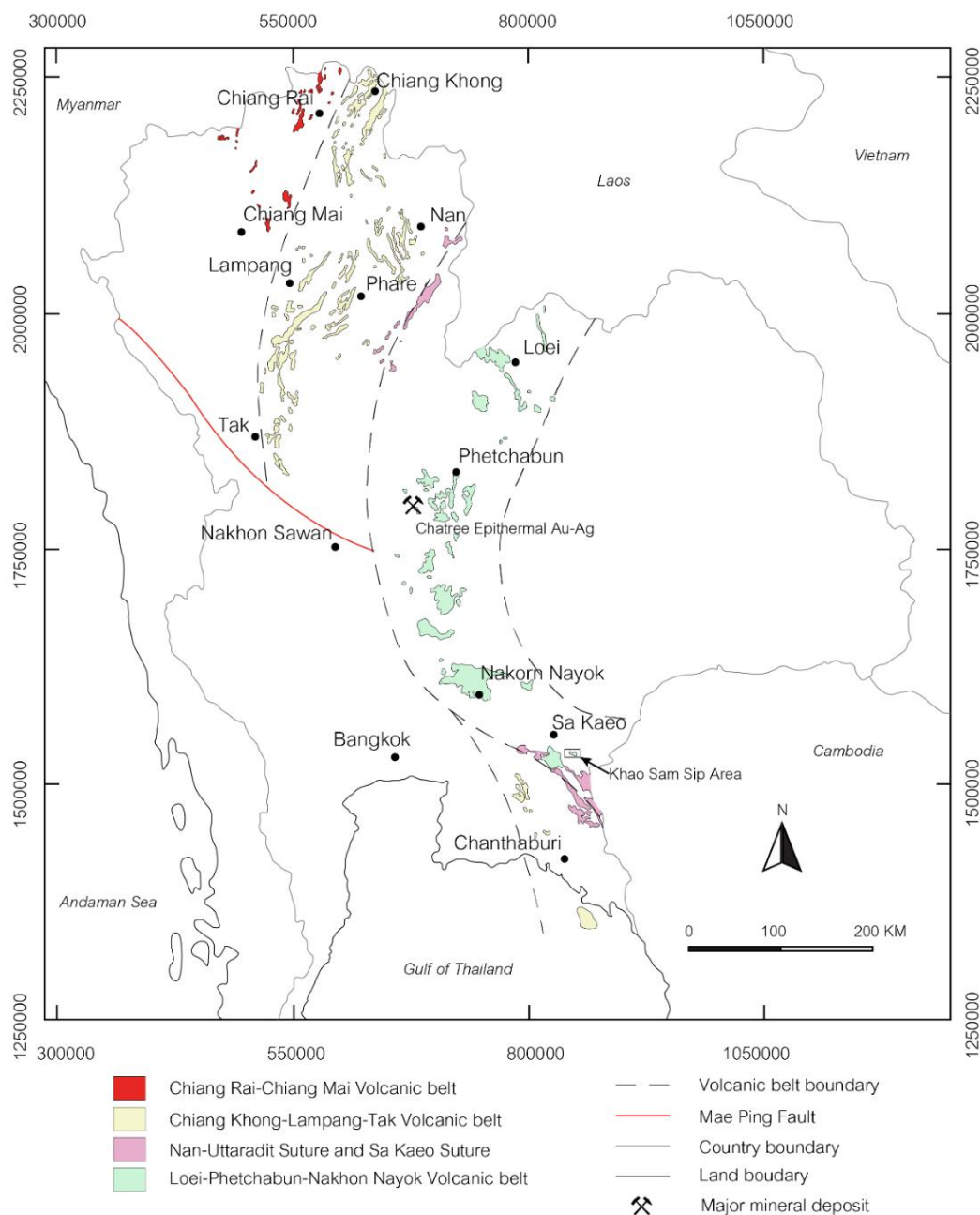


Fig. 3 The distribution of Paleozoic-Mesozoic volcanic rocks in Thailand (after Junyusuk and Khositant (1992); Kosuwan et al. (2017); Panjasawatwong (2003); Panjasawatwong et al. (2006))

these volcanic rocks suggesting they are mainly basaltic composition formed as lava flows, pillow breccia/hyaloclastite, and dykes in an extensional environment and characterized by transitional between tholeiitic and alkalic basalt. Subsequently, Panjasawatwong, Kanpeng, and Ruangvatanasirikul (1995) investigated basaltic lavas in the southern and western Li basin showing transitional tholeiites and alkalic basalt.

This study showed the possible southern extension of the CR-CM volcanic belt. In addition, Phajuy, Panjasawatwong, and Osataporn (2005) studied the volcanic rocks in Phrao area reporting that the rocks here were basaltic lava and dyke rocks. These rocks were interpreted to be formed in a major ocean environment. Meanwhile, Phajuy (2008) has studied in several areas along the Chiang Rai-Chiang Mai volcanic belt and suggested that there are two episodes of volcanism. The first episode was formed in immature back arc basin in the Silurian-Devonian and the second episode was formed in mature back arc basin and a major ocean basin in the Carboniferous to Late Triassic period. Subsequently, Shen et al. (2009); Wang et al. (2017); Zhang et al. (2016) reported that the volcanic rocks in the Chiang Mai zone were dominantly with alkali basalt and minor with the sub-alkalic basalt. These rocks were suggested to be formed in oceanic island environment. In addition, Wang et al. (2017) also reported the  $^{40}\text{Ar}/^{39}\text{Ar}$  ages of  $282.3 \pm 1.4$  Ma from basaltic sample and suggested that the Inthanon zone might represent the main Paleo Tethys suture zone linked with the Changning-Menglian suture zone of Southwest China.

The Chiang Khong-Lampang-Tak (CLT) volcanic belt extends southward from Chiang Rai through Lampang and Phrae to Tak and Eastern of Thailand (Fig. 3) (Barr et al., 2000; Junyusuk and Khositantont, 1992; Sone, Metcalfe, and Chaodumrong, 2012). A possible northern extension of the CLT volcanic belt was reported as the eastern part of the Lincang-Jinghong volcanic belt in Yunnan based on the similar ages of rocks and stratigraphy (Feng et al., 2005; Fontaine et al., 2012; Qian et al., 2017; Yang et al., 1994). Junyusuk and Khositantont (1992) reported that there are two episodes of volcanic activity during Permo-Triassic and Late Triassic to Early Jurassic existed along the Tak-Chiang Khong volcanic belt. Subsequently, many studies were reported to thoroughly identify characteristic and environment of the volcanic rocks in the CLT volcanic belt; for example, Barr et al. (2000); Barr et al. (2006); Panjasawatwong (2003); Qian et al. (2016a, 2016b); Srichan et al. (2010); Srichan, Crawford, and Berry (2009). Barr et al. (2000) characterized the volcanic rocks in Lampang area into Triassic dacitic to rhyolitic with subordinate rocks in andesitic and rare basaltic compositions and

probably erupted in a continental volcanic arc. The age dating of rhyolite sample from Lampang volcanic belt yielded U-Pb zircon age of  $240 \pm 1$  Ma. In addition, Panjasawatwong (2003) studied the Permo-Triassic volcanic rocks in the Chiang Khong area. These rocks were mainly rhyolite, dacite, andesite, basalt and their pyroclastic equivalents such as well-bedded andesite tuff, rhyolitic tuff and agglomerate, conformably sequenced with Permian-Triassic sedimentary rocks in a continental volcanic arc. Barr et al. (2006) suggested that the rhyolitic tuff in the Chiang Khong area was calc-alkalic composition and the age dating of rhyolitic tuff yielded a U-Pb zircon of  $232.9 \pm 0.4$  Ma. These rocks were correlated with Lampang area further to the south and north of Linchang-Jinhong belt in Yunnan; thus, these correlations supported the location of the Paleo Tethys suture along the west of the SFB. Moreover, Srichan et al. (2009) studied the volcanic rocks in the Chiang Khong area and reported that these volcanic rocks comprised of three sub-parallel belts: 1) Western Sub-belts 2) Central Sub-belts and 3) Eastern Sub-belts. The Western Sub-belts and Central Sub-belts were dominantly felsic volcanic sequences and minor of mafic dykes with high-K calc-alkalic composition. Significantly, the fractionation levels of high field strength element contents in the Western Sub-belt lavas have slightly lower than the equivalent rocks from the Central Sub-belt. On the other hands, The Eastern Sub-belt was dominantly mafic lavas and dykes which ranged in composition between E-MORB and back-arc basin basalts. As the result, the mafic rocks in the Chiang Khong area were interpreted to be formed in the continental volcanic arc while the felsic volcanic sequences were alternatively suggested to be formed in the post-collisional extensional setting and yielded the U-Pb of zircon age of 233-220 Ma. Similarly, Qian et al. (2016a, 2016b) reported the U-Pb zircon ages of  $229 \pm 4$  Ma from andesite samples and the U-Pb zircon age of  $230.7 \pm 1.1$  Ma from rhyolite samples which were slightly younger than timing of the continental volcanic arc proposed by Srichan et al. (2009). Subsequently, Qian et al. (2017) studied the volcanic rocks in the Lampang-Denchai area which ranged from intermediate to felsic rocks with calc-alkaline composition. The zircon U-Pb age dating was performed for andesitic and rhyolitic samples yielding  $240.4 \pm 1.7$  Ma and  $240.6 \pm 1.9$  Ma,

respectively. Their geochemical data confirmed the presence of Middle Triassic arc volcanism.

The Late Triassic-Early Jurassic volcanic rocks consist of andesite, rhyodacite, rhyolite and tuff. Volcanic rocks in the Chiang Khong-Lampang-Tak volcanic belts are underlain by non-marine red-beds and overlain by lower Jurassic sedimentary rocks (Junyusuk and Khositant, 1992; Panjasawatwong, 2003). Srichan et al. (2010) reported two representative felsic volcanic rocks yielded U-Pb zircon ages of 186-187 Ma (Late Early Jurassic) in the Nan-Wiang Sa area where inferred as the part of the CLT volcanic belt.

The Nan-Uttaradit-Sa Kaeo (NUS) volcanic belt extends southward from Nan province through Uttaradit to Sa Kaeo (Fig. 3). A possible northern extension of this volcanic belt was reported as Luang Prabang volcanic belt in Lao (Barr et al., 1985). Barr and Macdonald (1987) studied the ophiolitic mafic and ultramafic rocks in the Nan river suture and interpreted that these rocks were formed in a back-arc or inter-arc setting. Subsequently, Panjasawatwong (1993) reported that mafic-ultramafic igneous rocks in the Nan suture occurred as blocks which consisted of ocean-island basalts, back-arc basin basalts and andesites, island-arc basalts and andesites and supra-subduction mafic cumulates in the mélangé during Carboniferous to Permo-Triassic times. Some post-Triassic basaltic lavas were petrochemically examined as alkalic rocks and proposed to be formed in the intraplate continental setting during the Late Cenozoic time. In addition, Chutakositkanon and Hisada (2008) reported the Late Paleozoic blocks in mélangé of the Sa Kaeo-Chanthaburi area which might be correlated with the Nan Suture as an accretionary complex. These blocks were characterized by basaltic pillow lava, hyaloclastite, chert, limestone, and serpentinites formed in oceanic environment, and were collided by the east-dipping subduction during the Uppermost Permian. Meanwhile, Yang et al. (2016) studied zircon U-Pb ages of gabbro and metabasalt from the Nan-Uttaradit suture, and the crystallization ages of rocks yield zircon U-Pb ages of  $311 \pm 10$  and  $316 \pm 3$  Ma, respectively, co-existed with the Ailaoshan-Jinshajiang Ocean in China.

Previous studies suggest that the Nan-Uttaradit Suture represents the Paleotethys ocean; for example, Bunopas and Vella (1983); Singharajwarapan (1994); Singharajwarapan and Berry (2000). However, Hara et al. (2018); Sone and Metcalfe (2008); Ueno and Hisada (2001) suggested that the Nan-Uttaradit Suture might be correlated with the Sa Kaeo Suture and interpreted that this suture represented the Permian back-arc basin.

The Loei-Phetchabun-Nakhon Nayok (LPN) volcanic belt extends southward from Loei through Phetchabun and Nakhon Nayok to Sa Kaeo (Fig. 3). The volcanic rocks in the LPN volcanic belt are composed of lavas and volcanoclastic rocks showing a wide range from felsic to mafic rocks with mainly calc-alkalic composition. This LPN volcanic belt may include erupted products more than one tectonic setting during middle Devonian, Permo-Triassic to late Tertiary. The volcanic rocks in the Loei area can be divided into eastern, central and western sub-belts. The eastern sub-belt consists of lava and pyroclastic of rhyolitic composition underlain by Middle Permian marine limestone and overlain by Phu Kradung formation of the Early Jurassic. The central sub-belt consists mainly of basaltic pillow lava, hyaloclastite and pillow breccia with minor stratified volcanic tuff. The western sub-belt composes mainly of andesite porphyry and andesitic breccia with subordinate rhyolite, rhyolitic tuff and dacite (Junyusuk and Khositantont, 1992; Panjasawatwong et al., 2006). Intasopa (1993) studied the volcanic rocks in the Loei, Phetchabun and Lopburi areas. The rhyolites in eastern sub-belt of the Loei area were suggested to be generated by partial melting of continental crust and having a Rb-Sr age of 374 Ma (Intasopa, 1994) while the ocean floor basalts in the central sub-belt were generated in a spreading center in the ocean. These basalts were proposed to be formed in the younger magmatism with Rb-Sr age of  $361 \pm 11$  Ma and their compositions were tholeiitic basalts and spilitic basalts. Moreover, the basalts, basaltic andesites and andesites from the Phetchabun area were interpreted to be the products of arc volcanism from east dipping subduction under Indochina terrane and have hornblende  $^{40}\text{Ar}/^{39}\text{Ar}$  ages of  $238 \pm 4$  and  $237 \pm 12$  Ma (Intasopa, 1994). Subsequently, Panjasawatwong et al. (2006) studied geochemistry of the central Loei

volcanic rocks such as tholeiitic basalt and calc-alkalic basalt and andesite. The geochemistry and interpretation suggested that these rocks were formed in oceanic island-arc setting and associated with the mid-ocean ridge. Moreover, Khositantont et al. (2008) suggested the two volcanoclastic facies: 1) Ban Na Ngiew volcanoclastic unit and 2) Ban Na Ko volcanoclastic unit located in the northern Loei province. These volcanoclastic units have rhyolitic composition with calc-alkaline affinity and the negative Eu anomalies. Regarding their geochemical properties, Zhao, Qian, and Feng (2016) suggest these rhyolitic rocks are typical arc-related rocks and have the U-Pb zircon age of  $423.7 \pm 2.7$  Ma in accordance with Khositantont et al. (2008).

Junyusuk and Khositantont (1992) have reported that the volcanic rocks in Phetchabun area range from basalt to rhyolite, but basaltic andesite and andesite are most abundant. Andesitic tuff and agglomerate are found to interbed with Middle Permian sandstone and the andesite dykes have been observed to cross-cut the Triassic sedimentary rocks in the Phetchabun basin, these appearances indicated more than one generation of magmatism. Subsequently, Kamvong, Charusiri, and Intasopa (2006) studied petrochemistry of the volcanic rocks in the eastern Wang pong area. These volcanic rocks compose of andesite porphyry, agglomerate and crystal tuff and have mantle source similar to OIB-type mantle in accordance with Intasopa (1993). The well-studied volcanic rocks of LPN volcanic belt are at the area of Phichit-Phetchabun or also known as the Chatree volcanic complex (e.g. Boonsoong, Panjasawatwong, and Metpasopsan (2011); Cumming (2004); Salam (2013)). Cumming (2004) studied the volcanic facies at the Chatree gold mine. The volcanic facies at the Chatree mine are mainly polymictic andesitic lithic breccia which were underlain by a silicified pumice and overlain by feldspar-phyric pumice breccia and siltstone. Minor sedimentary facies were found associating with the polymictic lithic breccia. These facies consist of a volcanogenic sandstone, laminated and commonly carbonaceous siltstone and thinly bedded limestone. The coherent facies at the Chatree mine consist of the andesitic rocks which are conformable with sedimentary bedding, and the andesitic to basaltic rocks which cross-cut the bedding. Subsequently, Boonsoong et al. (2011) studied the

volcanic rocks in the Chon Dean-Wang Pong and suggested that these rocks have composition of tholeiitic andesite/basalt and calc-alkaline andesite with the negative Nb anomalies relative to N-MORB. As the result, the volcanic rocks in the Chon Dean-Wang Pong area were interpreted to be related with volcanic arc setting. The Chatree volcanic complex has been thoroughly studied in volcanic stratigraphic sequence, geochemistry and mineralization by Salam (2013) and Salam et al. (2014). The volcanic stratigraphic sequence comprised of porphyritic andesite unit, polymictic mafic-intermediate breccia unit, volcanogenic sedimentary unit and fiamme breccia unit from the base to the top. This host sequence was intruded by two series of dykes: 1) xenolithic dykes, and 2) basaltic to andesitic dykes. In addition, the geochemical studies suggested that the host volcanic rocks at Chatree comprise two volcanic suites: 1) a more depleted mantle in the Late Permian (258.6 to 250 Ma) (Volcanic Suite 1) and 2) Volcanic Suite 2 in the Early Triassic (250 to 247 Ma). The volcanic suite 1 was proposed to be formed just after the beginning of subduction in the island arc setting while the volcanic suite 2 was proposed to be formed during ongoing subduction.

The volcanic rocks of LPN volcanic belt, which extended eastward to the Phai Sali and southward to Saraburi, Nakorn Nayok and Sa Kaeo areas (Fig. 3), are insufficiently documented in the literatures. Junyusuk and Khositantont (1992) reported that volcanic rocks in Phai Sali are mainly rhyolitic and minor andesitic to basaltic compositions. The rhyolitic rocks occur as flow and tuff overlain by basaltic andesitic flow. These volcanic rocks were suggested to erupt after Middle Permian due to their occurrences which flowed over and crosscut the Middle Permian limestone. In addition, the Saraburi-Prachinburi pre-Jurassic volcanic rocks are also reported by Junyusuk and Khositantont (1992) that these rocks consist of porphyritic rhyolite, porphyritic basaltic andesite and their pyroclastic equivalents. These rocks were found to be underlain and crosscut Permian limestone, and overlain by Jurassic sedimentary rocks, so they were suggested to be formed in Middle Permian or after and prior to Jurassic ages. Meanwhile, Arboit et al. (2016), who studied geochronology and geochemistry of mafic and intermediate dykes from the Khao Khwang Fold-Thrust Belt, reported that mafic

dykes have tholeiitic to mostly calc-alkalic composition with the negative Nb anomalies. Their geochemical characteristics suggest that these dykes were formed in the volcanic arc setting and quite similar to the mafic dykes from the Chiang Khong volcanic suite and LPN volcanic belt. The  $^{40}\text{Ar}/^{39}\text{Ar}$  age dating and a U-Pb zircon age dating were examined, as a result,  $^{40}\text{Ar}/^{39}\text{Ar}$  age of  $255 \pm 6$  Ma (Early Triassic) from the andesitic dykes and U-Pb zircon age  $207 \pm 2$  Ma (Late Triassic) from the rhyolitic rocks were reported (Arboit et al., 2016). Moreover, the least-documented volcanic rocks of LPN volcanic belt is at the Sa Kaeo area. Junyusuk and Khositantont (1992) reported that these volcanic rocks consist of Permian-Triassic aphanitic rhyolite, rhyolite, rhyolite porphyry, rhyolitic tuff, and subordinate andesite porphyry and aphanitic andesite. However, the petrological and geochemical data of these volcanic rocks need to be constrained thoroughly for giving more details of the Loei-Phetchabun-Nakorn Nayok volcanic belt.

### 2.3. An overview geology of the study area

The study area is Khao Sam Sip area in the Sa Kaeo Province showing the distribution of rocks of LPN volcanic belt. The geological map of Batdambang ND 48-9 (Scale 1:250,000) was compiled by Polprasit et al. (1985) (Fig. 4). The area is made up of igneous and sedimentary rocks with Triassic ages and unconsolidated sediments of Quaternary age.

The Triassic volcanic rocks are constituted largely by pyroclastic rocks such as flow breccias associated with lapilli tuff, laminated and cross bedded tuff, with minor basaltic to andesitic lava flows, agglomerate and intrusions of gabbro, pyroxenite and hornblende including epidotization and bearing quartz lodes (Polprasit et al., 1985).

The Triassic sedimentary rocks occur in the southern part of the study area, and comprise the Triassic conglomerate (Tr) and the Pong Nam Ron Formation (Trp) (Chaodumrong, 1992; Polprasit et al., 1985). The Triassic conglomerate unconformably overlies the Permian Ratburi Group and consists of conglomerate with sub-rounded to rounded pebbles and boulders of granite, andesite, chert, limestone, slate and rhyolite.

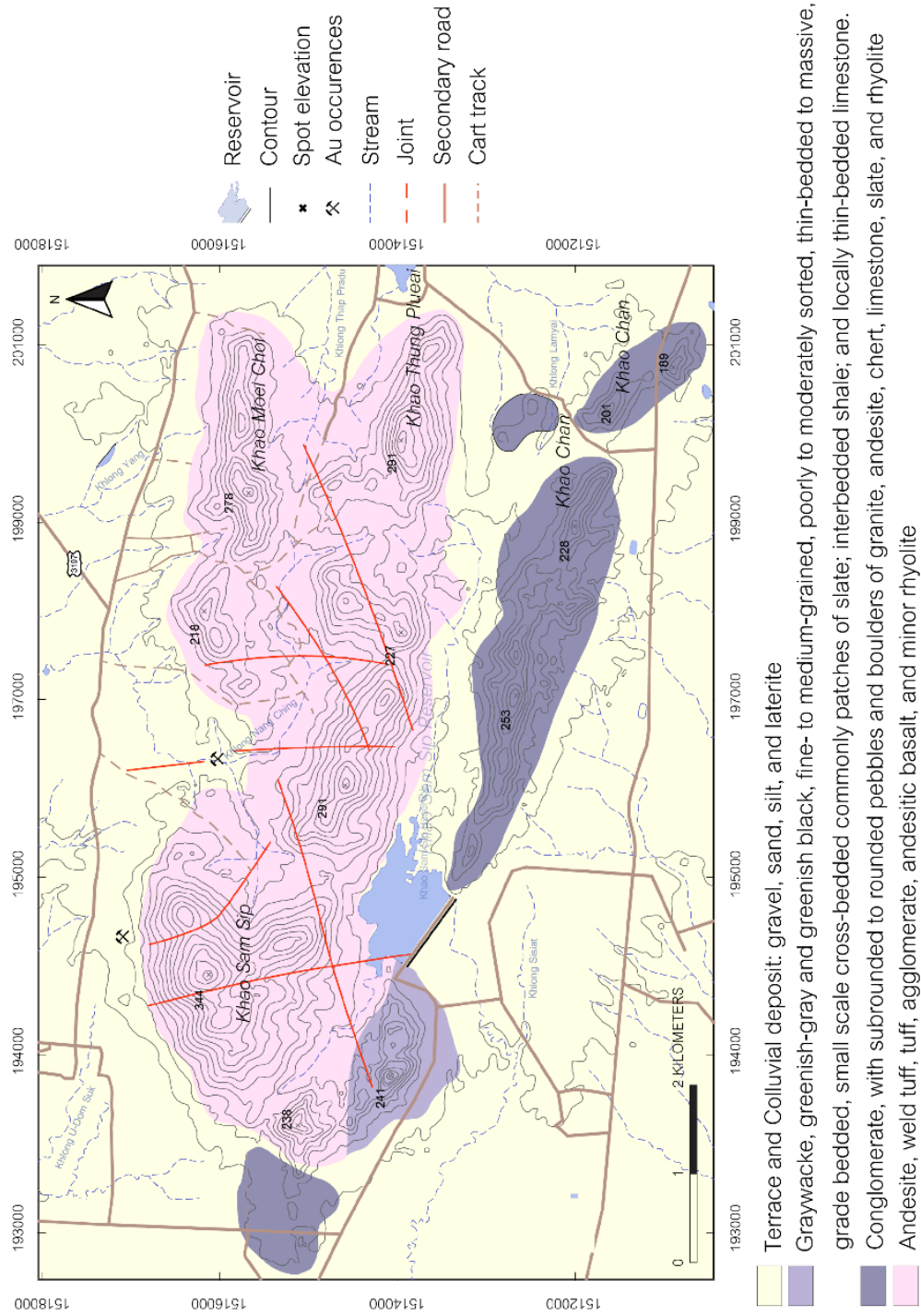


Fig. 4 Regional geology of the Khao Sam Sip area (Modified from Chaodumrong (1992); Polprasit et al. (1985)).

The Pong Nam Ron Formation overlies conformably the Triassic conglomerate and consists of greenish-gray and greenish-black fine- to medium-grained graywacke. They are poorly to moderately sorted, thin-bedded to massive, grade bedded, small scale cross-bedded. Patches of shale, interbedded shale, and thin-bedded limestones have been locally observed.

The Quaternary sediments in this area are distributed along drainage patterns. These sediments form as terrace and colluvial deposits (Polprasit et al., 1985). The terrace and colluvial deposits include gravel, sand, silt, and laterite.

#### 2.4. Economic Potential

The Khao Sam Sip area has favorable features of hosting economic metallic minerals and precious metals. The history of gold mining can be dated back for no less than a hundred years, and villagers have worked on placer gold by panning. Yet, there were small underground mines in several locations within the Khao Sam Sip area, for example, Ban Bo Nang Ching and Khao Sam Sip (Department of Mineral Resources, 2011).



## CHAPTER 3

### VOLCANIC PETROGRAPHY

#### 3.1. Introduction

This chapter describes occurrence, lithology and petrography, relation between the volcanic rocks and mineralization in the Khao Sam Sip area. There are mainly four rock units in the study area. Rock names which are found in drill cores and field outcrops are described based on their textures (grain size, sorting and shape) and mineral constituents.

#### 3.2. Method of study

Representative samples of rock units were collected from the field (e.g. Unit 1, Unit 2, Unit 3 and Unit 4) covering the areas of Khao Sam Sip, Khao Moei Choi and Khao Thung Plueai (Fig. 5). Hand specimen and thin sections of the rock samples were selected and studied microscopically to characterize primary mineral compositions, alterations and textures representing each volcanic rock at the Department of Geological Sciences, Faculty of Science, Chulalongkorn University. The lithology and petrography were described and discussed in the following sections.

#### 3.3. Petrography

##### Unit 1: Basalt-andesite unit

The basalt-andesite unit is the lowest part of the sequence (Fig. 5) consisting of olivine-pyroxene-plagioclase basalt, pyroxene basalt, hornblende-plagioclase andesite and plagioclase andesite.

##### Olivine-pyroxene-plagioclase basalt

Olivine-pyroxene-plagioclase basalt is exposed in quarry (Fig. 6A, B) and intersected in a drill hole (BDH-3) of the north Khao Moei Choi and the Khao Sam Sip. The olivine-pyroxene-plagioclase basalt is greenish grey to greenish brown and is characterized by the uniform distribution of olivine, pyroxene and plagioclase phenocrysts (Fig. 6C). In the quarry, the rock is contacted at the top to pyroxene basalt which shows low degree of alteration and sulfide mineralization. The relationship

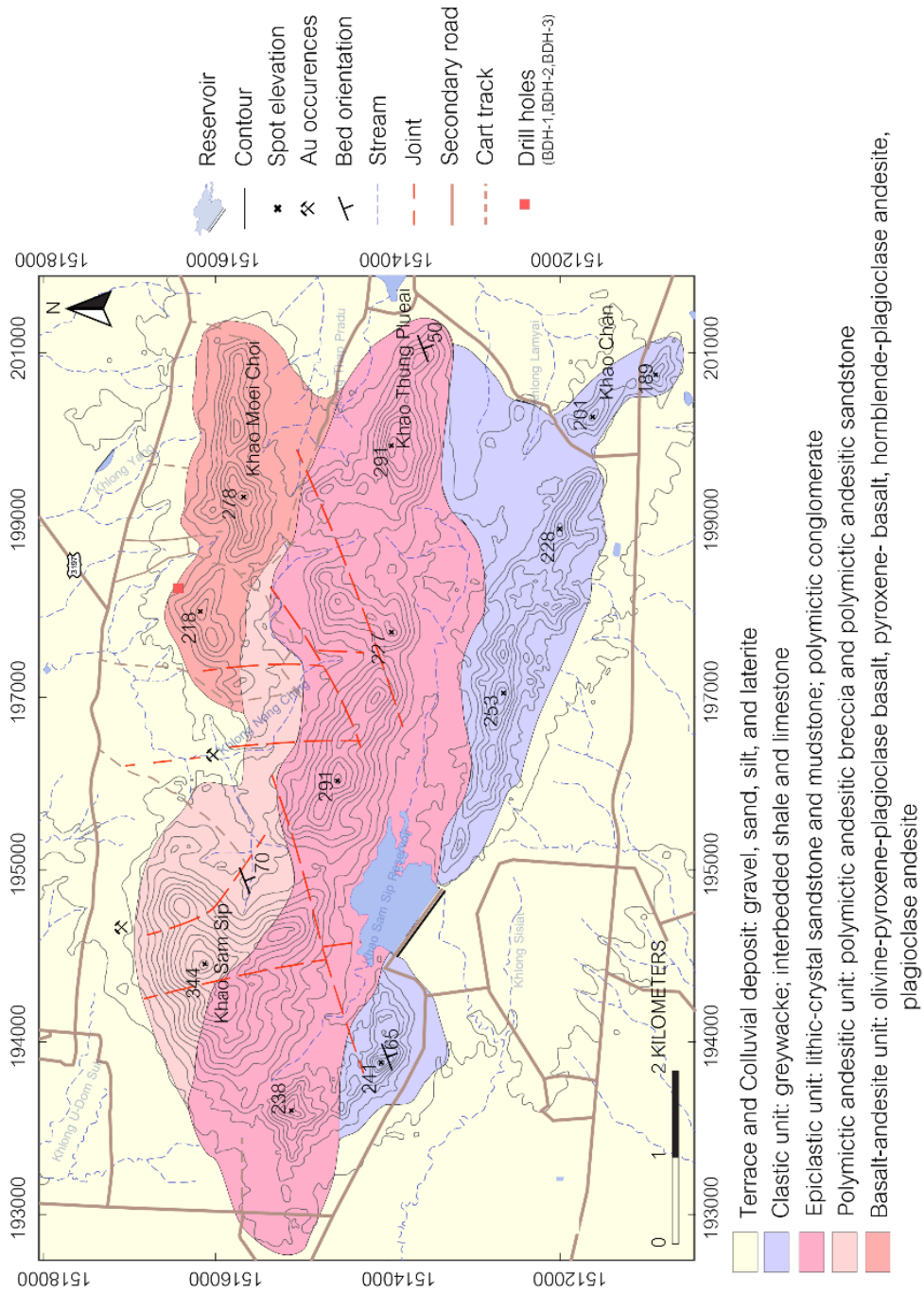


Fig. 5 Geological map of volcanic rocks and sedimentary rocks in the Khao Sam Sips area.

between olivine-pyroxene-plagioclase basalt and other coherent (coherent means lava) rock does not show in the survey area and drill cores due to high degree weathering of outcrops. However, the olivine-pyroxene-plagioclase basalt shows in the polymictic breccia as high altered greenish brown blocky clasts. Thus, the olivine-pyroxene-plagioclase basalt was erupted before the pyroxene basalt and polymictic breccia.

Hand specimen has greenish grey to greenish black color and some metallic-oxide tarnishes on weathering surface. Phenocrysts are 2-3 mm subhedral plagioclase and 2-7 mm subhedral pyroxene. The pyroxene is partially replaced by epidote and chlorite. Pyrites are also distributed in the groundmass and veinlets. Tiny veins (sizes up to 2 mm thick) of chlorite, epidote, quartz and calcite are present.

The olivine-pyroxene-plagioclase basalt has fine-grained showing porphyritic texture (Fig. 6D). The groundmass dominantly consists of fine-grained (<1 mm), acicular plagioclase crystals with secondary minerals such as pyrite and chalcopyrite. It shows both trachytic and felted textures. Plagioclase in groundmass is subhedral and has a lath shape while plagioclase phenocrysts have subhedral to euhedral crystals (size up to 0.1 mm). Olivine phenocrysts are subhedral (sizes up to 3 mm across) and rounded edges. Some olivine crystals have been replaced by serpentine/chlorite and show euhedral opaque mineral inclusions. Clinopyroxene phenocrysts are euhedral (sizes up to 3 mm across) and partially replaced by chlorite/serpentine.

#### **Pyroxene basalt**

Hand specimen of pyroxene basalt has greenish grey to greenish brown color showing porphyritic texture. Phenocrysts are 2-3 mm euhedral to subhedral pyroxene with slight replacement of chlorite (Fig. 7A).

The pyroxene basalt has fine-grained showing moderately to strongly seriate texture (Fig. 7B). The groundmass dominantly consists of fine-grained (<1 mm), acicular plagioclase crystals and prismatic pyroxene and opaque minerals of titanomagnetite. Groundmass clinopyroxene is subhedral to euhedral crystal and is intergranular to plagioclase laths. Chlorite and small amounts of amphibole are slightly replaced the

groundmass clinopyroxene. Clinopyroxene phenocrysts are euhedral (sizes up to 3 mm across) and slightly replaced by chlorite/serpentine.

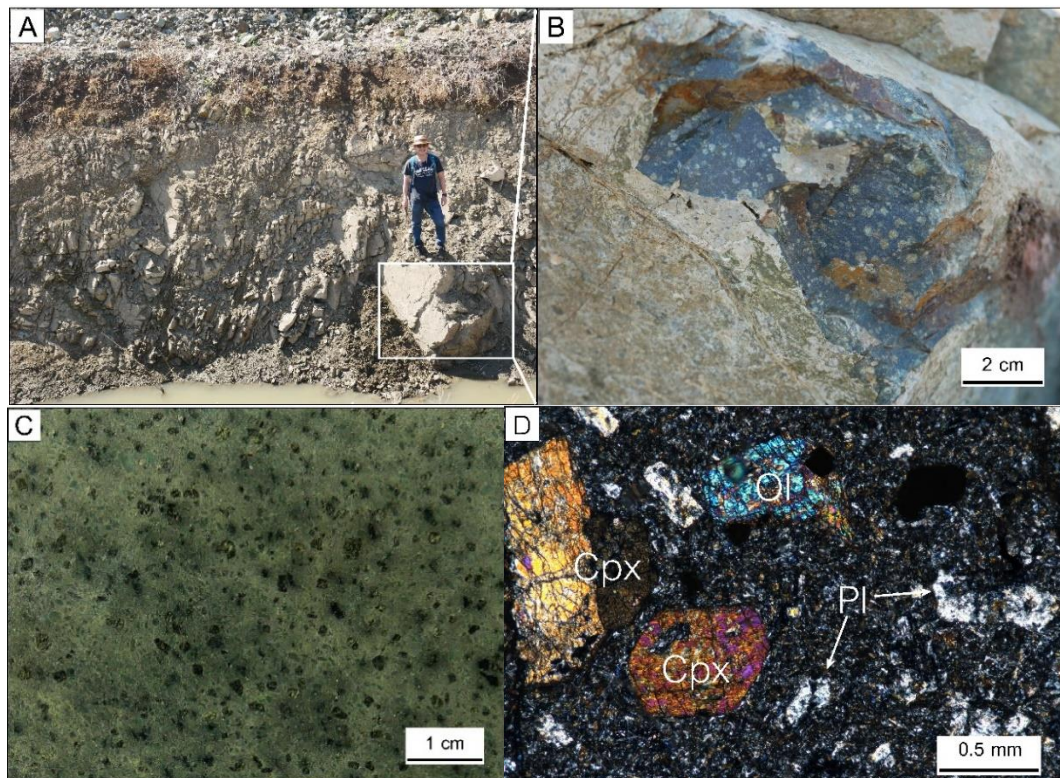


Fig. 6 Characteristics of olivine-pyroxene-plagioclase basalt and pyroxene basalt found at quarry and diamond drill core (BDH-3) at the north of Khao Moei Choi. A) Photograph of pit wall showing the olivine-pyroxene-plagioclase basalt and the pyroxene basalt on the pit wall of quarry. B) Photograph of Sample from the outcrop of olivine-pyroxene-plagioclase basalt showing dominated olivine phenocrysts. C) Photograph of hand specimen of olivine-pyroxene-plagioclase basalt showing olivine and pyroxene phenocrysts. D) Photomicrograph of olivine-pyroxene-plagioclase basalt showing plagioclase-rich groundmass with olivine, pyroxene and plagioclase phenocrysts.

#### Hornblende-plagioclase andesite

Hornblende-plagioclase andesite is exposed on surface in the north of Khao Moei Choi (Fig. 5) and intersected in drill holes (BDH-1, BDH-2 and BDH-3). The hornblende-plagioclase andesite shows greenish grey color and is characterized by porphyritic texture (Fig. 8A). In the drill cores, the hornblende-plagioclase andesite shows sharp contact with the plagioclase andesite. Moreover, the hornblende-plagioclase andesite is 5-7-meter-thick and crosscut by several quartz veins. Thus, the

hornblende-plagioclase andesite is younger than plagioclase andesite by law of crosscutting relationships.

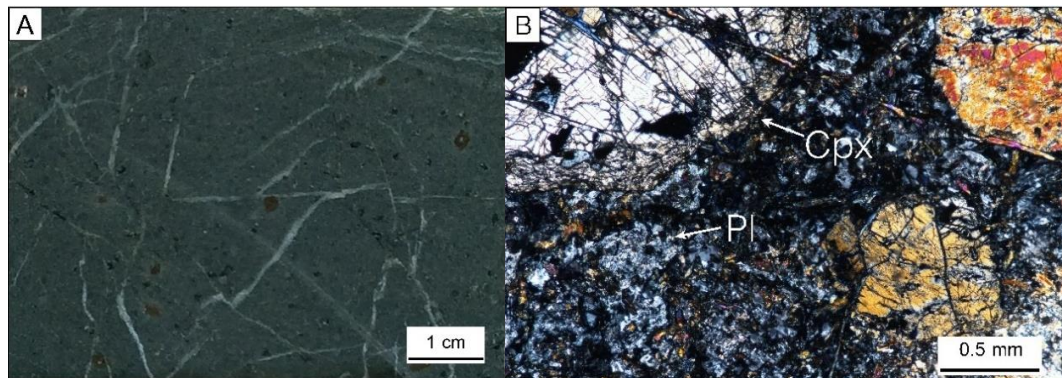


Fig. 7 Characteristics of pyroxene basalt found at quarry at the north of Khao Moei Choi. A) Photograph of hand specimen of pyroxene basalt showing pyroxene phenocrysts (black) and calcite veinlets. B) Photomicrograph of pyroxene basalt showing groundmass consisting of plagioclase with pyroxene phenocrysts.

In hand specimen, it has greenish grey to greenish black (Fig. 8A). The hornblende-plagioclase andesite has fine-grained groundmass showing aphyric texture. Major constituents of groundmass are plagioclase with minor hornblende and pyroxene. The pyroxene crystals are partly replaced by chlorite. Opaque minerals are also distributed in the groundmass, particularly close to quartz veins and veinlets. Tiny veins (sizes up to 2 mm thick) of chlorite, epidote, quartz and calcite are present.

Under microscope the hornblende-plagioclase andesite has fine-grained showing seriate texture (Fig. 8B). Groundmass is dominantly consisted of fine-grained (<1 mm) acicular plagioclase crystals, minor hornblende, pyroxene, opaque minerals and pyrite. Groundmass shows ophitic textures of lath shape plagioclase. Mafic minerals (mainly hornblende) are partly altered by chlorite and feldspar altered to sericite. The plagioclase phenocrysts/microphenocrysts are moderately to highly replaced by sericite and calcite. Hornblende phenocrysts have subhedral to anhedral crystals ranging in sizes from 0.1 to 0.2 mm. Clinopyroxene phenocrysts are anhedral to euhedral ranging in sizes from 0.1 mm across.

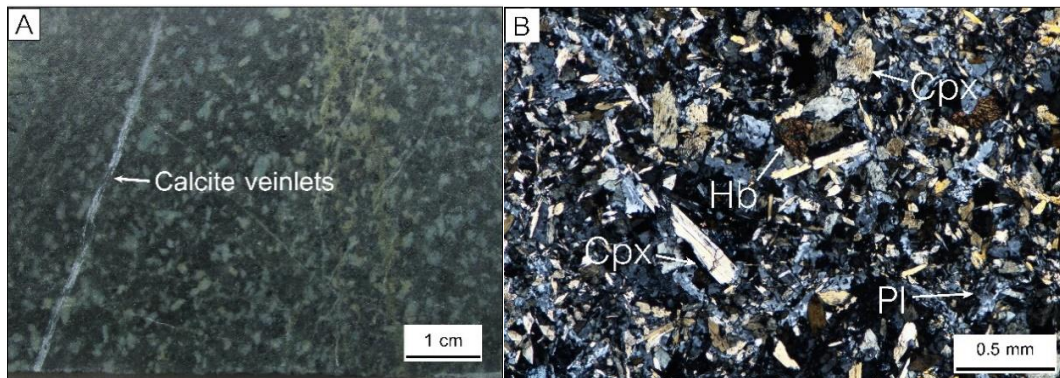


Fig. 8 Characteristics of hornblende-plagioclase andesite from drill core in the north of Khao Moei Choi area. A) Photograph hand specimen of hornblende-plagioclase andesite showing slightly porphyritic texture with calcite veinlets. B) Photomicrograph of hornblende-plagioclase andesite showing groundmass plagioclase with pyroxene, and hornblende crystals.

#### Plagioclase andesite

Plagioclase andesite and its monomictic breccia are exposed on surface in the north of Khao Moei Choi (Fig. 9A) and found in drill cores (BDH-1 and BDH-2). The plagioclase andesite explodes as a small outcrop and is characterized by the uniform distribution of plagioclase and small amount of pyroxene phenocrysts (Fig. 9B). In the diamond drill core, the plagioclase andesite shows strong silicified and sharp contact with hornblende-plagioclase andesite.

In hand specimen, the plagioclase andesite is greenish grey to greenish black (Fig. 9C). The rock has fine-grained groundmass showing moderately to strongly porphyritic texture. Phenocrysts are plagioclase and pyroxene dominated. Plagioclase phenocrysts are moderately altered to calcite and sericite while some pyroxenes are partly replaced by chlorite. Pyrite is common opaque mineral and distributes in the groundmass and quartz veinlets. Most veinlets are composed of chlorite, epidote, quartz and size up to 2 mm thick.

Petrographically, the plagioclase andesite has fine-grained showing porphyritic texture (Fig. 9D) in which pyroxene is major phenocrysts. The groundmass dominantly consists of fine-grained (<1 mm) acicular plagioclase crystals showing trachytic textures of lath shape plagioclase and are partly altered to sericite. Plagioclase phenocrysts are

subhedral to euhedral with sieve textures and embayed outlines and sizes up to 2 mm across. In some samples, the plagioclase phenocrysts are moderately to highly altered to fine white mica and sericite. Clinopyroxene phenocrysts are anhedral to euhedral, (grain sizes up to 2.5 mm across). Moreover, some clinopyroxene grains show zoning and sieve textures, or contain plagioclase inclusions.

#### **Monomictic breccia**

The monomictic breccia is found in the diamond drill cores and float rocks (Fig. 9B) which is characterized by a jigsaw-fit texture and high concentration of large blocky clasts with clast-supported. The rocks are several meters thick (5-10 m) in the drill cores (BDH-1 and BDH-2) which are crosscut by hornblende-plagioclase andesite and quartz veins. The small outcrops and float rocks distribute around Khao Moei Choi.

The monomictic breccia is clast-supported with a coarse sand- to silt- sized feldspar and pyroxene phyric greenish black matrix (Fig. 9C). The matrix has the same composition as the clasts showing phenocrysts with flow orientations in some samples. The clasts are very angular ranging in size from 2 to 10 cm. Some samples show vesicles filled up with secondary quartz and calcite.

Under microscope, the monomictic breccia contains 1-2 mm plagioclase and pyroxene phenocrysts in a fine-grained plagioclase-phyric groundmass. In addition, the groundmass composes of cumulated altered plagioclase and vesicles (Fig. 9E).

#### **Unit 2 Polymictic andesitic unit**

This unit is mainly distributed at the south of the Khao Moei Choi and the north of Khao Sam Sip and extends to the north of Khao Thung Plueai area (Fig. 5). It consists of polymictic andesitic breccia and polymictic andesitic sandstone.

#### **Polymictic andesitic breccia and polymictic andesitic sandstone**

The outcrops of this unit have been observed around Khao Sam Sip area (Fig. 10A). The polymictic breccia has matrix-supported with a coarse sand to silt sized particles showing 1 to 2 mm feldspar, lithic fragments and minor glass devitrified. The clasts are subangular to angular ranging from 2 to 15 cm. They are mainly 2-10 cm

andesitic breccia, 5-10 cm gabbro and 2-5 cm greenish grey mudstone clasts (Fig. 10B). Some outcrops are moderately to highly deformed. Quartz veins have size up to 10 cm and are commonly found in the unit.

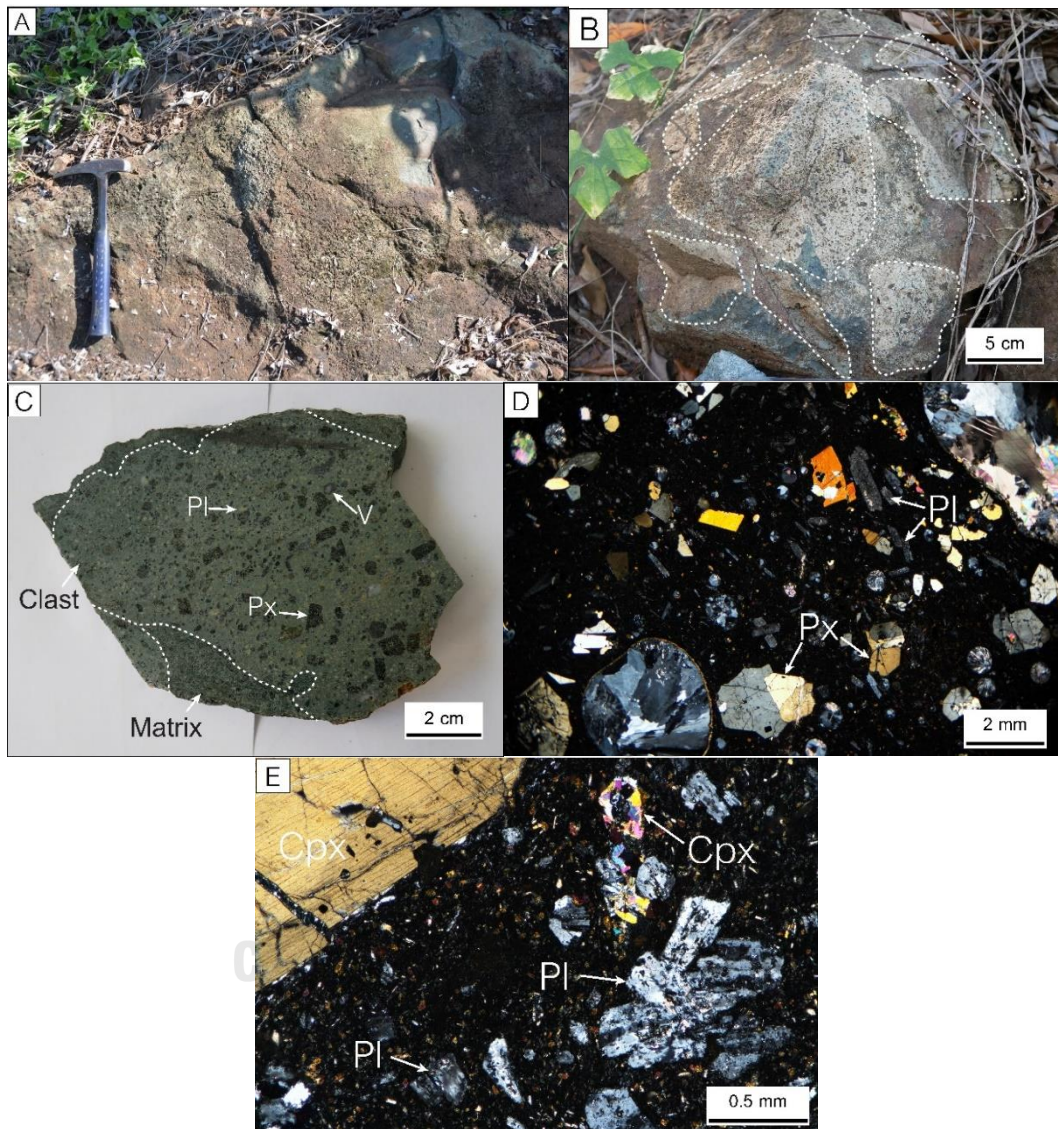


Fig. 9 Characteristics of plagioclase andesite from drill core and outcrop in the north of Khao Moei Choi. A) Photograph of outcrop of plagioclase andesite at the north of Khao Moei Choi. B) Photograph of float rock of monomictic breccia showing clast supported. C) Hand specimen showing blocky clasts of plagioclase andesite. D) Photomicrograph from clast in Fig. 9C showing groundmass and phenocryst of pyroxene (Px), plagioclase (Pl) with quartz and calcite. E) Photomicrograph from matrix in Fig. 9C showing groundmass and phenocrysts of clinopyroxene (Cpx) and plagioclase (Pl).

Petrographically, the matrix consists of plagioclase, pyroxene and rock fragments and glasses (Fig. 10C). The glasses in matrix are moderately devitrified and partly altered to sericite and chlorite. The andesitic breccia shows mainly plagioclase and clinopyroxene phenocrysts with vesicles (Fig. 10D). Some of the andesitic breccia shows glassy lenses with flame-like shapes or fiamme and vesicle filled up with secondary quartz. In addition, gabbroic breccia shows phaneritic texture and consist mainly of orthopyroxene and clinopyroxene (Fig. 10E).

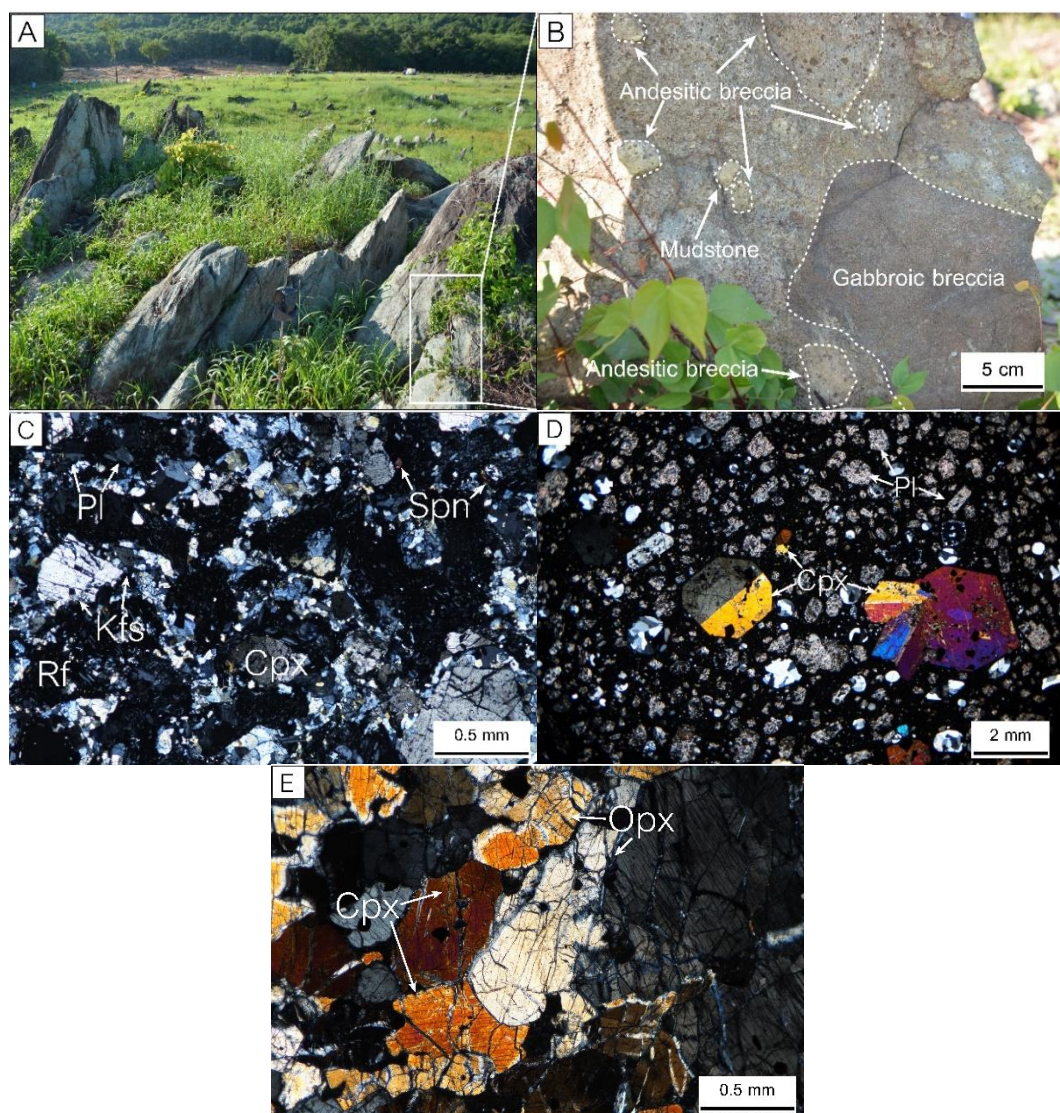


Fig. 10 Characteristics of polymictic andesitic breccia. A) Photograph of polymictic breccia and polymictic sandstone outcrop located at the north of the Khao Sam Sip B) Photograph of polymictic breccia outcrop showing clasts of gabbro and andesite. C) Photomicrograph of matrix of polymictic

breccia consisting of plagioclase (Pl), K-feldspar (Kfs), clinopyroxene (Cpx), sphene (Spn) and rock fragments (Rf). D) Photomicrograph of andesitic breccia clast consisting of plagioclase (Pl) and clinopyroxene (Cpx) phenocrysts. E) Photomicrograph of gabbro clast consisting of orthopyroxene (Opx) and clinopyroxene (Cpx).

### **Unit 3 Epiclastic unit**

This unit is mainly distributed at in the valley of Khao Sam Sip extending to Khao Thung Plueai (Fig. 5). It consists of lithic-crystal sandstone and mudstone and polymictic conglomerate.

#### **Lithic-crystal sandstone and mudstone**

The lithic-crystal sandstone and mudstone occurs as 3 meters height outcrop at the Khao Thung Plueai showing massive sandstone and sandstone interbedded with laminated siltstone and mudstone (Fig. 11A). It has NW-SE strike with 50-degree dipping angle to the southwest.

Hand specimen of lithic-crystal sandstone is greenish grey (Fig. 11B). This rock is fine-grained to medium-grained with upward gradation of grain size. It consists of plagioclase, rock fragments with minor quartz. For the mudstone, which is interbedded with the sandstone shows light green layer with thin beds ranging from 2 mm to 1 cm (Fig. 11C).

The sandstone consists of subhedral plagioclase feldspar crystals and fragments, subangular to angular quartz grains, basaltic lithic fragments ranging in sizes from 1 to 1.5 cm across and mudstone (Fig. 11D). The grain size ranges from fine- to medium-grained with gradation. The silty and mudstone layers generally occur with laminated greyish green bands and consists of mud and very fine-grained crystal fragments. Some laminated layers show dissemination of pyrite.

#### **Polymictic conglomerate**

The polymictic conglomerate occurs in the southern part of Khao Sam Sip as small outcrops (Fig. 12A). This conglomerate is mixed of volcanic and non-volcanic clasts consisting of basaltic rock, minor granite and mudstone clasts in medium-sand

matrix-supported (Fig. 12B). The clasts have size ranging from granule to boulder sized, rounded clasts and poorly sorting.

Petrographically, the matrix consists dominantly of medium- to coarse-grained quartz, mafic minerals and lithic fragments as basaltic rocks and mudstone (Fig. 12C). The grains are angular, low sphericity and highly altered to chlorite and epidote. The matrix resembles the lithic-crystal sandstone.

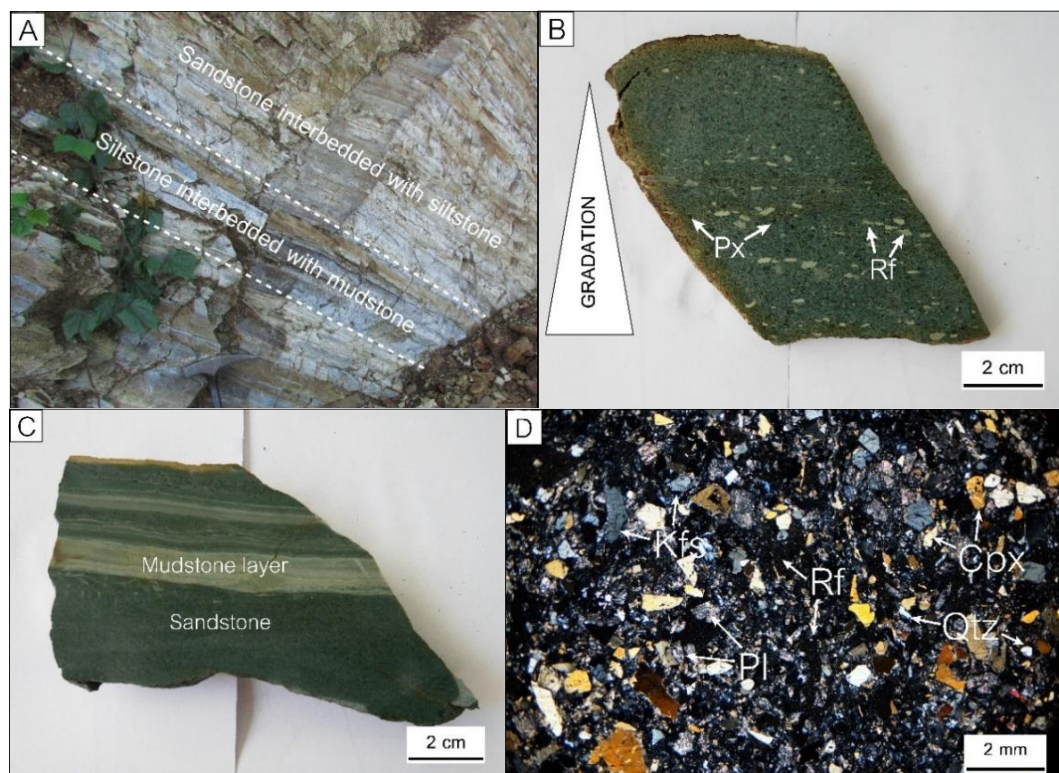


Fig. 11 Characteristics of lithic-crystal sandstone and mudstone. A) Photograph of outcrop located at the Khao Thung Plueai showing sandstone interbedded with siltstone and mudstone. B) Photograph of hand specimen of lithic-crystal sandstone showing gradation in grain size. C) Photograph of hand specimen of lithic-crystal sandstone and mudstone showing sandstone interbedded with mudstone layers. D) Photomicrograph of lithic-crystal sandstone consisting of plagioclase fragments (Pl), K-feldspar (Kfs), quartz (Qtz), rock fragments (Rf) and clinopyroxene (Cpx).

#### Unit 4 Clastic unit

This unit is mainly distributed in the south of Khao Sam Sip and extends to Khao Chan (Fig. 5). It consists of limestone and greywacke interbedded shale. The limestone has been observed in the field while the grey wacke interbedded shale that is

suggested to be Phong Nam Ron formation has not been observed during the field investigation

### Limestone

Limestone occurs in the southern part of Khao Sam Sip as a tall mountain (Fig. 13A). This limestone has grey to dark grey color with no fossil (Fig. 13B). It ranges in thickness from 5 to 10 cm of beds showing foliated texture by deformation



Fig. 12 Characteristics of polymictic conglomerate. A) Photograph of polymictic conglomerate outcrop located at the north of the Khao Sam Sip showing clasts of granite, basaltic rock fragments. B) Photograph of hand specimen of polymictic conglomerate showing clasts of basaltic rock fragments, clasts of mudstone and quartz pebble. C) Photomicrograph of polymictic conglomerate showing clast of basaltic rock in sandstone matrix which consists of quartz (Qtz), plagioclase (Pl), K-feldspar (Kfs), Clinopyroxene (Cpx) and rock fragments (Rf).

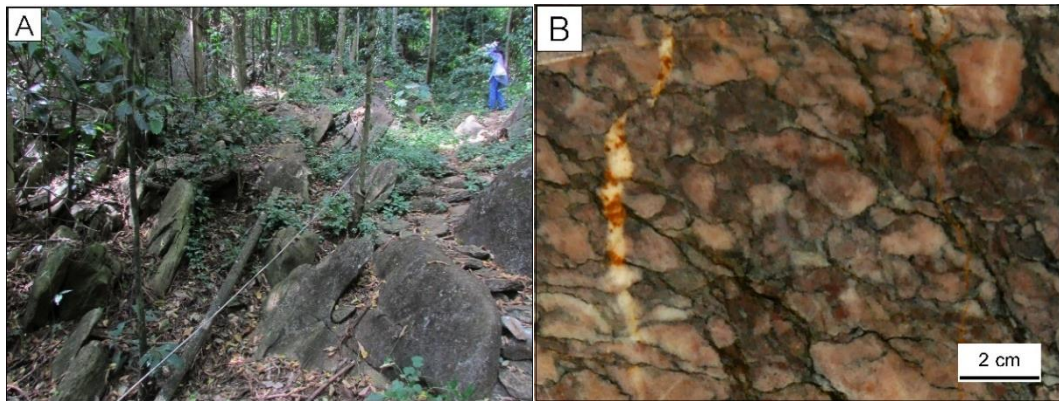


Fig. 13 Limestone outcrop located at the south of Khao Sam Sip A) Photograph of bedded limestone. B) Photograph of limestone hand specimen showing deformed texture.

### 3.4. Interpretation

The coherent lava (Unit 1: Basalt and andesite unit) is interpreted to be extruded as lava or syn-volcanic intrusion which has mafic component and shows massive of fine-grained lavas in the proximal part of the center of intrusions and the monomictic breccia as autobreccia in the distal part associated with its coherent volcanics. The polymictic andesitic breccia and sandstone (Unit 2: Polymictic andesitic unit) occurred in the Khao Sam Sip area and extended to the northern of Khao Thung Plueai. They are characterized by volcanic and non-volcanic clasts with matrix supported. Clasts of the polymictic breccia are interpreted to have transported from distal part due to sedimentary processes and deposited nearby the area of volcanic activity as the matrix is composed of devitrified glasses. The lithic-crystal sandstone and mudstone (Unit 3: Epiclastic unit) occurred in the southwestern part of the Khao Sam Sip area and the Khao Thung Plueai. The lithic-crystal sandstone has been interpreted to deposit nearby the source rock because of its composition of mainly crystal and lithic fragments. The interbedded sandstone with the laminated mudstone and siltstone suggests the sedimentary processes via water in low energy environment. The polymictic conglomerate (Unit 3: Epiclastic unit) is characterized by volcanic and non-volcanic clasts with matrix supported. The clasts have varied compositions and are rounded edge and well-sorted and their matrix consists of crystal and lithic fragments in medium grain sized. These rocks are interpreted to have been formed by weathering and erosion

processes due to the transportation features after the volcanism. Sedimentary rocks (Unit 4: Clastic unit) are mainly mudstone occurred in inter-mountain and limestone occurred as high mountain in the southwestern Khao Sam Sip area. The sedimentary rocks are interpreted to have formed after the formation of volcanic rock units due to its orientation. Furthermore, the rock units in the Khao Sam Sip area show slight deformation feature especially near shear zones which should have happened after their depositions.

Overall, the coherent lavas (Unit 1) in the Khao Sam Sip area is suggested to be the lowest unit which have erupted before other units (Unit 2, 3, 4). Subsequently, the polymictic breccia and polymictic sandstone (Unit 2) were deposited, and then eroded and deposited again as the lithic-crystal sandstone interbedded with the laminated mudstone and siltstone (Unit 3). Meanwhile, the polymictic conglomerate was deposited with several sources and overlain by sedimentary rocks such as limestone and shale. The Unit 2 might have been deposited by the sedimentary processes during the active volcanism while the Unit 3 and the Unit 4 might have been deposited after the cease of volcanism. Lastly, all of the rock units were undergone the deformations.

## CHAPTER 4

### GEOCHEMISTRY

#### 4.1. Introduction

This chapter describes the geochemistry of the basalt andesite unit in the Khao Sam Sip area. The objective of this study is to classify the volcanic rocks, understand how the geochemistry of the rocks has been affected by crystal fractionation, magma affinity and to constrain the tectonic setting of the rocks based on their whole rock geochemical analysis.

#### 4.2. Sampling and analytical methods

##### 4.2.1. Sample preparation

The least-altered samples of the basalt andesite unit were selected for whole rock geochemical analysis. There are four rock types: 1) olivine-pyroxene-plagioclase basalt, 2) pyroxene basalt, 3) hornblende-plagioclase andesite and 4) plagioclase andesite. The rock samples from Units 2 and 3 were not selected because their polymictic and mixed provenances are unsuitable for examine.

Twenty-four volcanic rock samples were selected from the drill cores (BDH-1, BDH-2, BDH-3) and five samples were selected from outcrops in the Khao Sam Sip area (Fig. 14). The samples were firstly examined for their lithology and mineralogy under the microscope, and then the least-altered samples were chosen for whole rock geochemical analysis. Fourteen of the twenty-nine samples were further analyzed for trace elements and rare earth elements (REE).

The chosen samples were needed to be cleaned and devoid of veins, vesicles, amygdales, xenocrysts and xenoliths. They were prepared by cutting off the weathering surface, and then splitting and crushing into small chips by Rocklabs Hydraulic Splitter and Jaw Crusher. Then, the cleaned rock chips were divided by quartering into 25 – 30 g and were pulverized by Rocklabs Tungsten Carbide Ring Mill. The crushing and the milling processes were performed at the Department of Geology, Chulalongkorn University, Thailand, and then transferred to the Department of Mineral Resources,

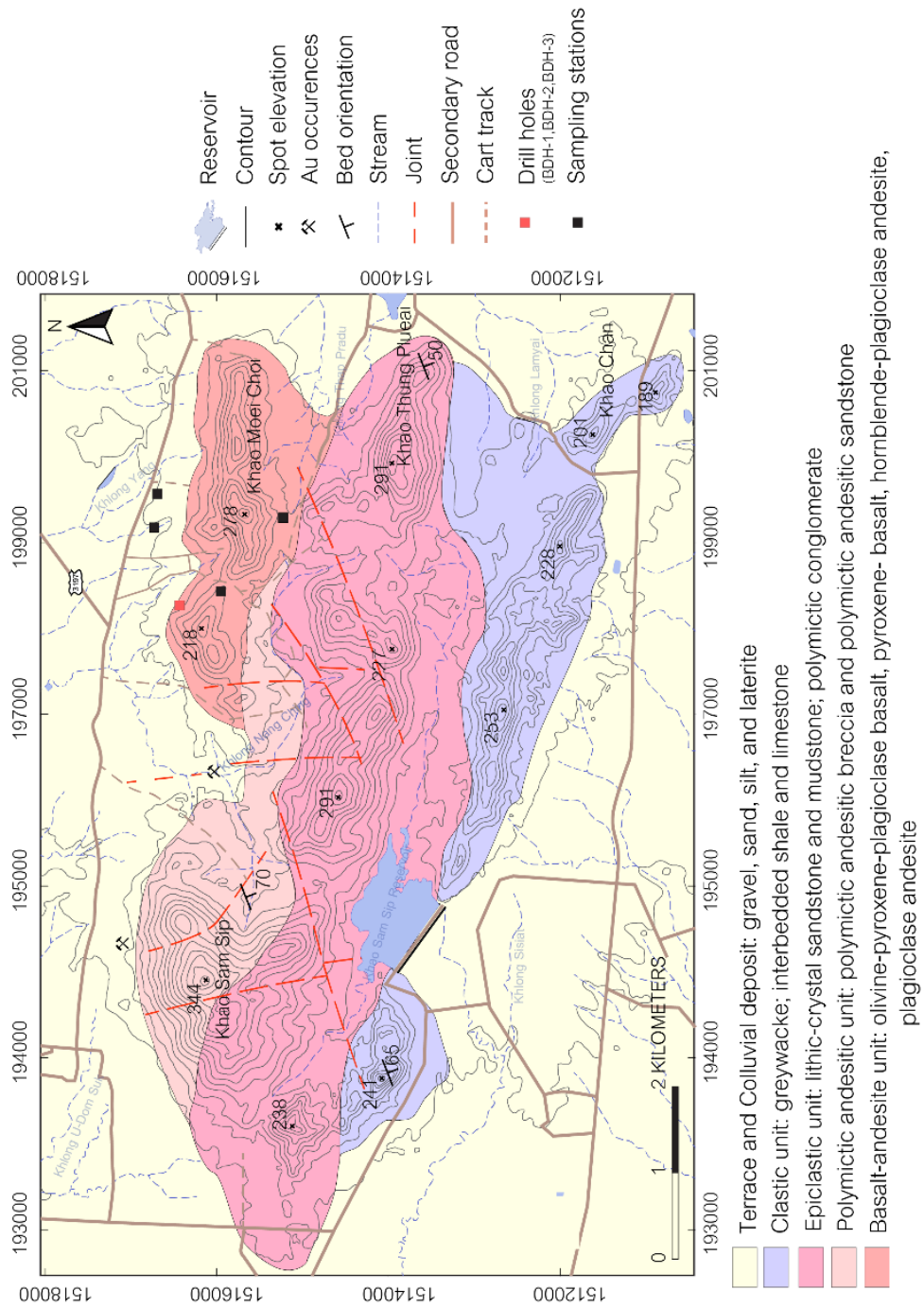


Fig. 14 Geological map of the Khao Sam Sip area with sampling stations.

Bangkok for Loss on Ignition (LOI.) and major oxides analysis.

#### 4.2.2. Loss on Ignition

Loss on ignition was determined at the Department of Mineral Resources, Bangkok by heating 1 g of each powder samples in ceramic crucibles, and then putting them in a furnace at 1000°C for 12 hours and reweighing the samples.

#### 4.2.3. Major oxides analysis

The fused discs were prepared by mixing 1.0000 g powder sample with a few lithium bromide (LiBr) and 5.00 g di-lithium tetraborate ( $\text{Li}_2\text{B}_4\text{O}_7$ ) in a platinum crucible. Then, the mixed was fused in a glass bead machine, installed at the Department of Mineral Resources, and then cooled down in a 3 cm-diameter platinum mold.

Chemical analysis for major oxides ( $\text{SiO}_2$ ,  $\text{TiO}_2$ ,  $\text{Al}_2\text{O}_3$ ,  $\text{FeO}$ ,  $\text{MnO}$ ,  $\text{MgO}$ ,  $\text{CaO}$ ,  $\text{Na}_2\text{O}$ ,  $\text{K}_2\text{O}$ , and  $\text{P}_2\text{O}_5$ ) was done by measuring the fused discs with PANalytical (Zetium) wavelength dispersive X-ray fluorescence spectrometer (WDXRF), installed at the Department of Mineral Resources. The element range for WDXRF goes for sodium to uranium (Na to U). The instrumental parameters are made up of (1) Rhodium (Rh) tube, 10 primary beam filter, 4 position collimator, 6 analyzer crystals, Vacuum seal, scintillation counter (for heavy elements) and flow proportion detectors (for light elements), and (2) X-Ray tube was operated at 60 kV and current of up to 160 mA; at a maximum power level of 4 kW. The net (background corrected) intensities were measured and the concentrations were calculated against the calibrations derived from 3 international standard reference materials (JGb-1, GBW03101, and JB-1a). The element constituent corrections were done by the Super Q version 6.1 program.

#### 4.2.4 Trace elements and REE analysis

The cleaned rock chips of fourteen representing samples were prepared for trace element and rare earth elements analysis at SGS company. The rock chips were pulverized by Rocklabs Ceramic grinder for powder sample, and then mixed the powder sample with Sodium peroxide. After that, the mixed was fused and digested by strong acid.

The selected samples were analyzed for trace elements (Rb, Sr, Zr, Y, Nb, Ni, Cr, V and Sc), REE, Hf, Th, and Ta by Elan 6100 inductive coupled plasma mass spectrometry (ICP-MS), installed at SGS company. The ICP-MS analysis was corrected for REE-oxide interferences at the acceptable for  $\pm 10\%$  of precision range of the measurement and monitored by blank and reference solution every twenty sample.

### 4.3. Geochemistry of volcanic rocks in the Khao Sam Sip area

Whole-rock geochemical data of the coherent volcanic rocks in the Khao Sam Sip area, Sa Kaeo Province are listed in Table 1 and Table 2.

#### 4.3.1 Major element geochemistry

The coherent volcanic rocks from the Khao Sam Sip area are classified based on their  $\text{SiO}_2$  content (basalt  $< 52$  wt. %, basaltic andesite 52-58 wt. %, andesite 58-63 wt. %, dacite to rhyolite  $> 63$  wt. %  $\text{SiO}_2$ ) as suggested by Cox, Bell, and Pankhurst (1979). Consequently, the rocks range in composition from 45 to 52 wt%  $\text{SiO}_2$  suggested as basaltic composition (Fig. 15).

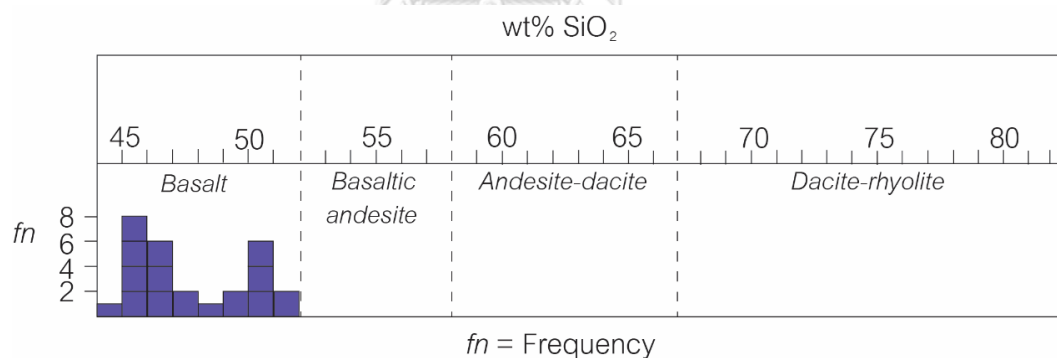


Fig. 15 Histograms of whole rock  $\text{SiO}_2$  content for the volcanic rocks from the Khao Sam Sip area. Note: Ranging of  $\text{SiO}_2$  for basalt, basaltic andesite, andesite and dacite field are based on Cox et al. (1979).

Although the samples were selected from the least-altered rocks, some samples might have been affected by secondary processes especially the hydrothermal alteration and hydrothermal mineralization presenting in the study area. Thus, to determine all selected samples in this study, the Madeisky (1996) diagram is used to evaluate the effect of hydrothermal mineralization on the volcanic rock samples (Fig. 16).

The diagram shows that all of the analyzed rock samples from the Khao Sam Sip area have molar  $(K + Na + 2Ca)/Al > 1$  considered to be unaltered rocks (Booden et al., 2010).

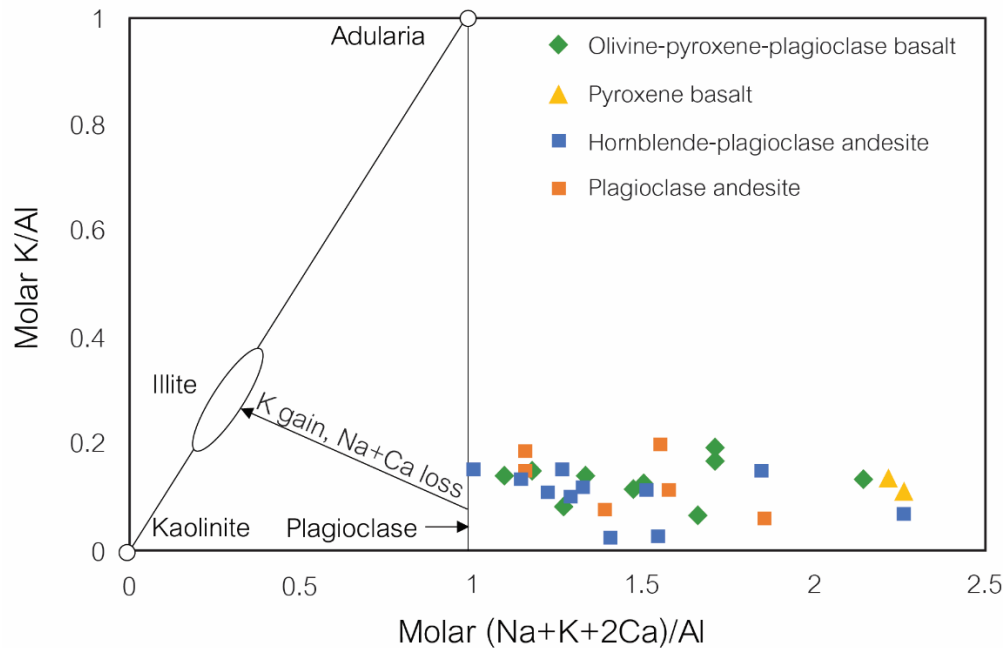


Fig. 16 Molar K/Al vs. molar  $(K + Na + 2Ca)/Al$  (Booden et al., 2010; Madeisky, 1996). In this diagram, the alteration minerals kaolinite, illite and adularia plot on a line of slope 1. Unaltered basaltic to andesitic volcanic rocks typically have molar  $(K + Na + 2Ca)/Al$  values  $> 1$ . Potassium metasomatism leads to decreasing molar  $(K + Na + 2Ca)/Al$  and increasing molar K/Al values. Most of the Khao Sam Sip rocks have molar  $(K + Na + 2Ca)/Al > 1$  and are considered to be the least-altered rocks.

The four coherent volcanic rock types, which are classified by their petrography (in the chapter 3), are analyzed geochemically as alkalic affinity and plotted in trachybasalts, basaltic trachyandesites and basalt field on TAS diagram ( $Na_2O + K_2O$  vs  $SiO_2$  diagram)(Irvine and Barager, 1971; Le Maitre et al., 1989)(Fig. 17).

**Table 1** Geochemistry of least altered volcanic rocks in the Khao Sam Sij area, Sa Kaeo Province.

Sample No.	14.15- BDH-3	21.10- BDH-3	22.35- BDH-3	29.50- BDH-3	40.00- BDH-3	41.00- BDH-3	47.00- BDH-3	KS1-f Pit	KS2 Pit	KS8 KMJ	34.05- BDH-3	KS1 Pit	14.05- BDH-1	15.00- BDH-1	39.70- BDH-1
Rock Types	OB	OB	OB	OB	PB	PB	HPPA	HPPA	HPPA						
SiO <sub>2</sub>	45.04	45.42	50.68	51.72	48.23	45.90	49.28	47.34	46.20	50.60	45.55	46.09	50.71	50.25	45.26
TiO <sub>2</sub>	0.89	0.83	0.82	0.81	0.84	0.84	0.85	0.99	0.70	0.93	0.80	0.70	0.69	0.85	0.80
Al <sub>2</sub> O <sub>3</sub>	16.74	14.04	17.28	16.56	14.91	16.19	14.34	18.15	11.33	16.65	12.66	11.61	20.94	17.91	14.48
FeO <sub>t</sub>	10.47	11.40	9.74	9.57	10.72	10.11	11.74	10.70	12.87	10.04	10.42	11.00	5.23	9.71	14.32
MnO	0.13	0.15	0.12	0.13	0.17	0.13	0.17	0.15	0.16	0.17	0.15	0.14	0.11	0.12	0.27
MgO	6.61	9.76	5.78	5.82	7.28	6.63	7.90	6.28	10.76	5.07	10.50	10.60	5.05	5.04	9.32
CaO	11.19	10.82	6.49	6.68	10.59	12.66	8.21	6.90	11.38	8.57	13.50	12.47	6.21	6.36	6.81
Na <sub>2</sub> O	1.59	0.93	3.56	4.54	2.68	1.14	2.74	2.90	1.21	2.51	1.07	1.34	3.96	3.91	2.22
K <sub>2</sub> O	1.98	2.55	2.44	1.29	0.92	2.52	1.53	2.36	1.41	2.21	1.59	1.21	3.00	2.24	1.50
P <sub>2</sub> O <sub>5</sub>	0.43	0.30	0.22	0.24	0.29	0.40	0.27	0.34	0.25	0.33	0.28	0.26	0.26	0.26	0.19
LOI	4.28	3.18	2.11	2.01	2.69	2.93	2.26	3.33	3.43	2.59	2.86	4.13	3.29	2.62	3.96
Sum	99.36	99.38	99.25	99.36	99.31	99.44	99.28	99.43	99.69	99.67	99.40	99.54	99.43	99.26	99.13
Mg#	38.71	46.13	37.26	37.82	40.45	39.60	40.21	37.00	45.53	33.52	50.19	49.08	49.13	34.16	39.42

Abbreviation: BDH-1 = Bo Nang Ching Drill Hole 1, BDH-2 = Bo Nang Ching Drill Hole 2, BDH-3 = Bo Nang Ching Drill Hole 3, KMJ = Khao Moei Joi, OB = Olivine-pyroxene-plagioclase basalt, PB = Pyroxene basalt, HPPA = Hornblende-plagioclase andesite, PPA = Plagioclase andesite.

Table 1 (Continued)

Sample	41.45-	19.0-	51.25-	51.85-	53.65-	45.20-	8.5-8.65	48.50-	29.35-	38.60-	24.30-	25.15-	42.00-	25-13
No.	41.55	19.15	51.45	52.0	53.75	45.40		48.70	29.40	38.65	24.45	25.30	42.15	
Area	BDH-1	BDH-2	BDH-2	BDH-2	BDH-2	BDH-2	BDH-3	BDH-3	BDH-1	BDH-1	BDH-2	BDH-2	BDH-2	KMJ
Rock Types	HPPA	HPPA	HPPA	HPPA	HPPA	HPPA	HPPA	HPPA	PPA	PPA	PPA	PPA	PPA	PPA
SiO <sub>2</sub>	51.48	50.82	45.29	45.58	46.55	47.84	44.26	49.49	44.95	46.86	45.66	46.38	50.69	46.68
TiO <sub>2</sub>	0.88	0.69	0.89	0.76	0.81	0.92	0.91	0.99	0.81	0.77	0.76	0.81	0.90	0.97
Al <sub>2</sub> O <sub>3</sub>	15.36	15.26	15.89	13.36	13.27	16.35	17.13	16.12	16.53	14.31	15.21	17.81	15.36	15.81
FeO <sub>t</sub>	9.22	8.00	12.30	10.51	11.71	10.81	10.78	10.15	13.61	11.00	10.46	10.01	10.55	12.28
MnO	0.18	0.14	0.18	0.20	0.21	0.20	0.14	0.13	0.17	0.18	0.20	0.16	0.17	0.17
MgO	7.88	4.08	7.94	7.64	9.73	5.84	6.27	6.75	7.18	8.87	8.20	6.25	5.64	4.81
CaO	6.21	8.28	7.83	15.35	11.49	7.62	11.36	8.69	7.01	8.91	9.52	7.37	7.08	13.74
Na <sub>2</sub> O	4.17	4.88	2.04	0.79	0.95	3.53	1.93	3.86	2.33	2.80	1.93	2.27	4.38	1.98
K <sub>2</sub> O	1.50	0.40	2.28	0.87	1.86	1.80	1.81	0.41	2.29	1.53	2.82	3.15	1.12	0.92
P <sub>2</sub> O <sub>5</sub>	0.37	0.82	0.32	0.20	0.20	0.41	0.45	0.26	0.24	0.30	0.34	0.45	0.26	0.50
LOI	2.15	6.13	4.56	4.19	2.72	4.07	4.35	2.56	4.12	3.72	4.34	4.75	2.84	1.62
Sum	99.40	99.49	99.50	99.44	99.48	99.38	99.38	99.42	99.24	99.25	99.44	99.41	98.99	99.48
Mg#	46.11	33.77	39.21	42.10	45.39	36.76	35.07	39.92	34.54	44.63	43.96	38.42	34.82	28.13

Abbreviation: BDH-1 = Bo Nang Ching Drill Hole 1, BDH-2 = Bo Nang Ching Drill Hole 2, BDH-3 = Bo Nang Ching Drill Hole 3, KMJ = Khao Moei Joi, OB = Olivine-pyroxene-plagioclase basalt, PB = Pyroxene basalt, HPPA = Hornblende-plagioclase andesite, PPA = Plagioclase andesite.

**Table 2** Trace elements and REE compositions (in ppm) determined by ICP-MS analysis of least altered volcanic rocks from the Khao Sam Sij Area, Sa Kao Province.

Sample No.	22.35- 22.65	KS1-F	KS2	KS8	KS1-C	14.05- 14.10	19.00- 19.15	45.20- 45.40	51.85- 52.00	8.50-8.65	48.50- 48.70	24.30- 24.45	42.00- 42.15	25-13
Area	BDH-3	Pit	Pit	KMJ	Pit	BDH-1	BDH-2	BDH-2	BDH-2	BDH-3	BDH-3	BDH-2	BDH-2	KMJ
Rock Types	OB	OB	OB	OB	PB	HPPA	HPPA	HPPA	HPPA	HPPA	HPPA	PPA	PPA	PPA
Ba	49.90	4.00	43.70	25.70	17.30	17.50	228.00	93.60	135.00	55.60	23.30	27.60	44.20	10.10
Cu	15.00	5.00	9.00	6.00	21.00	8.00	8.00	9.00	9.00	9.00	21.00	15.00	14.00	7.00
Ni	8.00	6.00	5.00	6.00	6.00	13.00	14.00	13.00	8.00	11.00	12.00	11.00	18.00	7.00
Sr	15.20	4.90	19.50	10.50	9.50	9.30	38.20	20.30	25.30	17.90	13.80	8.50	12.00	7.70
Zn	65.00	138.00	352.00	39.00	84.00	66.00	59.00	53.00	39.00	88.00	53.00	49.00	85.00	43.00
Ce	83.00	35.10	285.00	159.00	45.30	285.00	132.00	162.00	148.00	84.80	150.00	58.60	78.10	78.10
Dy	7.44	2.89	27.50	21.20	10.10	13.20	6.73	11.90	18.20	7.12	10.30	13.50	15.20	14.00
Er	3.81	1.43	14.10	11.30	5.73	7.03	3.49	6.82	11.00	4.36	6.12	9.08	10.30	8.55
Eu	0.27	0.05	0.68	0.41	0.08	0.32	0.57	0.34	0.39	0.22	0.20	0.10	0.12	0.10
Gd	6.38	2.29	28.80	20.30	7.10	15.30	7.31	11.30	13.90	5.11	6.85	8.76	10.50	10.40
Hf	4.00	3.00	10.00	6.00	4.00	15.00	11.00	8.00	9.00	5.00	8.00	12.00	17.00	6.00
Ho	1.45	0.51	5.14	3.95	1.93	2.46	1.32	2.42	3.79	1.45	2.13	2.96	3.27	2.85
La	37.60	15.50	130.00	93.00	19.20	91.00	45.70	76.30	63.10	21.70	48.50	14.10	31.50	36.90
Lu	0.64	0.37	2.35	1.85	1.18	1.14	0.64	1.13	1.88	0.76	1.06	1.76	2.04	1.57
Nb	33.00	121.00	136.00	60.00	58.00	76.00	43.00	56.00	54.00	57.00	65.00	63.00	72.00	59.00
Nd	31.50	13.10	154.00	108.00	19.90	84.40	42.10	60.80	55.50	18.60	34.10	17.10	32.30	31.60
Pb	68.00	93.00	207.00	150.00	104.00	306.00	176.00	130.00	149.00	124.00	34.00	348.00	58.00	127.00

Abbreviation: BDH-1 = Bo Nang Ching Drill Hole 1, BDH-2 = Bo Nang Ching Drill Hole 2, BDH-3 = Bo Nang Ching Drill Hole 3, KMJ = Khao Moei Joi, OB = Olivine-pyroxene-plagioclase basalt, PB = Pyroxene basalt, HPPA = Hornblende-plagioclase andesite, PPA = Plagioclase andesite.

Table 2 (Continued)

Sample No.	22.35- 22.65	KS1-F	KS2	KS8	KS1-C	14.05- 14.10	19.00- 19.15	45.20- 45.40	51.85- 52.00	8.50-8.65	48.50- 48.70	24.30- 24.45	42.00- 42.15	25-13
Area	BDH-3	Pit	Pit	KMJ	Pit	BDH-1	BDH-2	BDH-2	BDH-2	BDH-3	BDH-3	BDH-2	BDH-2	KMJ
Rock Types	OB	OB	OB	OB	PB	HPPA	HPPA	HPPA	HPPA	HPPA	HPPA	PPA	PPA	PPA
Rb	734.00	1310.00	805.00	811.00	972.00	284.00	666.00	629.00	979.00	713.00	602.00	904.00	500.00	564.00
Pr	9.22	3.91	41.10	29.00	5.50	24.10	12.00	18.20	16.00	5.47	10.30	4.42	8.79	9.25
Sb	0.70	0.50	0.60	0.40	0.40	0.90	0.50	0.50	0.90	1.70	1.30	0.30	2.10	0.60
Sm	7.60	3.00	36.70	26.60	7.40	19.50	9.10	13.40	13.80	5.10	7.30	6.50	10.20	9.40
Sn	100.00	365.00	65.00	97.00	324.00	103.00	59.00	89.00	86.00	131.00	117.00	158.00	294.00	138.00
Ta	12.60	60.50	20.40	18.00	26.50	16.30	8.70	12.00	13.60	21.20	15.50	26.20	26.90	17.80
Tb	1.24	0.46	4.74	3.58	1.64	2.37	1.19	2.01	2.78	1.07	1.54	2.02	2.21	2.13
Th	56.20	25.60	80.80	70.10	30.40	189.00	141.00	143.00	86.50	57.00	103.00	58.10	77.50	59.60
Tm	0.59	0.27	2.34	1.82	1.00	1.09	0.58	1.05	1.80	0.73	0.99	1.53	1.71	1.42
U	14.70	5.74	29.10	20.40	7.58	23.20	32.50	24.80	15.50	28.50	13.40	28.90	11.10	13.40
Y	43.50	17.20	153.00	116.00	61.70	72.70	32.40	73.80	125.00	45.00	67.20	96.50	95.90	87.00
Yb	4.00	2.30	16.10	12.50	7.70	7.40	4.10	7.20	12.50	5.10	6.80	10.80	12.90	9.70
Zr	106.00	49.20	233.00	120.00	49.00	328.00	299.00	191.00	247.00	89.10	211.00	243.00	311.00	109.00
Zr/Y	2.44	2.86	1.52	1.03	0.79	4.51	9.23	2.59	1.98	1.98	3.14	2.52	3.24	1.25
Ti/Y	113.54	345.35	27.23	48.00	67.52	56.97	126.91	74.32	36.20	121.48	88.30	46.90	56.06	66.76
[La/Sm]n	3.19	3.34	2.29	2.26	1.67	3.01	3.24	3.68	2.95	2.75	4.29	1.40	1.99	2.53
[Sm/Yb]n	2.11	1.45	2.53	2.36	1.07	2.93	2.47	2.07	1.23	1.11	1.19	0.67	0.88	1.08
[La/Yb]n	6.74	4.83	5.79	5.34	1.79	8.82	8.00	7.60	3.62	3.05	5.12	0.94	1.75	2.73

Abbreviation: BDH-1 = Bo Nang Ching Drill Hole 1, BDH-2 = Bo Nang Ching Drill Hole 2, BDH-3 = Bo Nang Ching Drill Hole 3, KMJ = Khao Moei Joi, OB = Olivine-pyroxene-plagioclase basalt, PB = Pyroxene basalt, HPPA = Hornblende-plagioclase andesite, PPA = Plagioclase andesite.

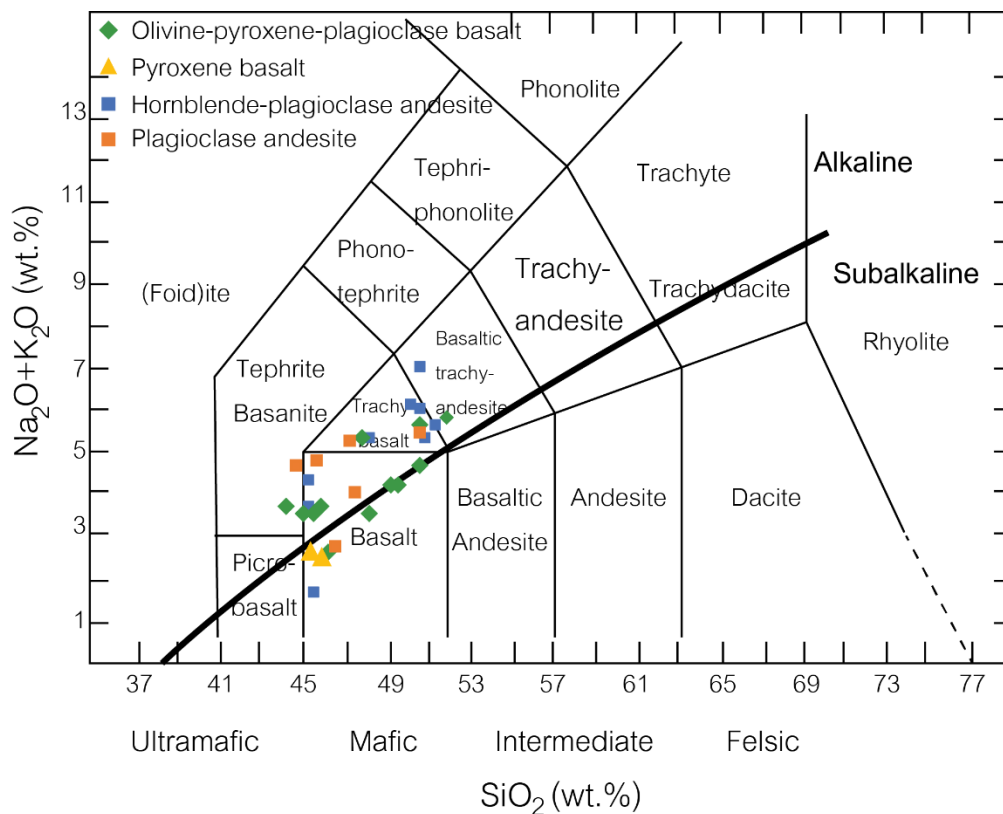


Fig. 17 TAS diagram ( $\text{Na}_2\text{O} + \text{K}_2\text{O}$  vs  $\text{SiO}_2$  diagram) (Irvine and Barager, 1971; Le Maitre et al., 1989)

In terms of immobile elements, the  $\text{Zr}/\text{TiO}_2$  vs  $\text{Nb}/\text{Y}$  diagram (Winchester and Floyd, 1977) is used to discriminate all the samples. Most sample are plotted to be trachyandesite, and some are on alkali basalt, rhyodacite, andesite and basanite fields (Fig. 18). Therefore, all the mafic rocks are grouped by their names which resemble their petrographic characteristics and their REE patterns.

Mg number (Mg#) was considered plotting against the major oxides (Fig. 19) and trace elements (Fig. 20) to show the variation of  $\text{TiO}_2$ ,  $\text{Al}_2\text{O}_3$ ,  $\text{FeO}_t$ ,  $\text{CaO}$  and  $\text{Na}_2\text{O}$  between the samples. The  $\text{TiO}_2$  contents are slightly increasing while  $\text{FeO}_t$  content is decreasing throughout the fractionation. Significantly, the  $\text{CaO}$  contents of pyroxene basalt are slightly higher than the other groups. The different values of trace elements were used to classify the characteristic of the volcanic rocks and determine in the next section.

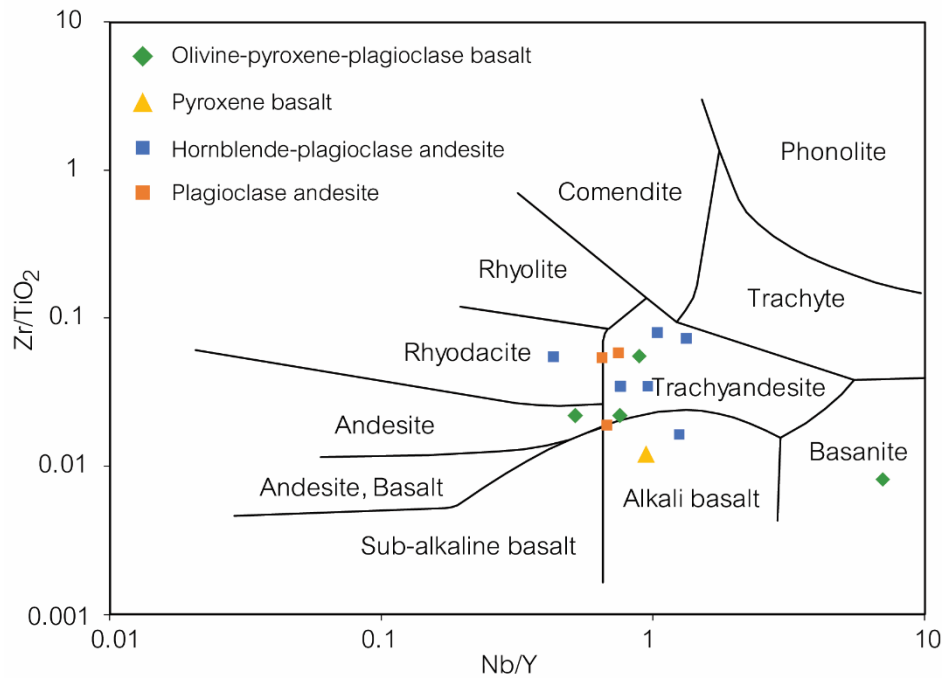


Fig. 18 Nb/Y and Zr/TiO<sub>2</sub> discrimination diagram by (Winchester and Floyd, 1977).

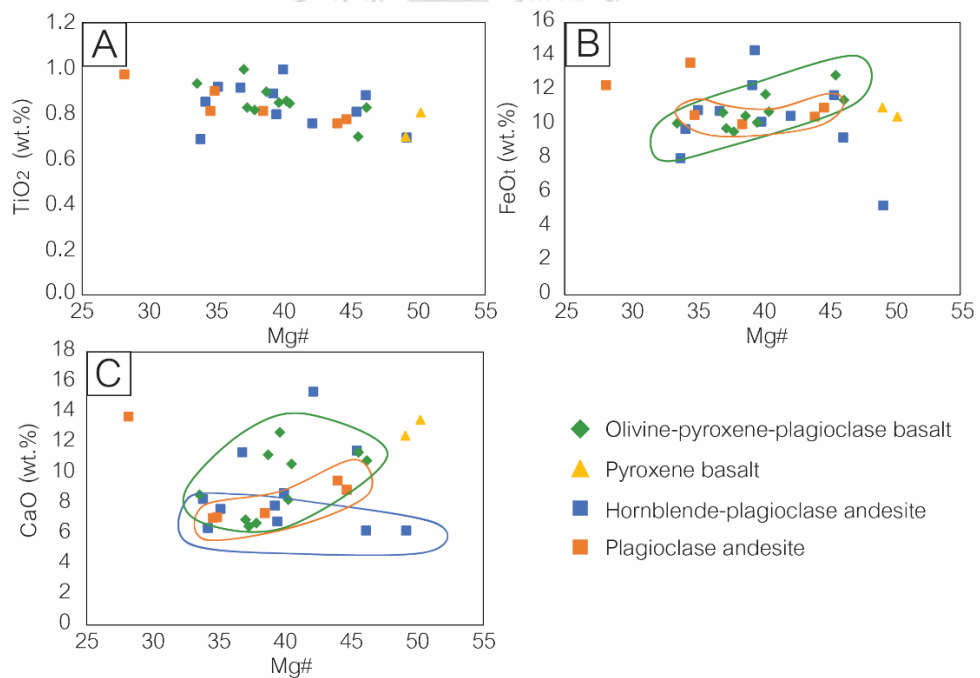


Fig. 19 Major element bivariate diagrams plotted against Mg# for the volcanic rocks from the Khao Sam Sip area. A) TiO<sub>2</sub> vs Mg# number showing an increase TiO<sub>2</sub> with decrease Mg#, B) FeO<sub>t</sub> vs Mg# showing a slightly positive trend to more mafic composition, C) CaO vs Mg# showing the different fields for the volcanic rocks.

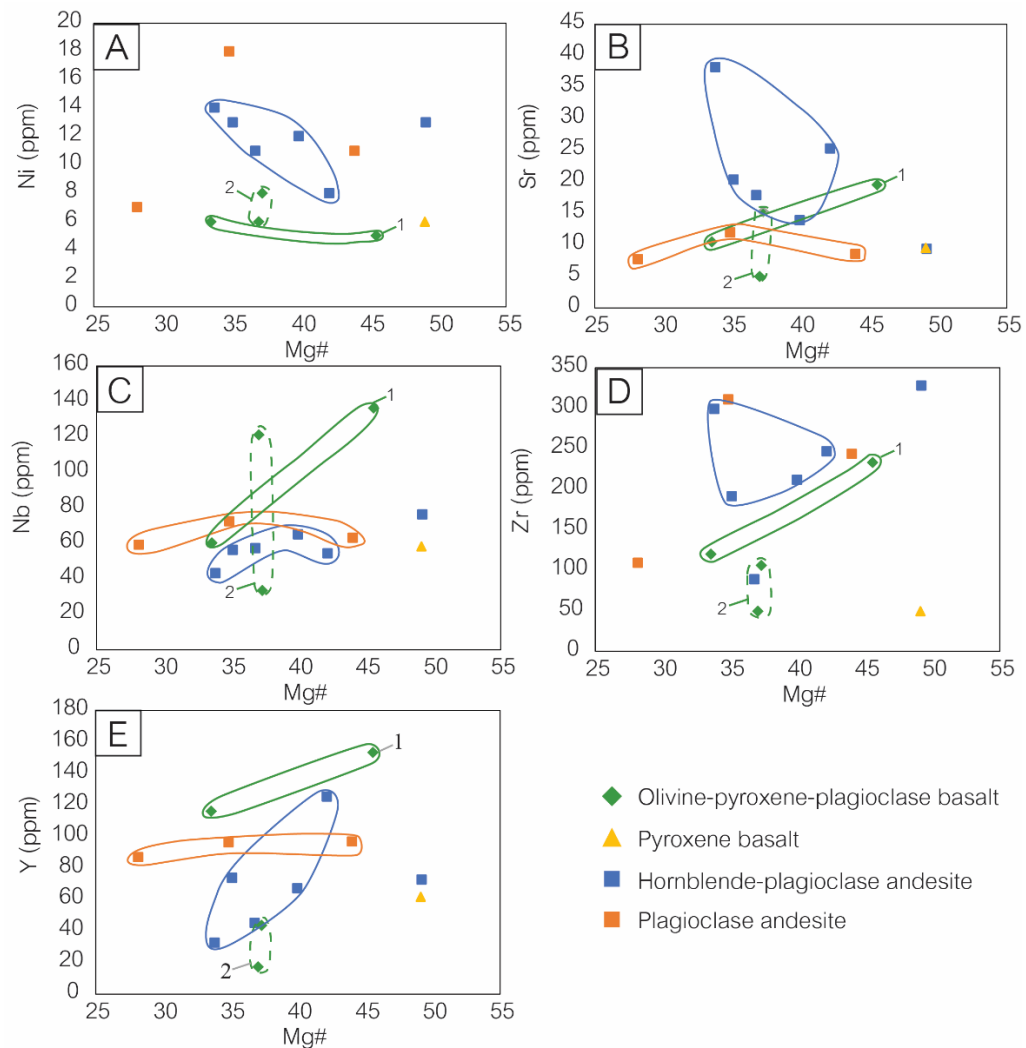


Fig. 20 Trace element bivariate diagrams plotted against Mg# for the volcanic rocks from the Khao Sam Sip area. A) Ni vs Mg#, B) Sr vs Mg#, C) Nb vs Mg#, D) Zr vs Mg#, and E) Y vs Mg#.

#### Olivine-pyroxene-plagioclase basalt

Olivine-pyroxene-plagioclase basalt possess variable  $\text{SiO}_2$  (45.04-51.72 wt. %) and MgO (5.07-10.76 wt. %), but coherent MnO (0.12-0.17 wt.%) contents. The  $\text{TiO}_2$  (0.70-0.99 wt. %) contents slightly increase with decreasing Mg# similar to the  $\text{Al}_2\text{O}_3$  (11.33-18.15 wt. %) contents whereas  $\text{FeO}_t$  (9.57-12.47 wt. %) is decreasing. They are also characterized with high CaO (6.49-11.38 wt. %) and moderate  $\text{P}_2\text{O}_5$  (0.22-0.43 wt. %) contents. Their  $\text{K}_2\text{O}$  (0.92- 2.55 wt. %) and  $\text{Na}_2\text{O}$  (0.93-4.54 wt. %) contents are diffused probably by hydrothermal alteration and mineralization.

The transitional elements (Ni), Large ion lithophile element (LILE: Sr) and High field strength element (HFSE: Nb, Y, and Zr) abundances show slight difference from the other rock types. The olivine-pyroxene-plagioclase basalt is characterized by low Ni (5.00-8.00 ppm) concentrations and Sr (4.90-19.50 ppm). Their Nb (33.00-136.00 ppm) and Y (43.50-153.00 ppm) concentrations are the lowest, but Zr (49.20-233.00 ppm) is higher than the other rock types (Fig. 20). In addition, The Zr and Y concentrations of this rock type can be classified into 2 subgroups in accordance with REE patterns.

The first subgroup of olivine-pyroxene-plagioclase basalt has Zr and Y concentrations between 120.0-233.00 ppm and 116.0-153.00 ppm. The REE abundances for 2 lavas of the first subgroup are presented in Table 2 and their chondrite-normalized values are plotted in Figure 21. Their REE patterns show markedly greater light rare earth element (LREE) enrichment relative to heavy rare earth element (HREE) which is characterized of typical alkaline magma. They have relatively LREE depletion with chondrite-normalized La/Sm (herein  $[La/Sm]_n$ ) between 2.26 to 2.29, and exhibit heavy REE (herein HREE) depletion with chondrite-normalized Sm/Yb (herein  $[Sm/Yb]_n$ ) ranging from 2.36 to 2.53. Most in this subgroup show depleted LREE pattern relative to HREE with chondrite-normalized La/Yb (herein  $[La/Yb]_n$ ) ranging from 5.34 to 5.79 and negative Eu anomaly ( $Eu/Eu^*=7-12$ ). Their La and Yb abundances vary from 392 to 549 and 74 to 95 times of chondritic values (Fig. 21).

N-MORB normalized multi-element patterns for the representative samples of the first subgroup display step-like pattern, typical of enriched mid-ocean ridge basalt (herein E-MORB) and within-plate basin (herein WPB). All representative samples represent negative Ba, Nb, Sr, P, Eu and Ti anomaly and the enrichment of Rb, Th, U, K, Ce, Sm and especially in Pb relative to other elements (Fig. 22).

The second subgroup of olivine-pyroxene-plagioclase basalt has Zr and Y concentration ranging from 49.20-106.00 ppm and 17.20-43.50 ppm. The REE abundances for 2 lavas of the second subgroup is presented in Table 2 and their chondrite-normalized values are plotted in Figure 21. Their REE patterns show markedly

greater LREE enrichment relative to HREE. These alkaline magma have relatively LREE depletion with chondrite-normalized La/Sm (herein  $[La/Sm]_n$ ) between 3.19 to 3.33, and exhibit heavy REE depletion (herein HREE) with chondrite-normalized Sm/Yb (herein  $[Sm/Yb]_n$ ) ranging from 1.45 to 2.11. Most in this subgroup show depleted LREE pattern relative to HREE with chondrite-normalized La/Yb (herein  $[La/Yb]_n$ ) ranging from 4.83 to 6.74 and negative Eu anomaly ( $Eu/Eu^*=1-5$ ). Their La and Yb abundances vary from 65 to 159 and 14 to 24 times chondritic values (Fig. 21).

N-MORB normalized multi-element patterns for the representative samples of the second subgroup display step-like pattern, typical of enriched mid-ocean ridge basalt (herein E-MORB) and within-plate basalt (herein WPB). All representative samples represent negative Ba, Nb, Sr, P, Eu and Ti anomalies and the enrichment of Rb, Th, U, K, Ce, Sm and especially in Pb relative to other elements (Fig. 22).

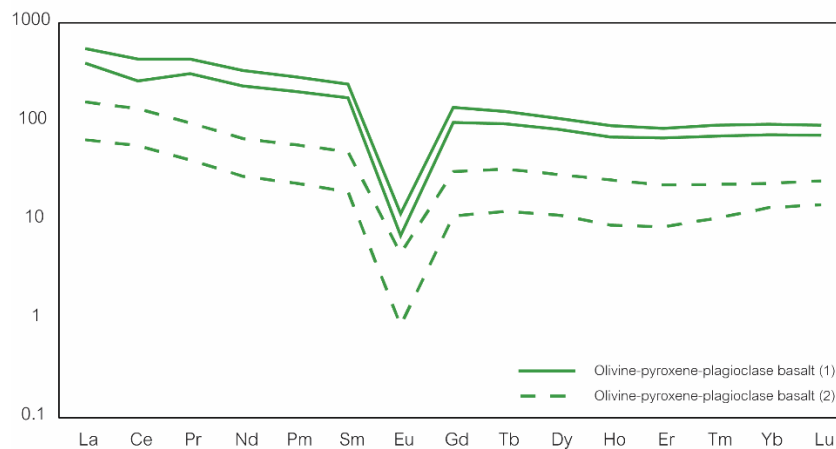


Fig. 21 Chondrite-normalized REE patterns for the olivine-pyroxene-plagioclase basalt. The chondrite-normalizing values are from (Sun and McDonough, 1989).

### Pyroxene basalt

Pyroxene basalt has coherent of composition due to small number of samples. It contains 45.55-46.09 wt. % of  $SiO_2$ , MgO (10.50-10.60 wt. %), MnO (0.14-0.15 wt.%),  $TiO_2$  (0.70-0.80 wt. %),  $FeO_t$  (10.42-11.00 wt. %),  $Al_2O_3$  (11.61-12.66 wt. %), and  $P_2O_5$  (0.26-0.28 wt. %). They are also characterized with moderate CaO (12.47-13.50 wt. %)

content. Their  $K_2O$  (1.21- 1.59 wt. %) and  $Na_2O$  (1.07-1.34 wt. %) contents are diffused by hydrothermal alteration.

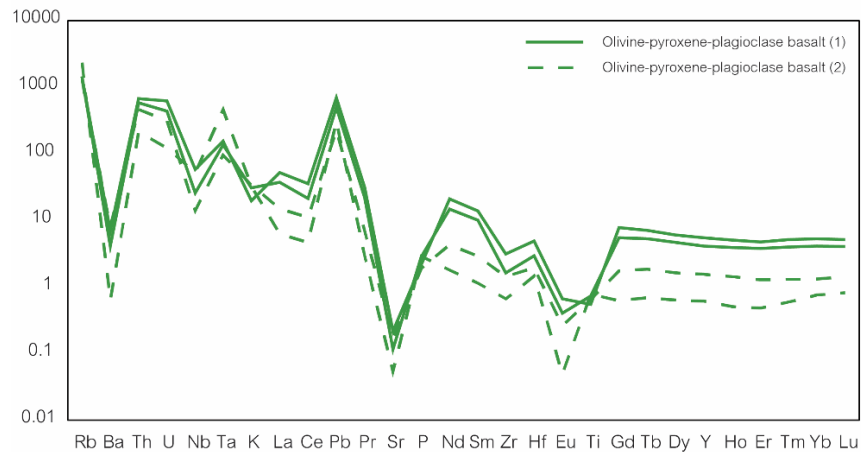


Fig. 22 N-MORB normalized multi-elements for the representative of the olivine-pyroxene-plagioclase basalt. The N-MORB normalizing values are from (Sun and McDonough, 1989).

The transitional elements (Ni), LILE (Sr) and HFSE (Nb, Y, and Zr) abundances show slight difference from the other rock types. These rocks are characterized by low Ni (6.00 ppm) concentrations and Sr (9.50 ppm), Nb (58.00 ppm) and Y (61.70 ppm), and Zr (49.00 ppm) (Fig. 20).

REE abundances for a pyroxene basalt is presented in Table 2, and their chondrite-normalized values are plotted in Figure 23. Its REE pattern shows slight LREE enrichment relative to HREE which characterize mildly alkaline magma. It has a slight depletion in LREE with chondrite-normalized La/Sm (herein  $[La/Sm]_n$ ) of 1.67, and flat HREE with chondrite-normalized Sm/Yb (herein  $[Sm/Yb]_n$ ) of 1.07. The pyroxene-phyric basalt shows a depleted LREE pattern relative to HREE with chondrite-normalized La/Yb (herein  $[La/Yb]_n$ ) 1.79 and negative Eu anomaly ( $Eu/Eu^*=1$ ). Their La and Yb abundances are 81- and 45-times of chondritic values (Fig. 23).

N-MORB normalized multi-element pattern for the representative sample of the pyroxene basalt displays step-like pattern, typical of enriched mid-ocean ridge basalt (herein E-MORB) and within-plate basalt (herein WPB). The representative sample

represents negative Ba, Nb, Sr, P, Eu and Ti anomalies and the enrichment of Rb, Th, U, K, Ce, Sm and especially in Pb relative to other elements (Fig. 24).

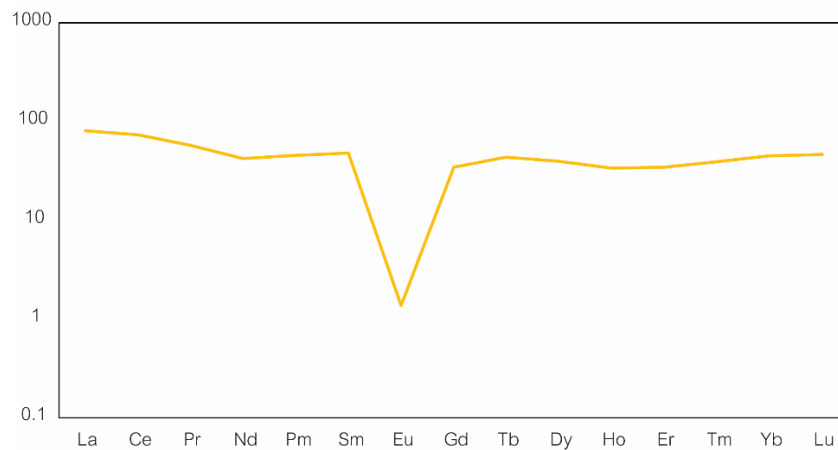


Fig. 23 Chondrite-normalized REE pattern for the pyroxene basalt. The chondrite normalizing values are from (Sun and McDonough, 1989).

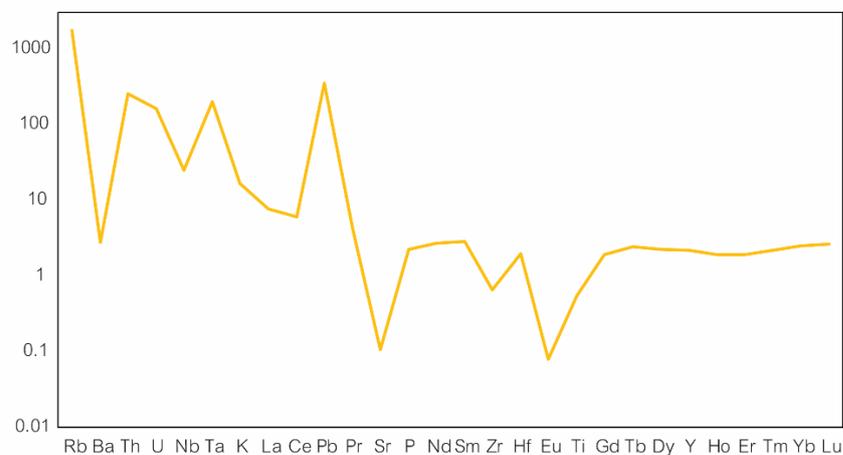


Fig. 24 N-MORB normalized multi-elements for the representative of the pyroxene-phyric basalt. The N-MORB normalizing values are from (Sun and McDonough, 1989).

#### Hornblende-plagioclase andesite

Hornblende-plagioclase andesite possess variable  $\text{SiO}_2$  (44.26-51.48 wt. %), and  $\text{MgO}$  (4.08-9.73 wt %), but coherent  $\text{MnO}$  (0.11-0.27 wt. %). The  $\text{TiO}_2$  (0.69-0.99 wt. %) contents slightly increase with decreasing  $\text{Mg\#}$  similar to  $\text{Al}_2\text{O}_3$  (13.27-20.94 wt. %) contents whereas the  $\text{FeO}_t$  (5.23-14.32 wt. %) is decreasing. They are also

characterized with lower CaO (6.21-15.35 wt. %) than the other rock types and  $P_2O_5$  (0.19-0.82 wt. %) are variable. Their  $K_2O$  (0.40- 3.00 wt. %) and  $Na_2O$  (0.79-4.88 wt. %) contents are diffused by hydrothermal alteration and mineralization.

The transitional elements (Ni), LILE (Sr) and HFSE (Nb, Y, and Zr) abundances show slight difference from the other rock types. The rocks are characterized by higher Ni (8.00-14.00 ppm) concentrations and Sr (9.30-38.20 ppm). In addition, Their Nb (43.00-76.00 ppm) and Y (32.40-125.00 ppm) concentrations are the lowest, but Zr (89.10-328.00 ppm) is higher than the other rock types (Fig. 20).

REE abundances for 6 lavas of hornblende-plagioclase andesite are presented in Table 2, and their chondrite-normalized values are plotted in Figure 25. Their REE patterns show markedly greater LREE enrichment relative to HREE which characterize typical alkaline magma. They have relative LREE depletion with chondrite-normalized La/Sm (herein  $[La/Sm]_n$ ) between 2.75 to 4.29, and exhibit HREE depletion chondrite-normalized Sm/Yb (herein  $[Sm/Yb]_n$ ) ranging from 1.11 to 2.93. Most samples in the hornblende-plagioclase andesite show a slight positive peak in Ce content and depleted LREE pattern relative to HREE with chondrite-normalized La/Yb (herein  $[La/Yb]_n$ ) ranging from 3.05 to 8.82 and negative Eu anomaly ( $Eu/Eu^*=3-10$ ). Their La and Yb abundances vary from 92 to 384 and 24 to 74 times of chondritic values (Fig. 25).

N-MORB normalized multi-element patterns for the representative samples of the hornblende-plagioclase andesite display step-like patterns, typical of enriched mid-ocean ridge basalt (herein E-MORB) and within-plate basalt (herein WPB). All representative samples represent negative Ba, Nb, Sr, P, Eu and Ti anomalies and the enrichment of Rb, Th, U, K, Ce, Sm and especially in Pb relative to other elements (Fig. 26).

#### **Plagioclase andesite**

Plagioclase andesite possess variable  $SiO_2$  (44.95-50.69 wt.%), MgO (4.81-8.87 wt.%), but coherent MnO (0.16-0.20 wt.%) content. The  $TiO_2$  (0.69-0.92 wt.%) contents slightly increase with decreasing Mg# similar to the  $Al_2O_3$  (14.31-17.81 wt.%) contents

whereas the  $\text{FeO}_t$  (10.01-13.61 wt. %) is decreasing. They are also characterized with higher CaO (7.01-13.74 wt.%) contents than hornblende-plagioclase andesite and  $\text{P}_2\text{O}_5$  (0.24-0.51 wt.%) contents are variable. Their  $\text{K}_2\text{O}$  (0.92- 3.15 wt.%) and  $\text{Na}_2\text{O}$  (1.93-4.38 wt.%) contents are diffused by hydrothermal alteration and mineralization.

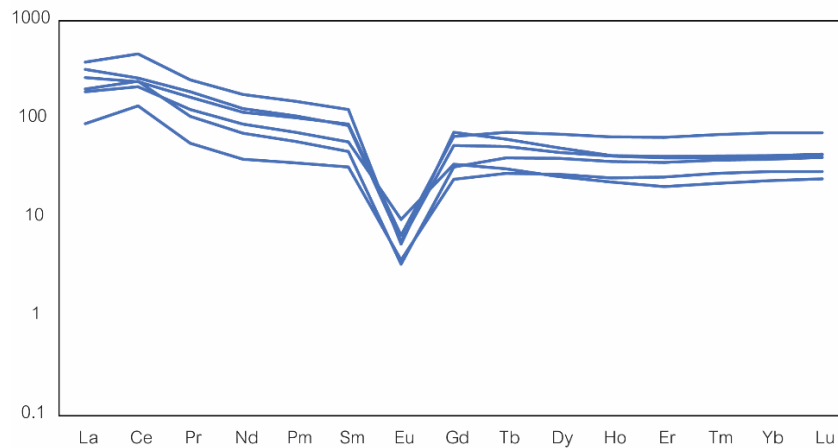


Fig. 25 Chondrite-normalized REE patterns for the hornblende-plagioclase andesite. The chondrite normalizing values are from (Sun and McDonough, 1989).

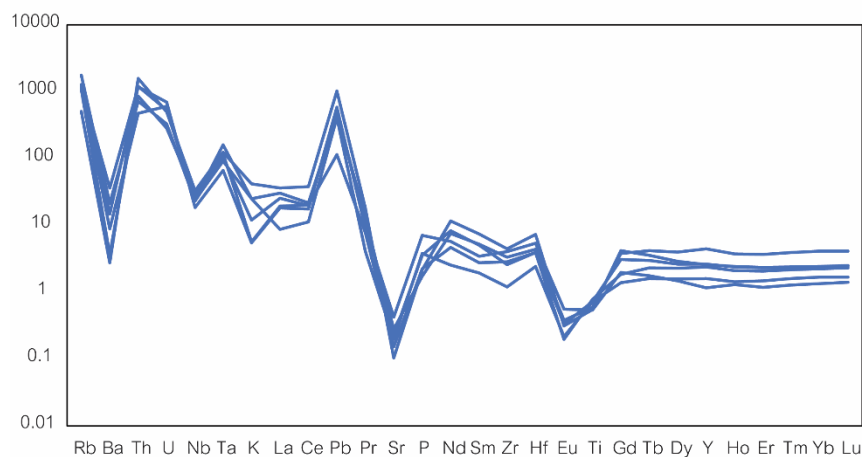


Fig. 26 N-MORB normalized multi-elements for the representative of the hornblende-plagioclase andesite. The N-MORB normalizing values are from (Sun and McDonough, 1989).

The transitional elements (Ni), LILE (Sr) and HFSE (Nb, Y, and Zr) abundances show slight difference from the other groups. These rocks are characterized by lower concentrations of Sr (7.70-12.00 ppm), but higher Nb (59.00-72.00 ppm) and constant Y

(87.00-96.50 ppm) than the other rock types. Significantly, the diagram of Ni (7.00-18.00 ppm) and Zr (109.00-311.00 ppm) concentrations show wide ranges (Fig. 20), and thus these diagrams cannot show typical values of the plagioclase andesite.

REE abundances for 3 lavas of plagioclase andesite are presented in Table 2, and their chondrite-normalized values are plotted in Figure 27. Their REE patterns show slight LREE enrichment relative to HREE which is characterized of mildly alkaline magma. They have LREE depletion with chondrite-normalized La/Sm (herein  $[La/Sm]_n$ ) between 1.40 to 2.53, and exhibit flat heavy REE (herein HREE) with chondrite-normalized Sm/Yb (herein  $[Sm/Yb]_n$ ) ranging from 0.67 to 1.08. One of three samples in the plagioclase-phyric andesite show a slight positive peak in Ce content, but all show slightly depleted LREE pattern relative to HREE with chondrite-normalized La/Yb (herein  $[La/Yb]_n$ ) ranging from 0.94 to 2.73 and negative Eu anomaly ( $Eu/Eu^*=2$ ). Their La and Yb abundances vary from 59 to 156 and 57 to 76 times of chondritic values (Fig. 27).

N-MORB normalized multi-element patterns for the representative samples of the plagioclase andesite display step-like pattern, typical of enriched mid-ocean ridge basalt (herein E-MORB) and within-plate basalt (herein WPB). All representative samples represent negative Ba, Nb, Sr, P, Eu and Ti anomalies and the enrichment of Rb, Th, U, K, Ce, Sm and especially in Pb relative to other elements (Fig. 28).

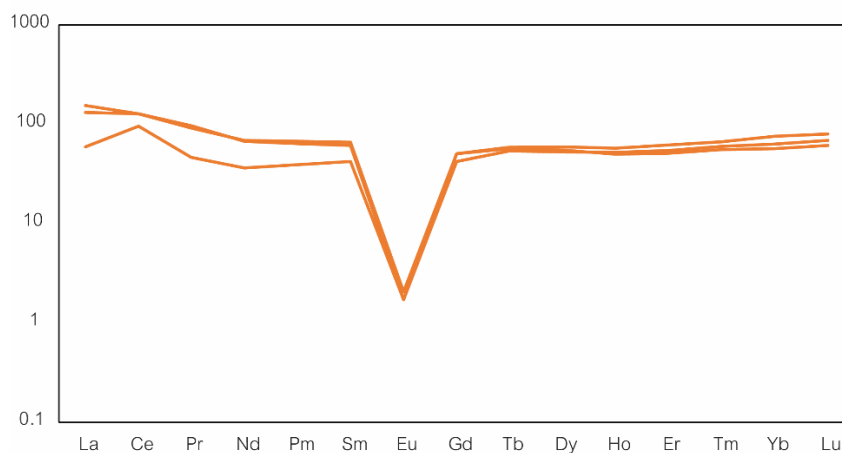


Fig. 27 Chondrite-normalized REE patterns for the plagioclase andesite. The chondrite normalizing values are from (Sun and McDonough, 1989).

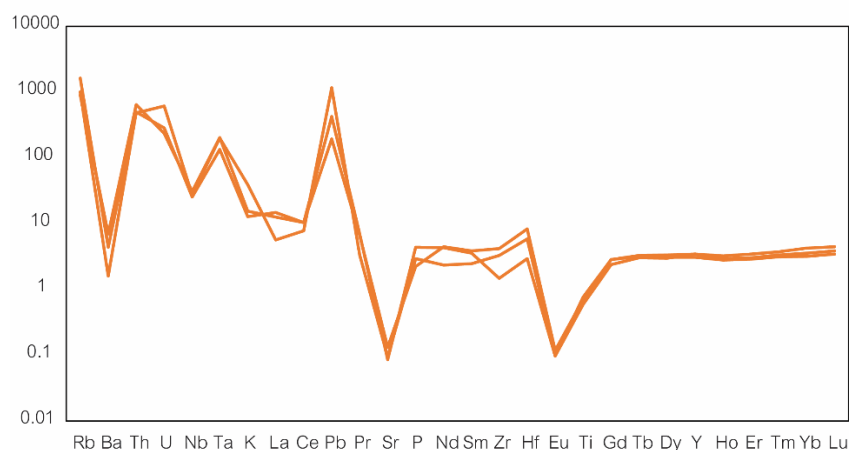


Fig. 28 N-MORB normalized multi-elements for the representative of the plagioclase andesite. The N-MORB normalizing values are from (Sun and McDonough, 1989).

#### 4.4. Tectonic Discrimination Diagrams

The diagrams used to discriminate tectonic environments of the studied rocks include  $MnO \cdot 10/TiO_2/P_2O_5$ ,  $TiO_2$  vs Zr, and Zr/Y vs Ti/Y diagrams. All of the volcanic groups appear to be island arc basalt, with calc-alkaline characters, as shown in the plots of  $MnO \cdot 10/TiO_2/P_2O_5$  (Fig. 29A)(Mullen, 1983). Their plots are correspondingly on the fields of volcanic arc basalt and plate margin in the  $TiO_2$ -Zr (Fig. 29B)(Pearce and Cann, 1973) and Zr/Y against Ti/Y (Fig. 29C)(Pearce, 1982) respectively.

In addition, the chondrite and N-MORB normalized multi-element patterns of the modern volcanic rocks were used to clarify the tectonic settings of formation. The representative of the olivine-pyroxene-plagioclase basalt is chemically analogous to the alkali rock from Valle del Leone, Etna Mount which is related the subduction zone (Armienti et al., 2004) as shown in Figure 30 and Figure 31 as well as the hornblende-plagioclase andesite. On the other hands, the representatives of the pyroxene basalt and the plagioclase andesite are most comparable in chemical composition with the alkali rock from Coriolis Trough basin, Vanuatu (Sun et al., 2003) (Fig. 30 and Fig. 31). This is marked by a flatter pattern compared to that of Etna Mount. Furthermore, all of the studied volcanic rock samples show strong negative Eu anomaly in REE patterns and fractionated patterns in trace elements diagrams compared to alkali rocks of Etna

and Vanuatu. This may suggest that volcanic rocks at Khao Sam Sip were formed from highly fractionated alkalic magmas related with subduction.

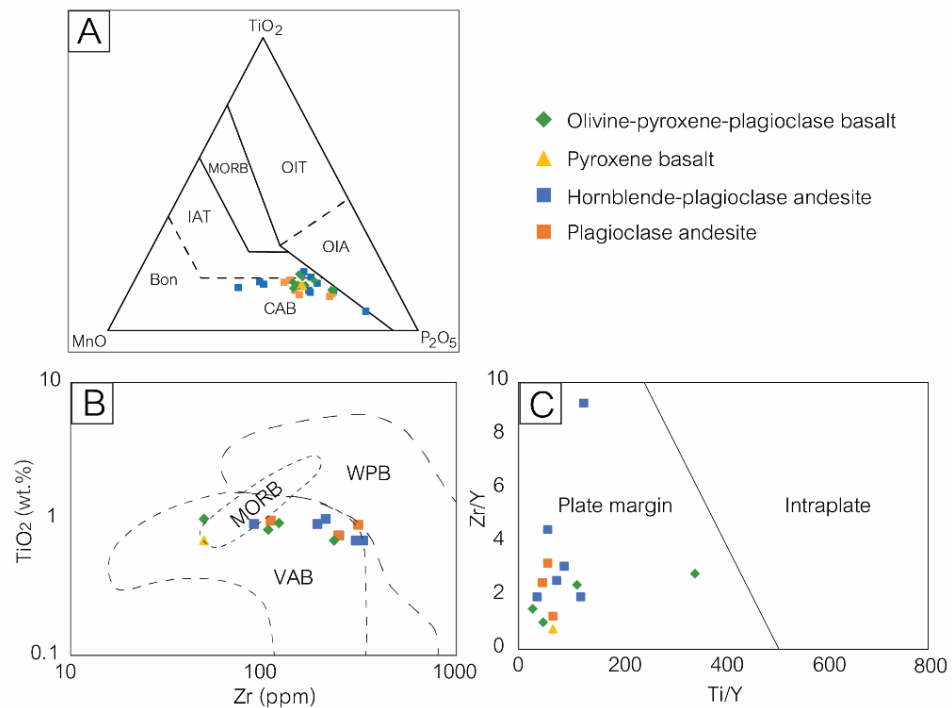


Fig. 29 Tectonic discrimination diagrams for volcanic rocks from the Khao Sam Sip are. **A)** Plot of  $\text{MnO} \cdot 10 - \text{TiO}_2 - \text{P}_2\text{O}_5 \cdot 10$  showing the field for MORB = mid ocean ridge basalt; OIT = ocean-island tholeiite or sea mount tholeiite; OIA = ocean-island alkali basalt or seamount alkali basalt; CAB = island-arc calc alkaline basalt; IAT = island-arc tholeiite; Bon = boninite (Mullen, 1983). Note that the volcanic rocks plot in the island arc calc-alkalic basalt field, **B)** Plot of  $\text{TiO}_2$  against Zr (Pearce and Cann, 1973). Note that the volcanic rocks plot in the volcanic arc basalt field, **C)** Plot of Zr/Y against Ti/Y (Pearce, 1982). Note that the volcanic rocks plot in the plate margin field.

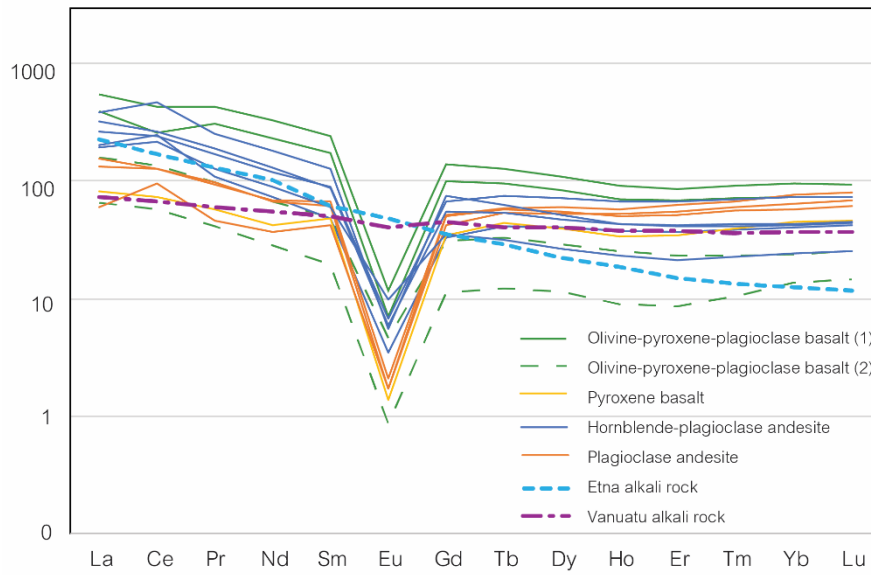


Fig. 30 Chondrite-normalized REE patterns of representative the volcanic rocks in the Khao Sam Sip plotted using chondrite normalizing values of (Sun and McDonough, 1989).

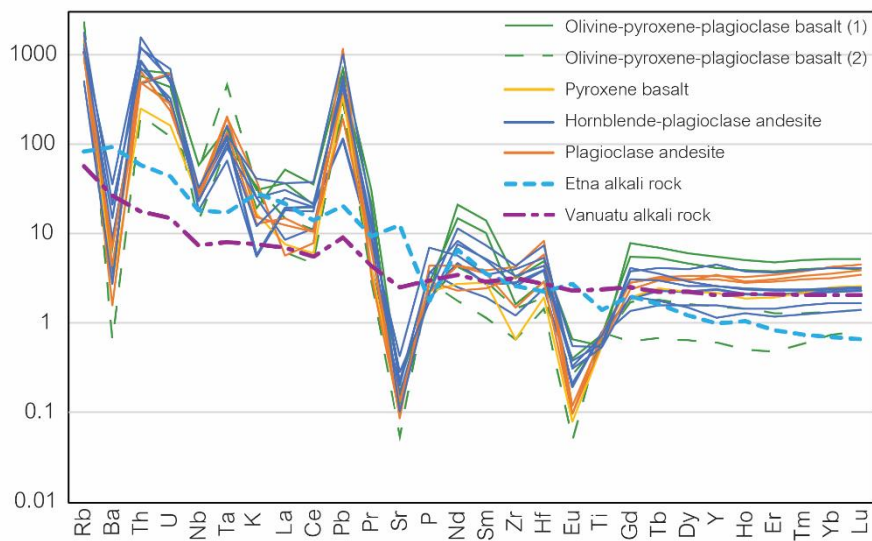


Fig. 31 N-MORB normalised trace elements patterns for the volcanic rocks in the Khao Sam Sip area. The N-MORB composition is taken from (Sun and McDonough, 1989).

## CHAPTER 5

### MINERALIZATION

#### 5.1. Introduction

This part documents mineralization characteristics found in the Khao Sam Sip area. However, information is very limited, due to 1) there are only three shallow drill holes which can be investigated for mineralization and no available outcrop samples were collected for this study, and 2) mineralization (or veining) is weakly developed in the three diamond drill holes. This chapter aims to give basic description of mineralization in terms of ore petrography and mineral paragenesis.

#### 5.2. Paragenesis and Mineralogy

At Khao Sam Sip, the mineralization occurs as veins and veinlets infilling fractures and faults. It is hosted in volcanic rocks (e.g. lava and volcanoclastic rocks), and the formation is controlled by structure (faults) and lithology. The best sulfide mineralization is developed in coherent volcanic unit such as plagioclase andesite and its autobreccia. Minor mineralization is also disseminated in other coherent rock types. Structurally, mineralization is mainly present along the NW-SE trending faults. The main Khao Sam Sip mineralization is characterized by quartz-carbonate-sulfide (chalcopyrite-pyrite-sphalerite). The mineralization occurs as veins, minor stockworks and patches.

Based on cross cutting relationships, mineral assemblages and vein textures, at least four stages of mineralization have been identified. They are; 1) Stage 1: Quartz-pyrite, 2) Stage 2: Quartz-calcite  $\pm$  sulfide (chalcopyrite-pyrite-sphalerite), 3) Stage 3: Chlorite-epidote, and 4) Stage 4: Quartz  $\pm$  calcite (Table 3).

##### Stage 1: Quartz-pyrite vein

The Stage 1 occurs as quartz-pyrite veins/veinlets containing predominant pyrite (Fig. 32A). Veins of this stage are often deformed and discontinued. Pyrite is the only sulfide mineral observed within this stage. Under microscope, quartz occurs at peripheral to veins. Pyrite forms as isolated grains to aggregates forming patches commonly along the center of vein (Fig. 32B). Pyrite forms as fine-grained crystal (less

than 50  $\mu\text{m}$  in diameter), subhedral to euhedral. Stage 1 vein is clearly crosscut by Stage 2 vein as observed in both in drill core and thin section under microscope (Fig. 32C).

**Table 3** Paragenetic diagram showing order of veins formation and the relative amount of mineral abundance (e.g. ore and gangue minerals).

Minerals	Stage 1	Stage 2	Stage 3	Stage 4
Quartz	---	—	---	—
Calcite		----		-----
Pyrite	—	---		
Chalcopyrite		—		
Sphalerite		---		
Epidote			—	
Chlorite			—	

#### Stage 2: Quartz-calcite-sulfide (chalcopyrite-pyrite-sphalerite)

The Stage 2 forms as veins/veinlets composed predominantly of quartz and minor carbonate (mainly calcite) and sulfides such as chalcopyrite, minor pyrite and sphalerite. Sulfides tend to form as patches enclosed by quartz and/or carbonate minerals and especially in center of quartz-carbonate veins (Fig. 33A). In Stage 2, chalcopyrite is the most abundant sulfide mineral with subordinate amount of pyrite (Fig. 33B) and minor amount of sphalerite. The pyrite forms as fine-grained, subhedral to euhedral crystals and mostly lies between euhedral quartz and chalcopyrite (Fig. 33B). Chalcopyrite occurs as isolated crystal and aggregates interstitially filled between quartz and carbonate (mainly calcite) (Fig. 33C). Pyrite in this stage is commonly at the peripheral of veins (Fig. 33B and D) suggesting it occurred earlier in Stage 2. Sphalerite has been identified only in some samples and constitutes in small amount and where present it is closely associated with pyrite. It occurs as fine-grained and anhedral crystals.

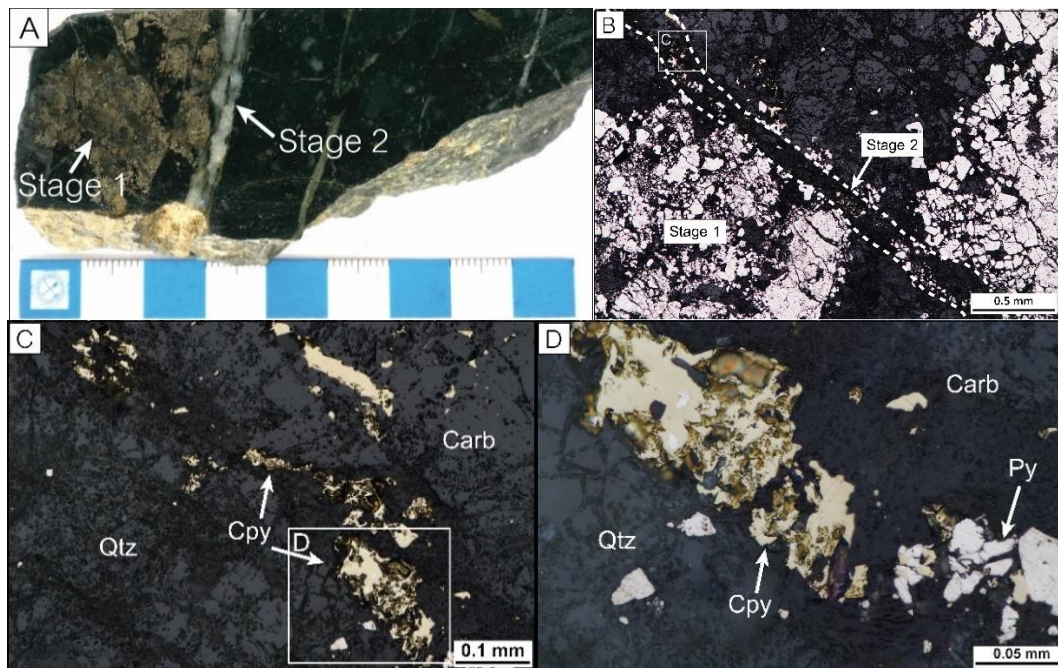


Fig. 32 Characteristics of Stage 1 veins/veinlets: A. Photograph of hand specimen showing Stage 1 vein consisting of massive pyrite aggregate and crosscut by Stage 2 quartz-carbonate-sulfides vein. B. Photomicrograph showing Stage 1 pyrite aggregate crosscut by Stage 2 quartz-carbonate-sulfide (mainly chalcopyrite) vein. C. Photomicrograph of Stage 2 zooming from area C in Fig. B showing vein dominated by chalcopyrite and minor pyrite. D. Photomicrograph enlarged from Fig. C showing presence of chalcopyrite and pyrite.

### Stage 3: Chlorite – epidote

In hand specimen, the Stage 3 forms as light to dark green vein/veinlets (Fig. 34A). Chlorite-epidote assemblage has been observed (Fig. 34B) with 1-2 mm width veinlets crosscut Stage 2 veins. No sulfide minerals have been observed in this stage.

### Stage 4: Quartz ± calcite

Stage 4 veins/veinlets are characterized by white to light cream color without sulfide minerals (Fig. 35A). Veins sometime can be several cm wide and widely distributed in the study area. It crosscuts veins/veinlets of all previous stages (Fig. 35A)

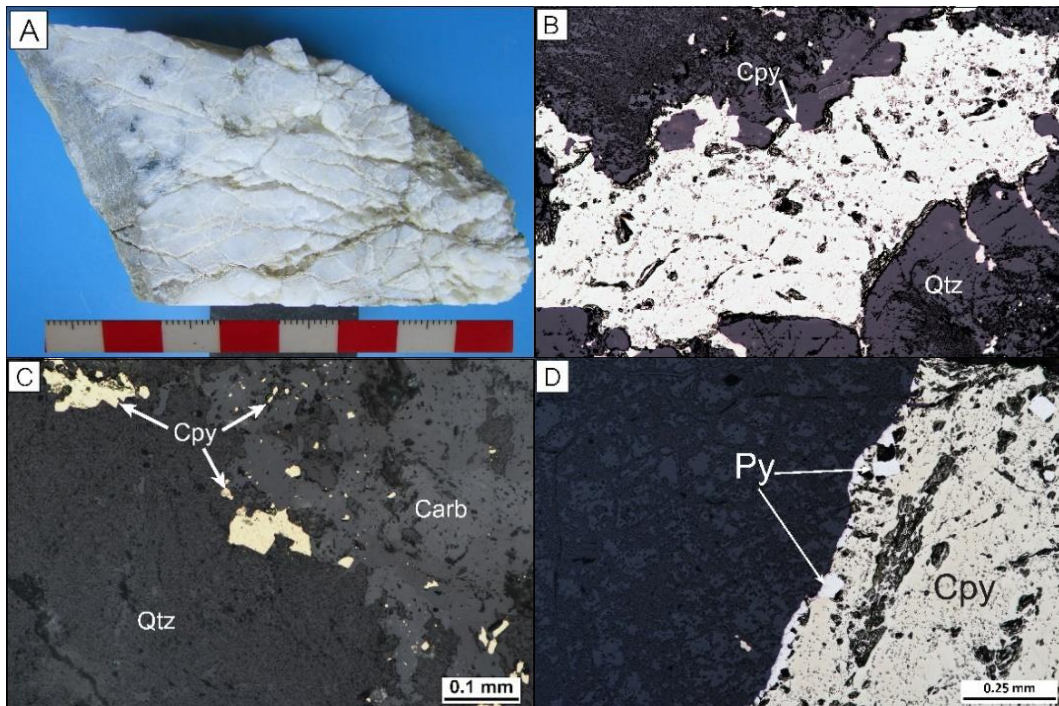


Fig. 33 Characteristics of Stage 2 veins: A. Photograph of diamond drill core showing Stage 2 vein consisting mainly of quartz and sulfide patches (dark). B. Photomicrograph showing mineral assemblage of Stage 2 vein comprising subhedral to euhedral quartz at the vein wall and pyrite (Py) and chalcopyrite (Cpy) at vein center. C. Photomicrograph showing presence of chalcopyrite crystals confined at the contact between quartz and carbonate bands. D. Photomicrograph showing massive chalcopyrite with euhedral pyrites at rim.

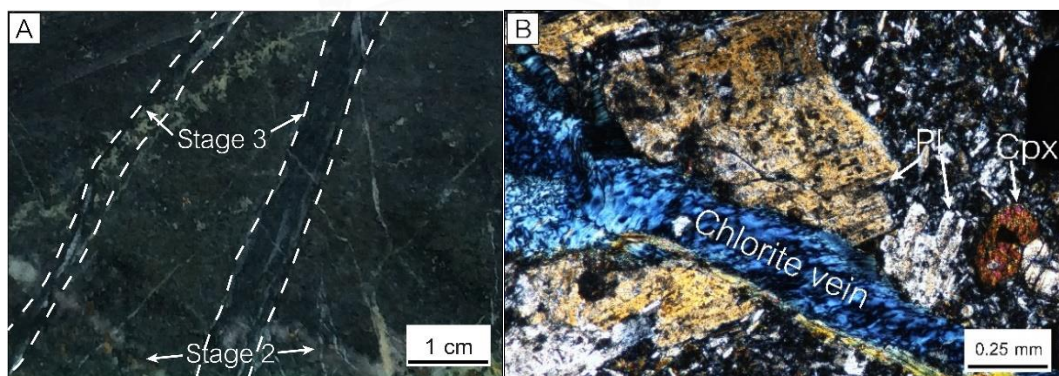


Fig. 34 Characteristics of Stage 3 veins/veinlets: A. Photograph of hand specimen showing Stage 3 vein consisting of quartz and chlorite. B. Photomicrograph showing minerals in Stage 3 comprise chlorite.



Fig. 35 Characteristics of Stage 4 veins/veinlets. A. Photograph of diamond drill core showing Stage 4 vein consisting mainly of quartz and carbonate.

### 5.3. Mineralogy

The mineralogy and ore textures are described for each mineralization stages including 1) Stage 1: Quartz-pyrite, 2) Stage 2: Quartz-calcite  $\pm$  sulfide (chalcopyrite-pyrite-sphalerite), 3) Stage 3: Chlorite – epidote, and 4) Stage 4: Quartz  $\pm$  calcite.

#### 5.3.1. Ore mineralogy

Ore minerals which can be observed in the mineralized veins/veinlets in the Khao Sam Sip area consist of sulfide minerals such as pyrite, sphalerite, and chalcopyrite.

Pyrite is the most abundant sulfide, which occurs in the Stage 1 and Stage 2 veins. In the Stage 1, it forms as isolated fine-grained crystal to patches and subhedral to euhedral crystal (Fig 36A). It is commonly associated with minor quartz. In the Stage 2, pyrite tends to associate with chalcopyrite and minor sphalerite (Fig. 36B). Pyrite is subhedral to euhedral in shape and associates with chalcopyrite in the center of quartz veins. Chalcopyrite forms only in Stage 2. It usually associates with quartz and carbonate and often displays chalcopyrite disseminate in patches of carbonate minerals. Sphalerite is present as small amount in the Stage 2 veins. It forms as anhedral, fine-grained crystals.

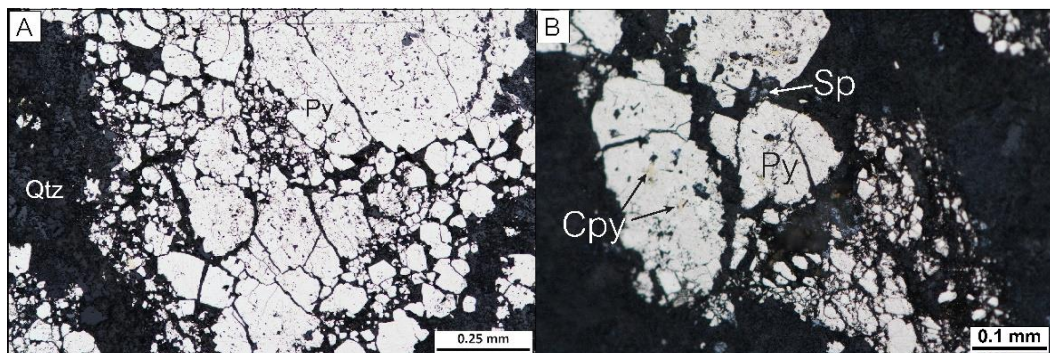


Fig. 36 Characteristics of vein infills: A. Photomicrograph showing Stage 1 pyrite aggregate. B. Photomicrograph showing mineral assemblage of Stage 2 vein comprising pyrite (Py), chalcopyrite (Cpy) and sphalerite (Sp).

### 5.3.2. Gangue mineralogy

Quartz is the most common gangue mineral and present in all stages. In stage 1, it forms in small amount at peripheral of veins. In Stage 2, quartz forms as subhedral to euhedral of coarse- to fine-grained crystals and is generally associated with sulfide minerals. Quartz in Stage 3 forms in small amount associated with epidote and chlorite. Calcite is more abundant in Stage 4 in comparison to the Stage 2. In stage 2, calcite occurs in minor amounts in association with chalcopyrite while calcite in the stage 4 is associated with coarse-grained quartz. In addition, epidote-chlorite assemblage is particularly abundant in Stage 3 veins/veinlets. Numerous chlorites form as tabular aggregated.

### 5.3.3. Minerals chemistry

The study of minerals chemistry is mainly focused on Stage 1 quartz-pyrite veins and stage 2 quartz-calcite-chalcopyrite-pyrite-sphalerite veins in which gold might be present. This study uses Electron Probe Micro Analyzer (EPMA) to measure the mineral composition in terms of elements (e.g. Cu, Fe, S, As, Zn, Au, Ag, Pb, Si, Al, Mg, and Ca). The results of EPMA analyzes can be confirmed the ore petrographic examination.

The EPMA mapping of quartz-calcite-chalcopyrite-pyrite-sphalerite veins (Stage 2) particularly on sulfide minerals (chalcopyrite, and pyrite) and gold showing in Figure

37. EPMA image confirmed the presence of pyrite, chalcopyrite but no gold has been detected neither free grain nor inclusion in sulfide (especially pyrite) of Stage 1.

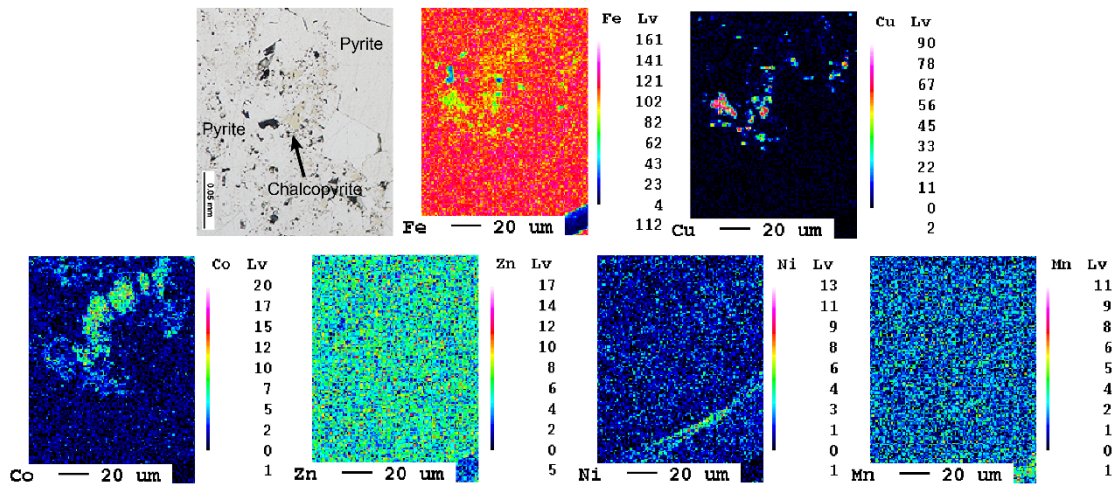


Fig. 37 EPMA Mapping of pyrite-chalcopyrite bearing quartz vein (Stage 1) showing mostly pyrite with small amount of fine-grained chalcopyrite.

The EPMA mapping of Stage 2 veins particularly on sulfide mineral assemblage (chalcopyrite-pyrite-sphalerite) and gold showing in Figure 38. EPMA image confirmed the presence of chalcopyrite, and pyrite but no gold has been detected neither as free gold grain nor inclusion in the sulfides (pyrite and chalcopyrite).

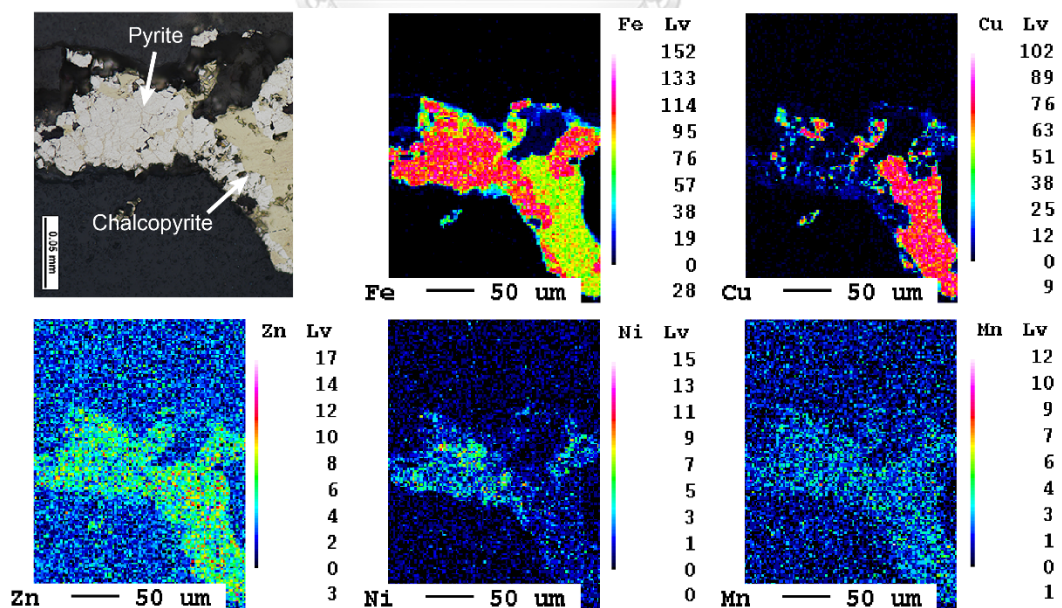


Fig. 38 EPMA Mapping of chalcopyrite-pyrite bearing quartz vein (Stage 2) confirming the present of chalcopyrite and pyrite but no gold.

## CHAPTER 6

### DISCUSSION AND CONCLUSION

Based on the detailed descriptions given in Chapter 3 and Chapter 4, the magmatic suites, the magma source and the tectonic setting are discussed below as well as the mineralization characteristics in the Khao Sam Sip area from Chapter 5:

#### 6.1. Magmatic suites at the Khao Sam Sip

Based on field observation and petrographic characteristics, the volcanic rocks at the Khao Sam Sip contain 3 volcanic rock units: a) Basalt-andesite unit, b) Polymictic andesitic unit and c) Epiclastic unit. The volcanic units in the Khao Sam Sip area might erupt and deposit showing their characteristics by different processes. Almost all rocks of the Basalt-andesite unit (Unit 1) comprise lavas showing evenly distributed, euhedral crystal and porphyritic texture which should have formed from the cooling and solidification of molten lava or magma (McPhie, Doyle, and Allen, 1993). The hornblende-plagioclase andesite shows ophitic texture which generally represents dyke rocks. The other volcanic units (Unit 2 and 3) might be deposited by the sedimentary processes. The polymictic andesitic unit (Unit 2) may have been deposited by the sedimentary processes nearby the area of volcanic activity because its matrix is composed of devitrified glasses and juvenile clasts. The epiclastic unit (Unit 3) shows laminated and graded bedded layers that commonly suggest deep-water depositional environment.

Only the least altered coherent volcanic rocks are presented in detail in this study because they are suitable for identifying the tectonic setting of the source magmas. There are 4 rock types: 1) Olivine-pyroxene-plagioclase basalt, 2) Pyroxene basalt, 3) Hornblende-plagioclase andesite, 4) Plagioclase andesite. The coherent volcanic rocks are ranged in rhyodacite, andesite, trachyandesite, alkali basalt, and basanite in chemical compositions with alkalic affinity. They have distinct chemical characteristics for each rock type: 1) Olivine-pyroxene-plagioclase basalt is characterized by low Ti, Ni, and Zr, moderate Sr and Nb. 2) Pyroxene basalt is

characterized by low Ti, Ni, Sr, Nb, Zr, and Y; however, the pyroxene basalt has been examined only one sample. To give more precise characteristic of the pyroxene basalt more samples need to be analyzed 3) Hornblende-plagioclase andesite is characterized by high Ni, Sr and Zr whereas low Nb and Y. 4) Plagioclase andesite is characterized by low Ti, various in Ni and Zr but constant Nb and Y. Although variations of the trace elements have been considered, they show slight differences.

Thus, the REE patterns, LILE and HFSE abundances of the analyzed rocks are used to confirm that the four coherent rock types have different characteristics. Significantly, compiling all geochemical data and their petrographical results shows the accordant results that the olivine-pyroxene-plagioclase basalt, the pyroxene basalt and plagioclase andesite, which have formed as lava flows, have moderate in trace element, LILE, and HFSE. On the other hands, the hornblende-plagioclase andesite, which has occurred at several depths in drill cores and been suggested to be dyke, has high transition elements, LILE and HFSE except for Nb.

## 6.2. Magma sources

The REE have been used to establish petrochemical characteristic and magma source of the coherent volcanic rocks. These coherent volcanic rocks are divided into two magmatic suites, as evidenced by narrow ranges of least-mobile element ratios (e.g., La/Sm, Sm/Yb, and La/Yb). Suite 1 shows more enrichment of LREE relative to HREE than suite 2. The olivine-pyroxene-plagioclase and the hornblende-plagioclase andesite show higher least-mobile element ratios in comparison to the pyroxene basalt and the plagioclase basalt.

In addition, a comparison of the collected data from Khao Sam Sip with those from modern analogs has been carried out. As a result, the olivine-pyroxene-plagioclase basalt and the hornblende-plagioclase andesite are similar to the alkali rock from Valle del Leone, Etna Mount (Armienti et al., 2004) while the pyroxene basalt and the plagioclase andesite are similar to the alkali rock from Coriolis Trough basin, Vanuatu (Sun et al., 2003). However, all the studied volcanic rock samples consistently show strong negative Eu anomaly in REE patterns and fractionated patterns in trace elements

diagrams compared to alkali rocks of Etna and Vanuatu. Since the presence of negative Eu anomaly commonly suggests that plagioclase and/or potassic feldspar might retain in the source from the partial melting or the plagioclase and/or potassic feldspar have been removed from the melt (Rollinson, 1983; Winter, 2010), this may indicate that volcanic rocks at Khao Sam Sip were formed from highly fractionated alkalic magmas related to subduction (Armienti et al., 2004; Gill, 2010; Sun et al., 2003; Winter, 2010).

### 6.3. Tectonic setting implication

The coherent volcanic unit at the Khao Sam Sip area shows enrichment in LILE, and low abundances of Nb and Ti relative to N-MORB, indicating a subduction-related magmatic setting (Fitton et al., 1988; Pearce, 1982; Stolz, 1995). The reason of enrichment is the addition of LILE and LREE to the mantle source as well as Pb and Th by liquid phases from the subduction of the oceanic crust (Bebout, 2007; Elliott et al., 1997; Hawkesworth et al., 1993; Pearce and Peate, 1995; Spandler and Pirard, 2013). For the depletion of Nb corresponding with depletions of Ti, the immobility of Nb and Ti in subduction zone fluids (Brenan, Shaw, and Ryerson, 1995; Brenan, Shaw, Ryerson, et al., 1995; Keppler, 2017; Tatsumi, 2005) suggests crustal contamination for the evolution of the volcanic rocks in arc-derived magmas (Kelemen et al., 1990; Ringwood, 1990; Ryerson and Watson, 1987).

The Mt. Etna is located on the east coast of Sicily in the converging system between the African and European plates. The evolution of Mt. Etna lava through times of eruption from sub-alkaline to alkaline affinity may reflect from the difference effects in the rising melt in the subduction related environment (Armienti et al., 2004). As the olivine-pyroxene-plagioclase basalt and the hornblende-plagioclase andesite are similar to the alkali rock from Valle del Leone, Etna Mount, the coherent volcanics in the Khao Sam Sip area may have formed by magmas which experienced increasing effect of fluids released by subducting slab enriching the mantle source as same as the Mt. Etna (Armienti et al., 2004).

In addition, the pyroxene basalt and the plagioclase andesite of Khao Sam Sip are similar to the alkali rock from Coriolis Trough basin, Vanuatu. Since the alkali rocks of Coriolis Trough basin are proposed to have derived from an enriched mantle source in the back-arc basin which close to an active arc (Sun et al., 2003), it may indicate that the pyroxene basalt and the plagioclase andesite have formed partially from magmas enriched in mantle source in Sa Kaeo back-arc basin (it now presents as Sa Kaeo Suture) which situates 20km south of the Khao Sam Sip area. However, the pyroxene basalt and the plagioclase andesite are suggested to be erupted in the volcanic arc environment by plotting on the discrimination diagrams of (Mullen, 1983; Pearce and Cann, 1973), suggesting that the mixture of magmas derived from such tectonic settings is proposed for Khao Sam Sip.

Furthermore, the magmatic affinity and the tectonic setting of the coherent volcanic unit are not in accordance with the data previously reported by Junyusuk and Khositantont (1992) and Khin et al. (2014) which suggested that the volcanic rocks in the LFB have a calc-alkalic affinity. However, some workers reported the presence of tholeiite at the Chatree mine in Phetchabun province (e.g., Salam et al. (2014)). The volcanic rocks in the LFB consist not only of the calc-alkaline affinity but also tholeiite and alkaline affinities.

Salam (personal communication, August 1, 2020) mentioned timing of magmatism of these volcanic rocks at Khao Sam Sip is indicated to be Early Triassic by zircon U-Pb age of  $246 \pm 3$  Ma for volcanic breccia collected from Unit 2. A similar age ( $247 \pm 6$  Ma) is also obtained from volcaniclastic rocks at the French Mine area about 30 km to the west of the Khao Sam Sip area (Khin et al., 2009). In general, the major volcanism/ period of the LFB is confined to Late Permian-Early Triassic (Intasopa, 1994; Junyusuk and Khositantont, 1992; Salam et al., 2014) and dominated by sub-alkaline rocks (tholeiite and calc-alkaline affinities). However, the volcanic rocks at Khao Sam Sip are identified to be Early Triassic alkaline series and this is a very unique characteristic for the volcanic rocks of the LFB.

#### 6.4. Mineralization

At Khao Sam Sip, the mineralizations are hosted in volcanic rocks particularly in the coherent volcanic unit (Unit 1). The main mineralizations are characterized by quartz-pyrite veins/veinlets (Stage 1) and quartz-carbonate-sulfides (chalcopyrite-pyrite-sphalerite) veins/veinlets (Stage 2). Gold has been reported in the assay of soil geochemical data in ppb level (Department of Mineral Resources, 2011). However, it has not been detected under a microscope during ore petrographic study and EPMA mapping. It could be interpreted as have been formed as refractory gold (in pyrite structure) or nano-size particles included in sulfide minerals especially pyrite. It should be noted that the limitation of the number of samples may also limit the chances to detect gold.

Based on mineral assemblages, textural features of Stage 1, and Stage 2 veins/veinlets couple with the presence of widespread chlorite-epidote veins/veinlets and alteration similar to those of retrograde skarn, the mineralization at Khao Sam Sip could be interpreted as a distal skarn similar to the gold skarn deposit at the French Mine (Khin Zaw et al., 2009). This skarn mineralization is likely to have been associated with Late Triassic ( $203 \pm 6$  Ma) diorite that has been responsible for gold skarn mineralization at the French Mine deposit (Khin Zaw et al., 2009).

Veins/veinlets are mainly trending NW-SE and controlled by fractures/faults. Based on available diamond drill holes at Khao Sam Sip, the copper mineralization is spatially confined to the basalt-andesite unit (Unit 1). However, it cannot be ruled out that the copper mineralization is not hosted in other units. Considering in Unit 1, mineralization is weakly developed which may be due to poorly developed structures (e.g., fault) together with less suitable lithology (e.g., coherent rocks). In contrast, the large-scale Chatree epithermal deposit which is also hosted in volcanoclastics of similar ages in where mineralizations mainly occur in andesite breccia rather than coherent unit (Salam et al., 2014)

## 6.5. Conclusion

The field investigation, petrography and geochemistry of the volcanic rocks as well as mineralized rocks in the Khao Sam Sip area, Sa Kaeo province can draw the key conclusions below.

- 1) The Khao Sam Sip area comprises mainly four rock units namely: 1) Basalt-andesite unit, 2) Polymictic andesitic unit, and 3) Epiclastic unit, and 4) Clastic unit.
- 2) The coherent volcanics unit can be classified into four rock types namely, 1) olivine-pyroxene-plagioclase basalt, 2) pyroxene basalt, 3) hornblende-plagioclase andesite, and 4) plagioclase andesite.
- 3) The geochemical data of the coherent volcanic rocks show compositional ranges from basalt to andesite with major alkaline affinity.
- 4) Most of rock types of the coherent volcanics rock unit have narrow range in major oxide composition. Their trace elements are quite constant for the hornblende-plagioclase andesite while the olivine-pyroxene-plagioclase basalt, the pyroxene basalt, and the plagioclase andesite are slightly diffused. Thus, the REE patterns and the LREE/HREE ratios are used to confirm the characteristic for those rock types.
- 5) The enrichment of LILE, and low abundances of Nb and Ti relative to N-MORB indicates a subduction-related magmatic setting.
- 6) The trace element and REE data of the volcanic rocks are characterized by enrichment in HFSE (e.g., Th, U, Ta, Pb) and distinct negative Eu anomalies, indicating that they erupted from different magma sources which are highly fractionated magma from crustal contamination formed in volcanic arc system.
- 7) The magmatism responsible for the formation of volcanic rocks in Khao Sam Sip area is chronologically indicated to be a part of LFB, but has unique characteristics of alkaline affinity, which is rarely found among volcanic rocks of LFB.

- 8) The coherent volcanic rocks (Unit 1) host  $\text{Cu}\pm\text{Au}$  veins/veinlets, which can be classified as skarn or epithermal deposit types.

#### 6.6. Recommendations for future works

For the future works, to constrain on magma source, tectonic setting and mineralization in detail, the geochemical analysis is suggested to be studied.

- 1) In part of magma source and tectonic setting, the future study can be age dating in the basalt-andesite unit (Unit 1) and Isotope of Sr-Nd.
- 2) In part of mineralization, the future study can be about stable isotope e.g. oxygen isotope that can suggest types of mineralization (Epithermal or Skarn). More quality samples should be collected and examined to identify gold. In addition, the chemistry of pyrites can be examined for the refractory gold by using Laser Ablation Induced Coupled Plasma Mass Spectrometry (LA-ICP-MS).

## REFERENCES

- Arboit, F., Collins, A. S., Morley, C. K., Jourdan, F., King, R., Foden, J., and Amrouch, K. 2016. Geochronological and geochemical studies of mafic and intermediate dykes from the Khao Khwang Fold–Thrust Belt: Implications for petrogenesis and tectonic evolution. Gondwana Research 36: 124-141.
- Armienti, P., Tonarini, S., Orazio, D. M., and Innocenti, F. 2004. Genesis and evolution of Mt. Etna alkaline lavas: petrological and Sr-Nd-B isotope constraints. Periodico di Mineralogia 73: 29-52.
- Barr, S. M., and Charusiri, P. 2011. The Geology of Thailand. The Geological Society London.
- Barr, S. M., and Macdonald, A. S. 1978. Geochemistry and Petrogenesis of Late Cenozoic Alkaline Basalts of Thailand. Geological Society of Malaysia Bulletin 10: 25-52.
- Barr, S. M., and Macdonald, A. S. 1987. Nan River suture zone, northern Thailand. Geology 15: 907-910.
- Barr, S. M., and Macdonald, A. S. 1991. Toward a late Paleozoic-early Mesozoic tectonic model for Thailand. Journal of Thai Geosciences 1: 11-22.
- Barr, S. M., Macdonald, A. S., Dunning, G. R., Ounchanum, P., and Yaowanoyothin, W. 2000. Petrochemistry, U–Pb (zircon) age, and palaeotectonic setting of the Lampang volcanic belt, northern Thailand. Journal of the Geological Society, London 157: 553-563.
- Barr, S. M., Macdonald, A. S., Ounchanum, P., and Hamilton, M. A. 2006. Age, tectonic setting and regional implications of the Chiang Khong volcanic suite northern Thailand. Journal of the Geological Society, London 163: 1037-1046.
- Barr, S. M., Macdonald, A. S., Yaowanoyothin, W., and Panjasawatwong, Y. 1985. Occurrence of Blueschist in the Nan River Mafic-Ultramafic Belt, Northern Thailand. Warta Geologi (Newsletter of the Geological Society of Malaysia) 11: 47-50.
- Bebout, G. E. 2007. Trace element and Isotopic fluxes/ Subducted Slab. Treatise on

Geochemistry 3: 1-50.

- Booden, M. A., Smith, I. E. M., Mauk, J. L., and Black, P. M. 2010. Evolving volcanism at the tip of a propagating arc: The earliest high Mg- andesites in northern New Zealand. Journal of Volcanology and Geothermal Research 195: 83-96.
- Boonsoong, P., Panjasawatwong, Y., and Metpasopsan, K. 2011. Petrochemistry and tectonic setting of mafic volcanic rocks in the Chon Daen–Wang Pong area, Phetchabun, Thailand. Island Arc 20: 107-124.
- Brenan, J. M., Shaw, H. F., and Ryerson, F. J. 1995. Experimental evidence for the origin of lead enrichment in convergent-margin magmas. Nature 378: 54-56.
- Brenan, J. M., Shaw, H. F., Ryerson, F. J., and Phinney, D. L. 1995. Mineral-aqueous fluid partitioning of trace elements at 900<sup>o</sup>C and 2.0 GPa: Constraints on the trace element chemistry of mantle and deep crustal fluids. Geochimica et Cosmochimica Acta 59: 3331-3350.
- Bunopas, S., and Vella, P. Late Palaeozoic and Mesozoic structural evolution of northern Thailand a plate tectonic model. In Bangkok & Pattaya, 1978. Geological Society of Thailand.
- Bunopas, S., and Vella, P. Tectonic and geologic evolution of Thailand. In P. Nutalaya (ed.), Bangkok, 1983. pp. 307-322. Geological Society of Thailand and Geological Society of Malaysia.
- Chaodumrong, P. 1992. Continuation of geologic rock units among the 1:250,000 scale geologic map of Eastern Thailand.
- Charusiri, P., Clark, A. H., Farrar, E., Archibald, D., and Charusiri, B. 1993. Granite belts in Thailand: evidence from the <sup>40</sup>Ar/<sup>39</sup>Ar geochronological and geological syntheses. Journal of Southeast Asian Earth Science 8: 127-136.
- Chutakositkanon, V., and Hisada, K. Tectono-stratigraphy of the Sa Kaeo-Chanthaburi Accretionary Complex, Eastern Thailand: Reconstruction of Tectonic Evolution of Oceanic Plate-Indochina Collision. In Bangkok, Thailand, 2008.
- Cox, K. G., Bell, J. D., and Pankhurst, R. J. 1979. The interpretation of igneous rocks. George, Allen and Unwin, London.

- Cumming, G. V. 2004. Analysis of volcanic facies at the Chatree gold mine and in the Loei-Petchabun Volcanic belt, central Thailand. BSc. Geology, University of Tasmania.
- Department of Mineral Resources. 2011. Accelerated Mineral Resources Exploration and Evaluation Project (AMREEP): 1/2543 Khao Chakan. Mineral Resources division, Department of Mineral Resources, Bangkok.
- Elliott, T., Plank, T., Zindler, A., White, W., and Bourdon, B. 1997. Element transport from slab to volcanic front at the Mariana arc. Journal of Geophysical Research 102: 14991-15019.
- Feng, Q., Chonglakmani, C., Helmcke, D., Ingavat-Helmcke, R., and Liu, B. 2005. Correlation of Triassic stratigraphy between the Simao and Lampang-Phrae Basins: implications for the tectonopaleogeography of Southeast Asia. Journal of Asian Earth Sciences 24(6): 777-785.
- Fitton, J. G., James, D., Kempton, P. D., Ormerod, D. S., and Leeman, W. P. 1988. The role of lithospheric Mantle in the Generation of Late Cenozoic Basic Magmas in the Western United States. Journal of Petrology (Special Lithosphere Issue): 331-349.
- Fontaine, H., Hoang, T. T., Kavinat, S., Suteethorn, V., and Vachard, D. 2012. Permian fossils recently collected from limestone of Nan area, northern Thailand. Journal of Science and Technology Mahasarakham University 31: 51-62.
- Gill, R. 2010. Igneous Rocks and Processes. Wiley-Blackwell.
- Hara, H., Tokiwa, T., Kurihara, T., Charoentitirat, T., Ngamnithiporn, A., Visetnat, K., Tominaga, K., Kamata, Y., and Ueno, K. 2018. Permian–Triassic back-arc basin development in response to Paleo-Tethys subduction, Sa Kaeo–Chanthaburi area in Southeastern Thailand. Gondwana Research 64: 50-66.
- Hawkesworth, C. J., Gallagher, K., Hergt, J. M., and McDermott, F. 1993. Mantle and slab contributions in arc magmas. Annual Review of Earth and Planetary Sciences 21: 175-204.
- Intasopa, S. S. 1993. Petrology and geochronology of the volcanic rocks of the Central Thailand volcanic belt. PhD. Geology, Chulalongkorn University.

- Intasopa, S. S. 1994. Petrology and Sr-Nd isotopic systems of the basalts and rhyolites, Loei, Thailand.
- Irvine, T. N., and Barager, W. R. A. 1971. A guide to the chemical classification of the common volcanic rocks. Canadian Journal of Earth Sciences 8: 523-548.
- Junyusuk, N., and Khositant, S. Volcanic rocks and associated mineralization in Thailand. In C. Piencharoen (ed.), Department of Mineral Resources, Bangkok, 1992. pp. 522-538. Department of Mineral Resources.
- Kamvong, T., Charusiri, P., and Intasopa, S. S. 2006. Petrochemical Characteristics of Igneous Rocks from the Wang Pong Area, Phetchabun, North Central Thailand Implication for Tectonic Setting. Journal of the Geological Society of Thailand 1: 9-26.
- Kelemen, P. B., Johnson, K. T. M., Kinzler, R. J., and Irving, A. J. 1990. High field strength element depletions in arc basalts due to mantle-magma interaction. Nature 345: 521-524.
- Keppler, H. 2017. Fluids and trace element transport in subduction zones. American Mineralogist 12: 5-20.
- Khin, Z., Meffre, S., Kamvong, T., Khositant, S., Stein, H., Vasconceios, P., and Golding, S. Geochronological and metallogenic framework of Cu-Au skarn deposits along Loei Fold Belt, Thailand and Lao PDR. In Townsville, Australia, 17-20 August 2009, 2009. pp. 309-311.
- Khin, Z., Meffre, S., Lai, C.-K., Burrett, C., Santosh, M., Graham, I., Manaka, T., Salam, A., Kamvong, T., and Cromie, P. 2014. Tectonics and metallogeny of mainland Southeast Asia — A review and contribution. Gondwana Research 26(1): 5-30.
- Khositant, S., Panjasawatwong, Y., Ounchanum, P., Thanasuthipitak, T., Zaw, K., and Meffre, S. Petrochemistry and Zircon Age Determination of Loei-Phetchabun Volcanic Rocks. In Bangkok, Thailand, 2008.
- Kosuwan, P., J., Limtrakun, P., Boonsoong, P., and Panjasawatwong, Y. 2017. Petrography and REE Geochemical Characteristics of Felsic to Mafic Volcanic Hypabyssal Rock in Nakhon Sawan and Uthai Thani Provinces, Central Thailand.

Chiang Mai Journal Science 44(4): 1722-1734.

- Le Maitre, R. W., Bateman, P., Dudek, A., Keller, J., Lameyre Le Bas, M. J., Sabine, P. A., Schmid, R., Sorensen, H., Streckeisen, A., Woolley, A. R., and Zanettin, B. 1989. A classification of igneous rocks and glossary of terms. Blackwell, Oxford.
- Macdonald, A. S., and Barr, S. M. Tectonic Significance of a late Carboniferous volcanic arc in northern Thailand. In Bangkok & Pattaya, 1978. Geological Society of Thailand.
- Madeisky, H. E. 1996. A lithogeochemical and radiometric study of hydrothermal alteration and metal zoning at the Cinola epithermal gold deposit, Queen Charlotte Island, British Columbia.
- McPhie, J., Doyle, M., and Allen, R. 1993. Volcanic Textures: A guide to the interpretation of textures in volcanic rocks. Centre for Ore Deposit and Exploration Studies, University of Tasmania.
- Metcalf, I. 2009. Late Palaeozoic and Mesozoic tectonic and palaeogeographical evolution of SE Asia. Geological Society, London, Special Publications 315(1): 7-23.
- Metcalf, I. 2011. Tectonic framework and Phanerozoic evolution of Sundaland. Gondwana Research 19(1): 3-21.
- Metcalf, I. 2013. Gondwana dispersion and Asian accretion: Tectonic and palaeogeographic evolution of eastern Tethys. Journal of Asian Earth Sciences 66: 1-33.
- Morley, C. K. 2014. The widespread occurrence of low-angle normal faults in a rift setting: Review of examples from Thailand, and implications for their origin and evolution. Earth-Science Reviews 133: 18-42.
- Mullen, E. D. 1983. MnO/TiO<sub>2</sub>/P<sub>2</sub>O<sub>5</sub>: a minor element discriminant for basaltic rocks of oceanic environments and its implications for petrogenesis. Earth and Planetary Science Letters 62: 53-62.
- Nakapadungrat, S., and Putthapiban, P. 1992. Granites and associated mineralization in Thailand. Department of Mineral Resources, Bangkok, Thailand.

- Panjasawatwong, Y. 1993. Petrochemical study of post-Triassic basalts from the Nan Suture, northern Thailand. Journal of Earth Science 8: 147-158.
- Panjasawatwong, Y. 2003. Tectonic Setting of the Permo-Triassic Chiang Khong Volcanic Rocks, Northern Thailand Based on Petrochemical Characteristics. Gondwana Research 6(4): 743-755.
- Panjasawatwong, Y., Kanpeng, K., and Ruangvatanasirikul, K. Basalts in Li Basin, Northern Thailand: Southern Extension of Chiang Mai Volcanic Belt. In Khon Kaen, Thailand, 1995. pp. 225-234. Khon Kaen University.
- Panjasawatwong, Y., Zaw, K., Chantaraamee, S., Limtrakun, P., and Pirarai, K. 2006. Geochemistry and tectonic setting of the Central Loei volcanic rocks, Pak Chom area, Loei, northeastern Thailand. Journal of Asian Earth Sciences 26: 77-90.
- Pearce, J. A. 1982. Trace element characteristics of lavas from destructive plate boundaries. In Thorpe, R. S. (ed.), Andesites. Wiley. Chichester: 525-548.
- Pearce, J. A., and Cann, J. R. 1973. Tectonic setting of basic volcanic rocks determined using trace element analyses. Earth and Planetary Science Letters 19: 290-300.
- Pearce, J. A., and Peate, D. W. 1995. Tectonic implication of the composition of volcanic arc magmas. Annual Review of Earth and Planetary Sciences 23: 251-285.
- Phajuy, B. 2008. Petrochemistry and tectonic significance of mafic volcanic rocks in the Chiang Rai-Chiang Mai volcanic belt, northern Thailand. PhD. Geology, Chiang Mai University.
- Phajuy, B., Panjasawatwong, Y., and Osataporn, P. 2005. Preliminary geochemical study of volcanic rocks in the Pang Mayao area, Phrao, Chiang Mai, northern Thailand: tectonic setting of formation. Journal of Asian Earth Sciences 24(6): 765-776.
- Polprasit, C., Pajitpraporn, V., Thitisawan, V., and Tansathien, W. 1985. Geologic Map of Batdambang (Sheet ND 48-9, Scale 1:250,000). Geological Survey Division, Department of Mineral Resources, Bangkok.
- Qian, X., Wang, Y., Feng, Q., Zi, J.-W., Zhang, Y., and Chonglakmani, C. 2016a. Petrogenesis and tectonic implication of the Late Triassic post-collisional volcanic rocks in Chiang Khong, NW Thailand. Lithos 248-251: 418-431.

- Qian, X., Wang, Y., Feng, Q., Zi, J.-W., Zhang, Y., and Chonglakmani, C. 2016b. Zircon U–Pb geochronology, and elemental and Sr–Nd–Hf–O isotopic geochemistry of post-collisional rhyolite in the Chiang Khong area, NW Thailand and implications for the melting of juvenile crust. International Journal of Earth Sciences 106(4): 1375-1389.
- Qian, X., Wang, Y., Srithai, B., Feng, Q., Zhang, Y., Zi, J.-W., and He, H. 2017. Geochronological and geochemical constraints on the intermediate-acid volcanic rocks along the Chiang Khong–Lampang–Tak igneous zone in NW Thailand and their tectonic implications. Gondwana Research 45: 87-99.
- Ringwood, A. E. 1990. Slab-mantle interactions: Petrogenesis of intraplate magmas and structure of the upper mantle. Chemical Geology 82: 187-207.
- Rollinson, H. R. 1983. The geochemistry of mafic and ultramafic rocks from the Archaean greenstone belts of Sierra Leone. Mineralogical magazine 47: 267-280.
- Royal Thai Survey Department. 1999. AMPHOE KHAO CHAKAN 5436III Series: L7018 (WGS48). Royal Thai Survey Department.
- Ryerson, F. J., and Watson, E. B. 1987. Rutile saturation in magmas: implications for Ti–Nb–Ta depletion in island-arc basalts. Earth and Planetary Science Letters 86: 225-239.
- Salam, A. 2013. A geological, geochemical and metallogenic study of the Chatree Epithermal Deposit, Phetchabun Province, central Thailand. Geology, University of Tasmania.
- Salam, A., Zaw, K., Meffre, S., McPhie, J., and Lai, C. 2014. Geochemistry and geochronology of the Chatree epithermal gold-silver deposit: Implications for the tectonic setting of the Loei Fold Belt, central Thailand. Gondwana Research 26: 198-217.
- Shen, S., Feng, Q., Zhang, Z., and Chongpan, C. 2009. Geochemical characteristics of the oceanic island-type volcanic rocks in the Chiang Mai zone, northern Thailand. Chinese Journal of Geochemistry 28(3): 258-263.
- Singharajwarapan, S. 1994. Deformation and metamorphism of the Sukhothai fold belt,

- northern Thailand. PhD. University of Tasmania.
- Singharajwarapan, S., and Berry, R. 2000. Tectonic implications of the Nan Suture Zone and its relationship to the Sukhothai Fold Belt, Northern Thailand. Journal of Asian Earth Sciences 18: 663-673.
- Sone, M., and Metcalfe, I. 2008. Parallel Tethyan sutures in mainland Southeast Asia: New insights for Palaeo-Tethys closure and implications for the Indosinian orogeny. Comptes Rendus Geoscience 340(2-3): 166-179.
- Sone, M., Metcalfe, I., and Chaodumrong, P. 2012. The Chanthaburi terrane of southeastern Thailand: Stratigraphic confirmation as a disrupted segment of the Sukhothai Arc. Journal of Asian Earth Sciences 61: 16-32.
- Spandler, C., and Pirard, C. 2013. Element recycling from subducting slabs to arc crust: A review. Lithos: 208-303.
- Srichan, W., Chanthraprasert, S., Phajuy, B., Limtrakun, P., Srithai, B., and Meffre, S. Geochronology of igneous rocks from the Nan-Wiang Sa area, northern Thailand. In 2010. pp. 90-91.
- Srichan, W., Crawford, A. J., and Berry, R. F. 2009. Geochemistry and geochronology of Late Triassic volcanic rocks in the Chiang Khong region, northern Thailand. Island Arc 18(1): 32-51.
- Stolz, A. J. 1995. Geochemistry of the Mount Windsor Volcanics: Implications for the Tectonic Setting of Cambro-Ordovician Volcanic-Hosted Massive Sulfide Mineralization in Northeastern Australia. Economic Geology 90: 1080-1097.
- Sun, S.-s., and McDonough, W. F. 1989. Chemical and isotopic systematics of oceanic basalts: Implications for mantle composition and processes. Geological Society London Special Publications: 313-345.
- Sun, W., Bennett, V. C., Eggins, S. M., Arculus, R. J., and Perfit, M. R. 2003. Rhenium systematics in submarine MORB and back-arc basin glasses: laser ablation ICP-MS results. Chemical Geology 196: 259-281.
- Tatsumi, Y. 2005. The subduction factory: How it operates in the evolving Earth. GSA Today 15: 4-10.

- Ueno, K., and Hisada, K.-i. 2001. The Nan-Uttaradit-Sa Kaeo Suture as a Main Paleotethyan Suture in Thailand: Is it Real? Gondwana Research 4(4): 804-806.
- Wakita, K., and Metcalfe, I. 2005. Ocean Plate Stratigraphy in East and Southeast Asia. Journal of Asian Earth Sciences 24(6): 679-702.
- Wang, Y., He, H., Zhang, Y., Srithai, B., Feng, Q., Cawood, P. A., and Fan, W. 2017. Origin of Permian OIB-like basalts in NW Thailand and implication on the Paleotethyan Ocean. Lithos 274-275: 93-105.
- Winchester, J. A., and Floyd, P. A. 1977. Geochemical discrimination of different magma series and their differentiation products using immobile elements. Chemical Geology 20: 325-343.
- Winter, J. D. 2010. Principles of Igneous and Metamorphic Petrology. Prentice Hall.
- Yang, K., Mo, X., and Zhu, Q. 1994. Tectono-volcanic belts and late Paleozoic-early Mesozoic evolution of southwestern Yunnan, China. Journal of Southeast Asian Earth Science 10: 245-262.
- Yang, W., Qian, X., Feng, Q., Shen, S., and Chonglakmani, C. 2016. Zircon U-Pb geochronological evidence for the evolution of the Nan-Uttaradit suture in northern Thailand. Journal of Earth Science 27(3): 378-390.
- Zhang, Y., Wang, Y., Srithai, B., and Phajuy, B. 2016. Petrogenesis for the Chiang Dao Permian high-iron basalt and its implication on the Paleotethyan Ocean in NW Thailand. Journal of Earth Science 27(3): 425-434.
- Zhao, T., Qian, X., and Feng, Q. 2016. Geochemistry, zircon U-Pb age and Hf isotopic constraints on the petrogenesis of the Silurian rhyolites in the Loei Fold Belt and their tectonic implication. Journal of Earth Sciences 27: 391-402.



จุฬาลงกรณ์มหาวิทยาลัย  
**CHULALONGKORN UNIVERSITY**

## VITA

**NAME** Maythira Sriwichai

**DATE OF BIRTH** 2 April 1996

**PLACE OF BIRTH** Nakornping Hospital, Chiang Mai

**INSTITUTIONS ATTENDED** Bachelor of Sciences in Geology, Chiang Mai University,  
Chiang Mai, Thailand

**HOME ADDRESS** 20/32 Chiang Mai-Fang Road, Mae Sa Sub-District, Mae Rim  
District, Chiang Mai Province

**PUBLICATION** Sriwichai, M, Rachanark, B, Assavapanuvat, P,  
Wattanachareekul, P, Makakum, C, Watcharamai, T,  
Ardkham, P, Chaikam, C, Phujareanchaiwon, C, Srisunthon,  
P, Leknettip, S, Kaewpaluk, S, Khamsiri, S, Chawchai, S.  
2019. Preliminary study on petrography and geochemistry of  
basaltic rock in Central Phetchabun, Thailand. Publication in  
Bulletin of Earth sciences of Thailand (BEST), Chulalongkorn  
University, Bangkok, Thailand. Vol., 9, No. 1, 44-54.